

การจำลองพลวัตเชิงโมเลกุลบนพื้นฐานวิธีโอเนียม-เอ็กซ์เอสของไอออน
โลหะอัลคาไล (ไอออนลิเทียม ไอออนโซเดียม และไอออนโพแทสเซียม)
ในสารละลายน้ำ : จากความสามารถในการสร้างโครงสร้าง
คู่ความสามารถในการสลายโครงสร้าง



นางสาวภัทราวรรณ ศรีภา

วิทยานิพนธ์นี้เป็นส่วนหนึ่งของการศึกษาตามหลักสูตรปริญญาวิทยาศาสตรดุษฎีบัณฑิต
สาขาวิชาเคมี
มหาวิทยาลัยเทคโนโลยีสุรนารี
ปีการศึกษา 2557

**ONIOM-XS MD SIMULATIONS OF ALKALI METAL
IONS (Li^+ , Na^+ AND K^+) IN AQUEOUS SOLUTION :
FROM “STRUCTURE-MAKING” TO “STRUCTURE-
BREAKING” ABILITIES**



**A Thesis Submitted in Partial Fulfillment of the Requirements for the
Degree of Doctor of Philosophy in Chemistry
Suranaree University of Technology
Academic Year 2014**

**ONIOM-XS MD SIMULATIONS OF ALKALI METAL IONS
(Li⁺, Na⁺ AND K⁺) IN AQUEOUS SOLUTION : FROM
“STRUCTURE-MAKING” TO “STRUCTURE-BREAKING”
ABILITIES**

Suranaree University of Technology has approved this thesis submitted in partial fulfillment of the requirements for the Degree of Doctor of Philosophy.

Thesis Examining Committee

(Asst. Prof. Dr. Sanchai Prayoonpokarach)

Chairperson

(Assoc. Prof. Dr. Anan Tongraar)

Member (Thesis Advisor)

(Prof. Dr. Kritsana Sagarik)

Member

(Assoc. Prof. Dr. Albert Schulte)

Member

(Asst. Prof. Dr. Teerakiat Kerdcharoen)

Member

(Prof. Dr. Sukit Limpijumnong)

Vice Rector for Academic Affairs
and Innovation

(Assoc. Prof. Dr. Prapun Manyum)

Dean of Institute of Science

ภัทรารวรรณ ศรีภา : การจำลองพลวัตเชิงโมเลกุลบนพื้นฐานวิธีโอเนียม-เอ็กซ์เอส
ของไอออนโลหะอัลคาไล (ไอออนลิเทียม ไอออน โซเดียม และ ไอออนโพแทสเซียม)
ในสารละลายน้ำ : จากความสามารถในการสร้างโครงสร้างสู่ความสามารถในการสลาย
โครงสร้าง (ONIOM-XS MD SIMULATIONS OF ALKALI METAL IONS (Li^+ , Na^+
AND K^+) IN AQUEOUS SOLUTION : FROM “STRUCTURE-MAKING” TO
“STRUCTURE-BREAKING” ABILITIES) อาจารย์ที่ปรึกษา : รองศาสตราจารย์ ดร.
อนันต์ ทองระอา, 147 หน้า.

เทคนิคการจำลองพลวัตเชิงโมเลกุลที่ผสมผสานกลศาสตร์ควอนตัมและกลศาสตร์โมเลกุล
บนพื้นฐานวิธีโอเนียม-เอ็กซ์เอส (เรียกโดยย่อว่า การจำลองพลวัตเชิงโมเลกุลบนพื้นฐาน วิธี
โอเนียม-เอ็กซ์เอส) ได้ถูกนำมาประยุกต์ เพื่อศึกษาสมบัติเชิงโครงสร้างและเชิงพลวัตของไอออน
โลหะอัลคาไล ได้แก่ ไอออนลิเทียม ไอออน โซเดียม และ ไอออนโพแทสเซียม ในสารละลายน้ำ
การจำลองพลวัตเชิงโมเลกุลบนพื้นฐาน วิธีโอเนียม-เอ็กซ์เอส นี้ ได้ถูกเสนอ ขึ้นเพื่อปรับปรุง
ข้อบกพร่องของเทคนิคการจำลองพลวัตเชิงโมเลกุลที่ผสมผสานกลศาสตร์ควอนตัมและกลศาสตร์
โมเลกุลแบบดั้งเดิม (conventional QM/MM MD) โดยเทคนิค การจำลองพลวัตเชิงโมเลกุลบน
พื้นฐาน วิธีโอเนียม-เอ็กซ์เอส นี้ ระบบจะถูกแบ่งออกเป็นสองส่วน ส่วนที่ให้ความสำคัญมากที่สุด
จะเป็นส่วนเล็กๆ ในระบบ ได้แก่ ส่วนที่บรรจุ ไอออนเป็นศูนย์กลางทรงกลมและน้ำที่ล้อมรอบ
ไอออน ซึ่งจะอธิบายโดยใช้กลศาสตร์ควอนตัม และส่วนที่เหลือของระบบจะถูกอธิบายบนพื้นฐาน
ของกลศาสตร์โมเลกุล การศึกษาในครั้งนี้ การคำนวณทางกลศาสตร์ควอนตัมจะกระทำในระดับ
ฮาร์ตรี-ฟอร์ค (HF) โดยใช้เบสิสเซตชนิดดับเบิลเซต่าที่รวมการโพลาไรซ์ (DZP) สำหรับโมเลกุลน้ำ
และไอออนลิเทียม และใช้เบสิสเซตชนิดคิกซ์ยังผลชื่อ LANL2DZ สำหรับไอออน โซเดียมและ
ไอออนโพแทสเซียม ผลที่ได้จากการจำลองพลวัตเชิงโมเลกุลบนพื้นฐาน วิธีโอเนียม-เอ็กซ์เอส ทำ
ให้เข้าใจพฤติกรรมของไอออนทั้งสามที่เกี่ยวข้องกับความสามารถในการสร้างโครงสร้างและ
ความสามารถในการสลายโครงสร้างในสารละลายน้ำ ในกรณีของไอออนลิเทียม พบว่า ไอออนนี้ มี
การสร้างโครงสร้างไฮเดรชันที่ค่อนข้างชัดเจน โดยมีการจัดเรียงตัวของโมเลกุลน้ำรอบ ไอออน
จำนวนสี่โมเลกุลในลักษณะ โครงรูปเตตระฮีดรัล โครงสร้างไฮเดรชันมีความยืดหยุ่นอยู่บ้าง ทำให้
สามารถพบโครงสร้างลักษณะอื่นด้วย โดยเฉพาะ โครงสร้างที่ประกอบด้วยน้ำจำนวนห้าโมเลกุล
ในชั้นไฮเดรชันแรก ลักษณะที่พบดังกล่าว นำไปสู่ข้อเสนอนี้ว่า ความสามารถในการสร้าง
โครงสร้างของไอออนลิเทียมในสารละลายน้ำนั้นไม่แรงมากนัก เช่น หากเปรียบเทียบกับไอออน
แคลเซียมซึ่งมีความสามารถในการสร้างโครงสร้างที่แรงกว่ามาก สำหรับไอออน โซเดียม

ผลการศึกษา พบว่า ไอออนชนิดนี้ก็ยังแสดงความสามารถในการเหนี่ยวนำน้ำที่อยู่รอบๆ เพื่อสร้างโครงสร้างไฮเดรชันได้ดี โดยเกิดเป็นโครงสร้างไฮเดรชันหลักๆ สองชนิด ได้แก่ โครงสร้างไฮเดรชันที่มีน้ำจำนวนห้าและหกโมเลกุล ตามลำดับ สิ่งที่น่าสนใจ กล่าวคือ โครงสร้างทั้งสองชนิดนี้สามารถจะเกิดขึ้นสลับไปมาระหว่างกันและมีความยืดหยุ่นพอควร ลักษณะดังกล่าว สะท้อนให้เห็นความสามารถในการสร้างโครงสร้างของไอออนโซเดียมในสารละลายน้ำที่อ่อน ส่วนในกรณีของไอออน โพแทสเซียม เมื่อเปรียบเทียบกับไอออนลิเทียมและไอออนโซเดียมแล้ว พบว่าโครงสร้างไฮเดรชันของไอออนโพแทสเซียมจะยืดหยุ่นกว่าอย่างเห็นได้ชัด น้ำที่อยู่ล้อมรอบไอออนจะเคลื่อนที่ได้ง่ายและมีน้ำจำนวนหลากหลายโมเลกุลที่สามารถเกิดโครงสร้างไฮเดรชันกับไอออนโพแทสเซียม ทำให้ไอออนนี้มีเลขโคออร์ดิเนชันได้หลายค่า ลักษณะดังกล่าวบ่งบอกว่า ไอออนโพแทสเซียม อาจไม่สามารถเหนี่ยวนำน้ำที่อยู่รอบๆ ได้แรงนัก จึงสามารถจัดให้ไอออนโพแทสเซียมอยู่ในกลุ่มไอออนที่มีความสามารถในการสลายโครงสร้างในสารละลายน้ำ



PATRAWAN SRIPA : ONIOM-XS MD SIMULATIONS OF ALKALI METAL IONS (Li^+ , Na^+ AND K^+) IN AQUEOUS SOLUTION : FROM “STRUCTURE-MAKING” TO “STRUCTURE-BREAKING” ABILITIES.
THESIS ADVISOR : ASSOC. PROF. ANAN TONGRAAR, Ph.D. 147 PP.

Li^+ , Na^+ , K^+ / Structure-maker/breaker/ Molecular Dynamics, ONIOM-XS MD

A more sophisticated QM/MM MD technique based on the ONIOM-XS method, called briefly ONIOM-XS MD, has been applied for studying the hydration structure and dynamics of three essential alkali metal ions, namely Li^+ , Na^+ and K^+ , in aqueous solution. The ONIOM-XS MD technique has been proposed in order to improve the methodical drawbacks of the conventional QM/MM MD framework. Based on the ONIOM-XS MD technique, the system is composed of a “high-level” QM region, *i.e.*, a sphere which contains the ion and its surrounding water molecules, and the remaining “low-level” MM bulk waters. In this work, all interactions within the QM region were treated at the Hartree-Fock (HF) level of accuracy using a Dunning double- ζ plus polarization (DZP) basis set for water and Li^+ , and Los Alamos ECP plus DZ (LANL2DZ) basis set for Na^+ and K^+ , whereas the interactions within the MM and between the QM and MM regions were described by newly developed pair potentials. The results obtained by the ONIOM-XS MD simulations have provided more insights into the behaviors of these three ions with respect to their “structure-making” and “structure-breaking” abilities in aqueous solution. In the case of Li^+ , a well-defined tetrahedral geometry with the average coordination number of 4.1 is observed. The ONIOM-XS MD simulation clearly reveals that the

structure of the hydrated Li^+ is not rigid and that water molecules in the first hydration shell are somewhat labile, leading to a probability of finding other hydrated complexes, in particular the $\text{Li}^+(\text{H}_2\text{O})_5$ species. In this respect, the ONIOM-XS MD results clearly suggest that the “structure-making” ability of Li^+ in aqueous solution is not too strong, *i.e.*, compared to stronger “structure-makers”, such as Ca^{2+} . For Na^+ , the detailed analyzes of the ONIOM-XS MD trajectories show that this ion is able to order the structure of waters in its surroundings, forming two prevalent $\text{Na}^+(\text{H}_2\text{O})_5$ and $\text{Na}^+(\text{H}_2\text{O})_6$ species. Interestingly, it is observed that these 5-fold and 6-fold coordinated complexes can convert back and forth with some degrees of flexibility, leading to frequent re-arrangements of the Na^+ hydrates as well as numerous attempts of inner-shell water molecules to interchange with waters in the outer region. Such phenomenon clearly demonstrates the weak “structure-making” ability of Na^+ in aqueous solution. For K^+ , as compared to Li^+ and Na^+ , the first hydration shell is less structured and water molecules surrounding the K^+ ion are more labile, showing several re-arrangements of the hydrated K^+ complexes. This implies that this ion may not be able to form any specific geometrical order of its hydration shell, and thus, it can be classified as a “structure-breaker” in aqueous solution.

School of Chemistry

Academic Year 2014

Student's Signature _____

Advisor's Signature _____

ACKNOWLEDGEMENTS

First of all, I would like to thank my thesis advisor, Assoc. Prof. Dr. Anan Tongraar for his patience, motivation, and immense knowledge. His guidance encouraged me throughout the course of my graduate. I am also very thankful to the thesis examining committee for their useful comments and suggestions.

In addition to my advisor, I would like to thank Prof. Dr. Kritsana Sagarik and all instructors at School of Chemistry, Suranaree University of Technology (SUT), for their help to guide and develop the ideas of my thesis work with careful and instructive comments. I would also like to thank my friends at SUT, for their friendship.

I am grateful to Prof. Donald G Truhlar, who provided me new and worthy research experiences when I visited the University of Minnesota, United States of America.

Furthermore, I am thankful for the financial support from the National Research University (NRU) Project of Thailand, Office of the Higher Education Commission for giving me a grant under SUT-PhD program (Contract number : SUT PhD/01/2554). High-performance computer facilities provided by the National Electronics and Computer Technology Center (NECTEC) are also acknowledged.

Finally, I am deeply grateful to my parents and sister, for their understanding, support, encouragement, and love.

Pattrawan Sripa

CONTENTS

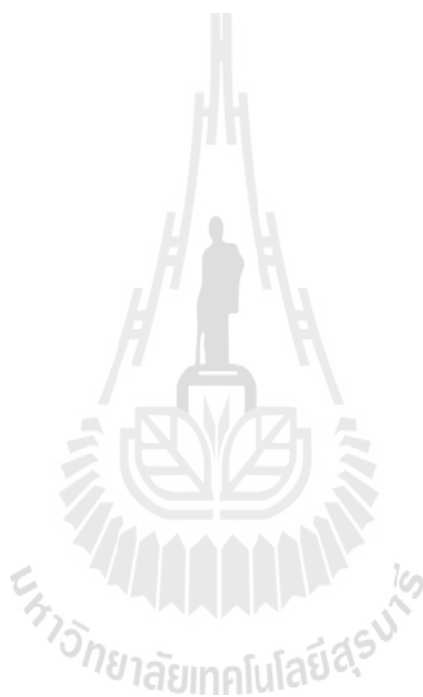
	Page
ABSTRACT IN THAI	I
ABSTRACT IN ENGLISH	III
ACKNOWLEDGEMENTS	V
CONTENTS	VI
LIST OF TABLES	X
LIST OF FIGURES	XII
LIST OF ABBREVIATIONS	XVI
CHAPTER	
I INTRODUCTION	1
1.1 Literature reviews	1
1.2 Research objectives	7
1.3 Scope and limitation of the study	7
1.4 References	9
II QUANTUM CHEMISTRY	21
2.1 Introduction to quantum chemistry	21
2.2 Schrödinger equation	21
2.3 The variation method	22
2.4 Born-Oppenheimer approximation	25
2.5 Molecular orbital theory	26

CONTENTS (Continued)

	Page
2.6 The LCAO-MO approach and basis sets	29
2.7 Basis Set Superposition Error (BSSE)	34
2.8 Hartree-Fock method	35
2.9 Electron correlation	41
2.10 References	42
III MOLECULAR DYNAMICS SIMULATIONS.....	45
3.1 Introduction to molecular dynamics (MD) simulations	45
3.2 Intermolecular potentials	48
3.3 Many-body interactions	48
3.4 Time integration algorithms	50
3.4.1 Verlet algorithm	51
3.4.2 Predictor-corrector algorithm	53
3.5 Periodic boundary conditions	54
3.6 Cut-off and minimum image convention	55
3.7 Non-bonded neighbor lists	59
3.8 Long-range interactions	60
3.9 Research methodology	62
3.9.1 Conventional QM/MM MD technique	62
3.9.2 QM/MM MD based on ONIOM-XS technique	64
3.10 Research procedures	67

CONTENTS (Continued)

	Page
APPENDIX D MANUSCRIPT	135
CURRICULUM VITAE	147



LIST OF TABLES

Table	Page
3.1 Optimized parameters of the analytical pair potentials for the interaction of water with Li^+ , Na^+ and K^+	68
3.2 Optimized geometries and corresponding many-body effects for $\text{Li}^+(\text{H}_2\text{O})_n$ complexes, as obtained by various QM methods using DZP basis set	69
3.3 Optimized geometries and corresponding many-body effects for $\text{Na}^+(\text{H}_2\text{O})_n$ complexes, as obtained by various QM methods using DZP basis set for H_2O and LANL2DZ basis set for Na^+	70
3.4 Optimized geometries and corresponding many-body effects for $\text{K}^+(\text{H}_2\text{O})_n$ complexes, as obtained by various QM methods using DZP basis set for H_2O and LANL2DZ basis set for K^+	71
4.1 Number of water exchange events (N_{ex}) and mean residence times (MRTs) of water molecules in the bulk and in the vicinity of ions, as obtained by the conventional QM/MM and ONIOM-XS MD simulations	96
4.2 D values of water molecules in the bulk and in the hydration shells of Li^+ , Na^+ and K^+ , as obtained by the ONIOM-XS MD simulations.....	107
4.3 Number of water exchange events (N_{ex}) and mean residence times (MRTs) of water molecules in the vicinity of ions and in the bulk, as obtained by ONIOM-XS MD simulations	109

LIST OF TABLES (Continued)

Table	Page
4.4 Vibrational frequencies of water molecules in the hydration shells of Li^+ , Na^+ , K^+ and in the bulk water	112



LIST OF FIGURES

Figure	Page
2.1 The Slater-type and Gaussian-type for 1s orbital	31
2.2 The STO-3G basis set representing the desired STO	32
3.1 The scheme of molecular dynamics simulation	47
3.2 The periodic boundary conditions in two dimensions	55
3.3 The spherical cut-off and the minimum image convention	56
3.4 A discontinuity of cut-off	57
3.5 The effect of a switching function applied on the Lennard-Jones potential	59
3.6 The non-bonded neighbor list	60
3.7 System's partition	62
3.8 Schematic diagram of the ONIOM-XS method	65
3.9 The <i>ab initio</i> interaction energies of a) $\text{Li}^+(\text{H}_2\text{O})_n$ complex, where $n = 1-4$, b) $\text{Na}^+(\text{H}_2\text{O})_n$ and c) $\text{K}^+(\text{H}_2\text{O})_n$ complexes, where $n = 1-6$, as obtained by various QM methods (HF, B3LYP, MP2 and CCSD) using DZP basis set for H_2O and Li^+ , and LANL2DZ basis set for Na^+ and K^+ , respectively.	73

LIST OF FIGURES (Continued)

Figure	Page
3.10 M-O distance of the optimized geometries of a) $\text{Li}^+(\text{H}_2\text{O})_n$ complex, where $n = 1-4$, b) $\text{Na}^+(\text{H}_2\text{O})_n$ and c) $\text{K}^+(\text{H}_2\text{O})_n$ complexes, where $n = 1-6$, as obtained by various QM methods (HF, B3LYP, MP2 and CCSD) using DZP basis set for H_2O and Li^+ , and LANL2DZ basis set for Na^+ and K^+ , respectively	74
3.11 Optimized geometries of $\text{Li}^+(\text{H}_2\text{O})_4$, $\text{Na}^+(\text{H}_2\text{O})_6$ and $\text{K}^+(\text{H}_2\text{O})_6$ complexes, as obtained by the HF calculations using different basis sets (3-21G, DZP, 6-311++G(d,p) and AUG-cc-pVDZ)	75
3.12 Requirements of CPU times for HF force calculations of $\text{Li}^+(\text{H}_2\text{O})_n$ complexes, where $n=1-16$, using DZP, 6-311++G(d,p) and AUG-cc-pVDZ basis sets. All QM calculations were performed on CCRL cluster .	76
3.13 Requirements of CPU times for HF force calculations of $\text{Na}^+(\text{H}_2\text{O})_n$ complex, where $n=1-16$, using DZP, 6-311++G(d,p) and AUG-cc-pVDZ basis sets for H_2O and LANL2DZ basis set for Na^+	77
3.14 Requirements of CPU times for HF force calculations of $\text{K}^+(\text{H}_2\text{O})_n$ complex, where $n=1-16$, using DZP, 6-311++G(d,p) and AUG-cc-pVDZ basis sets for H_2O and LANL2DZ basis set for K^+	78
3.15 Definition of mechanism of ligand exchange process	81

LIST OF FIGURES (Continued)

Figure	Page
4.1 a) Li-O and b) Li-H RDFs and their corresponding integration numbers, as obtained by the conventional QM/MM and ONIOM-XS MD simulations	88
4.2 Distributions of the coordination number of Li^+ , calculated within the first minimum of the Li-O RDFs, as obtained by the conventional QM/MM and ONIOM-XS MD simulations	89
4.3 Distributions of the O---Li---O angle, calculated within the first minimum of the Li-O RDFs, as obtained by the conventional QM/MM and ONIOM-XS MD simulations	90
4.4 Time dependence of a) Li^+ ---O distance and b) number of first-shell waters, as obtained from first 20 ps of the conventional QM/MM MD simulation	92
4.5 Time dependence of a) Li^+ ---O distance and b) number of first-shell waters, as obtained from first 20 ps of the ONIOM-XS MD simulation...	93
4.6 a) M-O and b) M-H RDFs and their corresponding integration numbers, as obtained by the ONIOM-XS MD simulations	98
4.7 Probability distributions of the coordination number of Li^+ , Na^+ and K^+ , calculated up to first minimum of the M-O RDFs	100

LIST OF FIGURES (Continued)

Figure	Page
4.8 Distributions of the O---M---O angle, calculated within first minimum of the M-O RDFs	102
4.9 Probability distributions of θ angle in the first hydration shells of Li^+ , Na^+ and K^+ , calculated within first minimum of the M-O RDFs	103
4.10 Time dependences of a) Na^+ ---O distance and b) number of first-shell waters, as obtained from first 20 ps of the ONIOM-XS MD simulation	105
4.11 Time dependences of a) K^+ ---O distance and b) number of first-shell waters, as obtained from first 20 ps of the ONIOM-XS MD simulation	106
4.12 Fourier transforms of the hydrogen velocity autocorrelation functions of a) bending vibrations (Q_2) and b) symmetric and asymmetric stretching vibrations (Q_1 and Q_3) of water molecules in the first hydration shells of Li^+ , Na^+ and K^+ and in the bulk	111

LIST OF ABBREVIATIONS

Å	=	Ångström
A	=	Associative exchange
ADF	=	Angular distribution function
au	=	Atomic unit
Aug-cc-pVDZ	=	Additional diffuse basis function and correlation consistent polarized valence double zeta
B3LYP	=	Becke three-parameter hybrid functional combined with Lee-Yang-Parr correlation function
BJH	=	Flexible water model developed by Bopp, Jancsó and Heinzinger
BLYP	=	Becke hybrid functional combined with Lee-Yang-Parr correlation function
BO	=	Born-Oppenheimer
BOMD	=	Born-Oppenheimer molecular dynamics
BSSE	=	Basis set superposition error
Ca ²⁺	=	Calcium ion
CCSD	=	Coupled cluster calculations using both single and double substitutions from Hartree-Fock determinant
CF2	=	Central force model version 2
cm ⁻¹	=	Wavenumber

LIST OF ABBREVIATIONS (Continued)

CN	=	Coordination number
CPMD	=	Car-Parrinello molecular dynamics
CPU	=	Central processing unit
D	=	Self-diffusion coefficient
D	=	Dissociative exchange
DFT	=	Density functional theory
DZP	=	Double zeta plus polarization
e	=	Electron charge
E_{tot}	=	Total interaction energy
E_{MM}	=	Interactions within MM region
E_{QM-MM}	=	Interactions between QM and MM regions
$E^{ONIOM-XS}$	=	The potential energy of the entire system for ONIOM-XS
ECP	=	Effective core potential
<i>etc</i>	=	et cetera
F_i	=	Force acting on each particle
F_{MM}	=	MM force
F_{QM}	=	QM force
fs	=	Femtosecond
GGA	=	Generalized gradient approximation
GTO	=	Gaussian-type orbital

LIST OF ABBREVIATIONS (Continued)

\hat{H}	=	Hamiltonian operator
HF	=	Hartree-Fock
I	=	Interchange mechanism
I _a	=	Associative-like interchange mechanism
I _d	=	Dissociative-like interchange mechanism
K	=	Kelvin
kcal/mol	=	Kilocalorie per mole
LANL2DZ	=	Los Alamos ECP plus DZ
LCAO-MO	=	Linear combination of atomic orbitals to molecular orbitals
l	=	Number of particles in the switching layer
M	=	Molarity
MC	=	Monte Carlo
MD	=	Molecular dynamics
MM	=	Molecular mechanics
MO	=	Molecular orbital
MP2	=	Second-order Møller-Plesset
MRT	=	Mean residence times
m	=	Mass
m_e	=	Mass of electron

LIST OF ABBREVIATIONS (Continued)

m_k	=	Mass of nucleus
n_1	=	Number of particles in the QM sphere
ND	=	Neutron diffraction
NVE	=	Microcanonical ensemble
NVT	=	Canonical ensemble
n_2	=	Number of particle in the MM region
N_{ex}	=	Number of exchange events
ONIOM	=	Own N-layered Integrated molecular Orbital and molecular Mechanics
ONIOM-XS	=	An extension of the ONIOM method for molecular simulation in condensed phase
PP	=	Pseudopotential
ps	=	Picosecond
QM	=	Quantum mechanics
QM/MM	=	Combined Quantum mechanics/molecular mechanics
RDF	=	Radial distribution function
RHF	=	Restricted Hatree-Fock
r_0	=	Distance characterizing the start of QM region
r_1	=	Distance characterizing the end of QM region
r_{min}	=	First minimum of RDF peak

LIST OF ABBREVIATIONS (Continued)

r_{max}	=	First maximum of RDF peak
SCF	=	Self-consistent field
STO	=	Slater-type orbital
SPC/E	=	Simple point charge effective pair water model
$S_m(r)$	=	Smoothing function
VACF	=	Velocity autocorrelation functions
XRD	=	X-ray diffraction
XAS	=	X-ray absorption spectroscopy
μ	=	Chemical potential
Φ	=	Trial function
h	=	Planck's constant
$^{\circ}$	=	Degree
τ_{H_2O}	=	MRT of water molecules
λ	=	Wavelength
t^*	=	Time for observing the number of exchange water
t_{sim}	=	Simulation time
$\chi(x)$	=	Spin orbital
∇^2	=	Laplacian operator
Ψ	=	Wavefunction
$(\Psi_{QM} \hat{H} \Psi_{QM})$	=	Interaction within QM region

CHAPTER I

INTRODUCTION

1.1 Literature review

Detailed knowledge of ions solvated in aqueous electrolyte solution has long been desirable for chemists and biologists in order to understand the role of these ions in chemical and biological processes (Hermansson and Wojcik, 1998; Misra and Draper, 1999). When ions interact with water, the effect of ions causes modifications in the local structure and changes in the dynamics properties of the surrounding water molecules. The manners in which ions order the structure of their surrounding waters are strongly related to the strength of ion-water interactions. For example, if the ion-water interactions are stronger than that of water-water interactions, such ions are classified as “structure-making” ions, *i.e.*, they can break H-bond structure of the surrounding water molecules and can order those water molecules to form specific ion-water complexes. In contrast, if the ion-water interactions are comparable or weaker than that of water-water interactions, such ions can be classified as “structure-breaker”. In this respect, water molecules surrounding the ions prefer to form H-bond network with their neighboring water molecules, rather than to form specific hydration structure with the ions. On the other hand, these “structure-breaking” ions are regarded as perturbation of the water’s H-bond structures (Tongraar, Liedl and Rode, 1998a; Tongraar and Rode, 2004).

During the past decades, the details with respect to behaviors of ions solvated in aqueous solution have been studied extensively, both by experiments (Bondarenko, Gorbaty, Okhulkov and Kalinichev, 2006; Caminiti, Licheri, Paschina, Piccaluga and Pinna, 1980; Cartailier, Kunz, Turq and Bellisent-Funel, 1991; Dang, Schenter, Glezakou and Fulton, 2006; Howell and Neilson, 1996; Kameda, Sugawara, Usuki and Uemura, 1998; Kulik, Marzari, Correa, Prendergast, Schwegler and Galli, 2010; Licheri, Piccaluga and Pinna, 1975; Mancinelli, Botti, Bruni, Ricci and Soper, 2007; Neilson and Skipper, 1985; Newsome, Neilson and Enderby, 1980; Novikov, Rodnikova, Savostin and Sobolev, 1999; Ohtomo and Arakawa, 1979; Ohtomo and Arakawa, 1980; Skipper and Neilson, 1989) and theoretical investigations (Azam, Hofer, Randolph and Rode, 2009; Azam, Zaheer ul and Fatmi, 2010; Bondarenko, Gorbaty, Okhulkov and Kalinichev, 2006; Carrillo-Tripp, Saint-Martin and Ortega-Blake, 2003; Chorny and Benjamin, 2005; Dang, Schenter, Glezakou and Fulton, 2006; Galamba and Costa Cabral, 2009; Grossfield, Ren and Ponder, 2003; Ikeda, Boero and Terakura, 2007; Kim, 2001; Lamoureux and Roux, 2006; Loeffler, Inada and Funahashi, 2006; Loeffler, Mohammed, Inada and Funahashi, 2003; Lyubartsev, Laasonen and Laaksonen, 2001; Megyes, Balint, Grosz, Radnai, Bako and Sipos, 2008; Obst and Bradaczek, 1996; Öhrn and Karlström, 2004; Ramaniah, Bernasconi and Parrinello, 1999; Rempe, Asthagiri and Pratt, 2004; Rempe, Pratt, Hummer, Kress, Martin and Redondo, 2000; Spangberg and Hermansson, 2004; Spangberg, Rey, Hynes and Hermansson, 2003; Sripa, Tongraar and Kerdcharoen, 2013; Tongraar, Liedl and Rode, 1998a; Tongraar, Liedl and Rode, 1998b; White, Schwegler, Galli and Gygi, 2000; Zhou, Lu, Wang and Shi, 2002). In particular for aqueous solutions of Li^+ , Na^+ and K^+ , a number of experiments and theoretical

investigations have been carried out, and the results are summarized in Tables A1-A6 (see Appendix A). With regard to the data in Tables A1-A6, however, it is apparent that significant discrepancies among those results still exist, even for such fundamental properties as the average coordination number and the mean ion-water distance.

With regard to experimental observations, X-ray diffraction (XRD) and neutron diffraction (ND) methods have proved to be valuable tools for determining the static structure factors of waters solvating a given ion (Ansell, Barnes, Mason, Neilson and Ramos, 2006; Ohtaki and Radnai, 1993). However, experimental measurements often yield an incomplete description of ionic solvation, due to, *e.g.* the lack of suitable isotope substitutions in ND experiments, or difficulties in separating the atomic correlations or different species in diffraction data (Chowdhuri and Chandra, 2003; Koneshan, Rasaiah, Lynden-Bell and Lee, 1998; Zhou, Lu, Wang and Shi, 2002). Recently, X-ray absorption spectroscopy (XAS), a powerful tool for local structural determination, has been employed for the study of such systems (Cappa, Smith, Messer, Cohen and Saykally, 2006; Kulik, Marzari, Correa, Prendergast, Schwegler and Galli, 2010). Nevertheless, this technique is mostly suitable for the treatment of systems that are relevant to hard atoms. According to the data in Tables A1, A3 and A5, for the aqueous solutions of Li^+ , Na^+ and K^+ , respectively, the observed discrepancy among the experimental data has been attributed mainly to the concentration dependence, as well as to the different experimental methods employed.

In conjunction with experiments, computer simulations, *i.e.*, by means of Monte Carlo (MC) and molecular dynamics (MD), have become an alternative way to provide microscopic details with respect to structural and dynamical properties of ions

in aqueous solutions. By the MC technique, each particle in the system will be moved randomly, through the energy criteria. In contrast to MC, the MD technique makes use of system's force to move all particles in the system. In this respect, the advantage of MD simulation over the MC technique is that it can provide not only the structural properties but also the dynamical details. The results obtained from various MC and MD simulations are summarized in Tables A2, A4 and A6 for the systems of Li^+ , Na^+ and K^+ in aqueous solutions, respectively. For earlier MC and MD simulations, most of which are based on molecular mechanical (MM) force fields (Lee, Tarakeshwar, Park, Kołaski, Yoon, Yi, Kim and Kim, 2004; Tanaka and Aida, 2004; Tongraar, Liedl and Rode, 1998a), the observed differences among the simulation results could be ascribed to the use of different MM force fields in describing the system's interactions. In this respect, the quality of the simulation results depends crucially on the quality of the ion-water and water-water potentials employed in the simulations (Rasaiah, Noworyta and Koneshan, 2000).

To obtain more reliable data, it has been demonstrated that the non-additive contributions as well as the polarization effects are significant and that the inclusion of these terms in the simulations through quantum mechanical calculations is mandatory (Impey, Madden and McDonald, 1983; Song Hi Lee and Rasaiah, 1996; Obst and Bradaczek, 1996; Rode, Schwenk and Tongraar, 2004). By means of *ab initio* (AI) MD techniques, Car-Parrinello (CP) and Born-Oppenheimer (BO) MDs are well-known. With regard to AI-MD technique, the whole system is treated quantum mechanically, most of which are based on density functional theory (DFT). In recent years, several AI-MD simulations have been performed for studying many aqueous ionic systems (Lyubartsev, Laasonen and Laaksonen, 2001; Ramaniah, Bernasconi

and Parrinello, 1999). However, some limitations of the AI-MD technique come from the use of simple generalized gradient approximation (GGA) functionals, such as BLYP and PBE and of the relatively small system size. In particular, it has been demonstrated that the use of small system size may lead to problems of ion-ion interactions (Lyubartsev, Laasonen and Laaksonen, 2001). Besides the AI-MD technique, an alternative approach is to apply a so-called combined quantum mechanical/molecular mechanical (QM/MM) technique (Field, Bash and Karplus, 1990; Singh and Kollman, 1986; Warshel and Levitt, 1976). By means of the QM/MM technique, the most interesting part of the system (*i.e.* a sphere which includes the ion and its surrounding solvent particles) is treated quantum mechanically, while the rest of the system is handled by simple MM force fields. This technique has been successfully applied for studying many condensed-phase systems (Gao, 2007; Kerdcharoen, Liedl and Rode, 1996; Rode, Schwenk and Tongraar, 2004; Sripa, Tongraar and Kerdcharoen, 2013; Thaomola, Tongraar and Kerdcharoen, 2012; Wanprakhon, Tongraar and Kerdcharoen, 2011). Interestingly, a combination of XAS measurements and QM/MM MD simulations has been successfully applied to investigate the hydration shell structures of Ca^{2+} and Cl^- (Tongraar, T-Thienprasert, Rujirawat and Limpijumnong, 2010).

Despite the QM/MM technique's successes, however, there are some unsolved problems that undermine the validity of this approach. For example, according to the conventional QM/MM scheme, a smoothing function is applied only for the exchanging particles that are crossing the QM/MM boundary. Such treatment is not realistic since an immediate exchange of particles between the QM and MM regions also affects the forces acting on the remaining QM particles. In addition, the

conventional QM/MM framework cannot clearly define the energy expression during the solvent exchange process (Kerdcharoen and Morokuma, 2002; Kerdcharoen and Morokuma, 2003). To solve these problems, a more sophisticated QM/MM MD technique based on ONIOM-XS method (which will be abbreviated throughout this work as “ONIOM-XS MD”) has been proposed (Kerdcharoen and Morokuma, 2003). The ONIOM method, originally developed by Morokuma *et al.* (Svensson, Humbel, Froese, Matsubara, Sieber and Morokuma, 1996), can handle not only the QM + MM combinations (which is implemented in the conventional QM/MM scheme), but also the QM + QM combinations. In addition, this technique allows forces on all QM particles to be smoothed during particle exchange, and thus, clearly defines the system’s energy expression. Recently, the ONIOM-XS MD technique has been successfully applied to various systems, such as Li^+ and Ca^{2+} in liquid ammonia (Kerdcharoen and Morokuma, 2002; Kerdcharoen and Morokuma, 2003), Na^+ , K^+ and Ca^{2+} in aqueous solution (Sripa, Tongraar and Kerdcharoen, 2013; Wanprakhon, Tongraar and Kerdcharoen, 2011) as well as liquid water (Thaomola, Tongraar and Kerdcharoen, 2012).

In the present study, the high-level ONIOM-XS MD technique will be applied for studying the behaviors of Li^+ , Na^+ and K^+ in aqueous solution. Of particular interest, the relationship of these three ions with respect to their “structure-making” and “structure-breaking” abilities will be evaluated and discussed. The results obtained by the ONIOM-XS MD simulations are expected to provide more reliable descriptions on the structure and dynamics of these hydrated ions.

1.2 Research objectives

1. To verify the reliability of the high-level ONIOM-XS MD technique for the treatment of aqueous ionic solutions.
2. To apply the ONIOM-XS MD technique for obtaining detailed knowledge with respect to the “structure-making” and “structure-breaking” abilities of Li^+ , Na^+ and K^+ in aqueous solution.

1.3 Scope and limitation of the study

In the case of aqueous Li^+ solution, to verify the reliability of the high-level ONIOM-XS MD technique for the study of such a condensed-phase systems, two QM/MM-based MD simulations, namely a conventional QM/MM and ONIOM-XS MDs, will be performed. The results obtained by the two QM/MM-based MD simulations will be compared and discussed with respect to the important treatment of the ONIOM-XS method for describing the “structure-making” ability of Li^+ in aqueous solution. Concurrently, a series of ONIOM-XS MD simulations will be performed to investigate the structural and dynamical properties of Na^+ and K^+ in aqueous solution. By the QM/MM-based MD techniques, the system is comprised of a “high-level” QM region, *i.e.*, a sphere which contains the ion and its surrounding water molecules, and the remaining “low-level” MM bulk waters. Since the QM region is considered as the most interesting part, the selection of QM method as well as the QM size and basis set is very crucial in order to obtain good results. In practice, these parameters must be optimized, compromising between the quality of the simulation results and the requirement of CPU time. In this context, it should be noted that the use of correlated QM calculations, even at the simple MP2-level, are still

beyond our current computational feasibility. Hence, all interactions within the QM region were evaluated by performing *ab initio* calculations at the Hartree-Fock (HF) level of accuracy using the DZP basis set (Dunning and Hay, 1977) for water and Li⁺ and LANL2DZ basis set (Boys and Bernardi, 1970; Check, Faust, Bailey, Wright, Gilbert and Sunderlin, 2001; Hay and Wadt, 1985) for Na⁺ and K⁺. The DZP and LANL2DZ basis sets employed in this work are considered as moderate basis sets, most of which have been successfully employed in previous conventional QM/MM and ONIOM-XS MD studies (Thaomola, Tongraar and Kerdcharoen, 2012; Wanprakhon, Tongraar and Kerdcharoen, 2011). For the QM size, a QM radius of 4.2 Å was chosen. This QM size is considered to be large enough to include most of the non-additive contributions and the polarization effects, *i.e.*, at least within the whole first hydration shell and major parts of the second hydration layer (*e.g.*, for Li⁺) of the ions. The structural properties of the hydrated Li⁺, Na⁺ and K⁺ will be analyzed in terms of radial distribution functions (RDFs) and their corresponding integration numbers, together with the angular distribution functions (ADFs) and dipole-oriented arrangements of water molecules surrounding the ions. The dynamics properties will be interpreted through mean residence times (MRTs) of water molecules and water exchange processes at the ion, together with water's intra-molecular vibrational frequencies. The results obtained by the ONIOM-XS MD simulations will be compared and discussed with available experimental data and other QM-based MD simulation results.

1.4 References

- Alam, T. M., Hart, D. and Rempe, S. L. B. (2011). Computing the ^7Li NMR chemical shielding of hydrated Li^+ using cluster calculations and time-averaged configurations from *ab initio* molecular dynamics simulations. **Physical Chemistry Chemical Physics**. 13: 13629-13637.
- Ansell, S., Barnes, A. C., Mason, P. E., Neilson, G. W. and Ramos, S. (2006). X-ray and neutron scattering studies of the hydration structure of alkali ions in concentrated aqueous solutions. **Biophysical Chemistry**. 124: 171-179.
- Azam, S. S., Hofer, T. S., Randolf, B. R. and Rode, B. M. (2009). Hydration of sodium(I) and potassium(I) revisited: A comparative QM/MM and QMCF MD simulation study of weakly hydrated ions. **The Journal of Physical Chemistry A**. 113: 1827-1834.
- Azam, S. S., Zaheer ul, H. and Fatmi, M. Q. (2010). Classical and QM/MM MD simulations of sodium(I) and potassium(I) ions in aqueous solution. **Journal of Molecular Liquids**. 153: 95-100.
- Birch, N. J. (1999). Inorganic pharmacology of lithium. **Chemical Reviews**. 99: 2659-2682.
- Bondarenko, G. V., Gorbaty, Y. E., Okhulkov, A. V. and Kalinichev, A. G. (2006). Structure and hydrogen bonding in liquid and supercritical aqueous NaCl solutions at a pressure of 1000 bar and temperatures up to 500 °C: A comprehensive experimental and computational study. **The Journal of Physical Chemistry A**. 110: 4042-4052.

- Boys, S. F. and Bernardi, F. (1970). The calculation of small molecular interactions by the differences of separate total energies. Some procedures with reduced errors. **Molecular Physics**. 19: 553-566.
- Caminiti, R., Licheri, G., Paschina, G., Piccaluga, G. and Pinna, G. (1980). Interactions and structure in aqueous NaNO_3 solutions. **The Journal of Chemical Physics**. 72: 4522-4528.
- Cappa, C. D., Smith, J. D., Messer, B. M., Cohen, R. C. and Saykally, R. J. (2006). Effects of cations on the hydrogen bond network of liquid water: New results from X-ray absorption spectroscopy of liquid microjets. **The Journal of Physical Chemistry B**. 110: 5301-5309.
- Carrillo-Tripp, M., Saint-Martin, H. and Ortega-Blake, I. (2003). A comparative study of the hydration of Na^+ and K^+ with refined polarizable model potentials. **The Journal of Chemical Physics**. 118: 7062-7073.
- Cartailler, T., Kunz, W., Turq, P. and Bellissent-Funel, M. C. (1991). Lithium bromide in acetonitrile and water: A neutron scattering study. **Journal of Physics: Condensed Matter**. 3: 9511.
- Check, C. E., Faust, T. O., Bailey, J. M., Wright, B. J., Gilbert, T. M. and Sunderlin, L. S. (2001). Addition of polarization and diffuse functions to the LANL2DZ basis set for P-Block elements. **The Journal of Physical Chemistry A**. 105: 8111-8116.
- Chorny, I. and Benjamin, I. (2005). Hydration shell exchange dynamics during ion transfer across the liquid/liquid interface. **The Journal of Physical Chemistry B**. 109: 16455-16462.

- Chowdhuri, S. and Chandra, A. (2003). Hydration structure and diffusion of ions in supercooled water: Ion size effects. **The Journal of Chemical Physics**. 118: 9719-9725.
- Dang, L. X., Schenter, G. K., Glezakou, V.-A. and Fulton, J. L. (2006). Molecular simulation analysis and X-ray absorption measurement of Ca^{2+} , K^+ and Cl^- ions in solution. **The Journal of Physical Chemistry B**. 110: 23644-23654.
- Dunning, T. H. and Hay, P. J. (1977). Methods of electronic structure theory. **Modern Theoretical Chemistry**. III, Plenum, New York.
- Enderby, J. E. and Neilson, G. W. (1981). The structure of electrolyte solutions. **Reports on Progress in Physics**. 44: 593.
- Field, M. J., Bash, P. A. and Karplus, M. (1990). A combined quantum mechanical and molecular mechanical potential for molecular dynamics simulations. **Journal of Computational Chemistry**. 11: 700-733.
- Galamba, N. and Costa Cabral, B. J. (2009). Born–Oppenheimer molecular dynamics of the hydration of Na^+ in a water cluster. **The Journal of Physical Chemistry B**. 113: 16151-16158.
- Gao, J. (2007). Methods and applications of combined quantum mechanical and molecular mechanical potentials. **Reviews in Computational Chemistry**. 119-185.
- Grossfield, A., Ren, P. and Ponder, J. W. (2003). Ion solvation thermodynamics from simulation with a polarizable force field. **Journal of the American Chemical Society**. 125: 15671-15682.

- Hay, P. J. and Wadt, W. R. (1985). *Ab initio* effective core potentials for molecular calculations. Potentials for the transition metal atoms Sc to Hg. **The Journal of Chemical Physics**. 82: 270-283.
- Heinzinger, K. (1985). The structure of aqueous electrolyte solutions as derived from MD (molecular dynamics) simulations, **Pure and Applied Chemistry**. 57: 1031.
- Hermansson, K. and Wojcik, M. (1998). Water exchange around Li^+ and Na^+ in $\text{LiCl}(\text{aq})$ and $\text{NaCl}(\text{aq})$ from MD simulations. **The Journal of Physical Chemistry B**. 102: 6089-6097.
- Howell, I. and Neilson, G. W. (1996). Li^+ hydration in concentrated aqueous solution. **Journal of Physics: Condensed Matter**. 8: 4455.
- Ibuki, K. and Bopp, P. A. (2009). Molecular dynamics simulations of aqueous LiCl solutions at room temperature through the entire concentration range. **Journal of Molecular Liquids**. 147: 56-63.
- Ikeda, T., Boero, M. and Terakura, K. (2007). Hydration of alkali ions from first principles molecular dynamics revisited. **The Journal of Chemical Physics**. 126: 034501-034509.
- Impey, R. W., Madden, P. A. and McDonald, I. R. (1983). Hydration and mobility of ions in solution. **The Journal of Physical Chemistry**. 87: 5071-5083.
- Kameda, Y., Sugawara, K., Usuki, T. and Uemura, O. (1998). Hydration structure of Na^+ in concentrated aqueous solutions. **Bulletin of the Chemical Society of Japan**. 71: 2769-2776.

- Kerdcharoen, T., Liedl, K. R. and Rode, B. M. (1996). A QM/MM simulation method applied to the solution of Li^+ in liquid ammonia. **Chemical Physics**. 211: 313-323.
- Kerdcharoen, T. and Morokuma, K. (2002). ONIOM-XS: An extension of the ONIOM method for molecular simulation in condensed phase. **Chemical Physics Letters**. 355: 257-262.
- Kerdcharoen, T. and Morokuma, K. (2003). Combined quantum mechanics and molecular mechanics simulation of Ca^{2+} /ammonia solution based on the ONIOM-XS method: Octahedral coordination and implication to biology. **The Journal of Chemical Physics**. 118: 8856-8862.
- Kim, H. S. (2001). Solvent effect on K^+ to Na^+ ion mutation: A Monte Carlo simulation study. **Journal of Molecular Structure: THEOCHEM**. 540: 79-89.
- Koneshan, S., Rasaiah, J. C., Lynden-Bell, R. M. and Lee, S. H. (1998). Solvent structure, dynamics, and ion mobility in aqueous solutions at 25 °C. **The Journal of Physical Chemistry B**. 102: 4193-4204.
- Kulik, H. J., Marzari, N., Correa, A. A., Prendergast, D., Schwegler, E. and Galli, G. (2010). Local effects in the X-ray absorption spectrum of salt water. **The Journal of Physical Chemistry B**. 114: 9594-9601.
- Lamoureux, G. and Roux, B. (2006). Absolute hydration free energy scale for alkali and halide ions established from simulations with a polarizable force field. **The Journal of Physical Chemistry B**. 110: 3308-3322.
- Lee, H. M., Tarakeshwar, P., Park, J., Kołaski, M. R., Yoon, Y. J., Yi, H.-B., Kim, W. Y., Kim, K. S. (2004). Insights into the structures, energetics, and vibrations of

- monovalent cation-(water)₁₋₆ clusters. **The Journal of Physical Chemistry A**. 108: 2949-2958.
- Lee, S. H. and Rasaiah, J. C. (1994). Molecular dynamics simulation of ionic mobility. I. Alkali metal cations in water at 25 °C. **The Journal of Chemical Physics**. 101: 6964.
- Lee, S. H. and Rasaiah, J. C. (1996). Molecular dynamics simulation of ion mobility. 2. Alkali metal and halide ions using the SPC/E model for water at 25 °C. **The Journal of Physical Chemistry**. 100: 1420-1425.
- Licheri, G., Piccaluga, G. and Pinna, G. (1975). X-ray diffraction study of LiBr aqueous solutions. **Chemical Physics Letters**. 35: 119-123.
- Loeffler, H. H. (2003). Many-body effects on structure and dynamics of aqueous ionic solutions. **Journal of Computational Chemistry**. 24: 1232-1239.
- Loeffler, H. H., Inada, Y. and Funahashi, S. (2006). Water exchange dynamics of lithium(I) ion in aqueous solution. **The Journal of Physical Chemistry B**. 110: 5690-5696.
- Loeffler, H. H., Mohammed, A. M., Inada, Y. and Funahashi, S. (2003). Lithium(I) ion hydration: A QM/MM-MD study. **Chemical Physics Letters**. 379: 452-457.
- Loeffler, H. H. and Rode, B. M. (2002). The hydration structure of the lithium ion. **The Journal of Chemical Physics**. 117: 110-117.
- Lyubartsev, A. P., Laasonen, K. and Laaksonen, A. (2001). Hydration of Li⁺ ion. An *ab initio* molecular dynamics simulation. **The Journal of Chemical Physics**. 114: 3120-3126.

- Mancinelli, R., Botti, A., Bruni, F., Ricci, M. A. and Soper, A. K. (2007). Perturbation of water structure due to monovalent ions in solution. **Physical Chemistry Chemical Physics**. 9: 2959-2967.
- Marcus, Y. (1988). Ionic radii in aqueous solutions. **Chemical Reviews**. 88: 1475-1498.
- Marcus, Y. (2009). Effect of ions on the structure of water: Structure making and breaking. **Chemical Reviews**. 109: 1346-1370.
- Megyes, T., Balint, S., Grosz, T., Radnai, T., Bako, I. and Sipos, P. (2008). The structure of aqueous sodium hydroxide solutions: A combined solution x-ray diffraction and simulation study. **The Journal of Chemical Physics**. 128: 044501-044512.
- Michaelian, K. H. and Moskovits, M. (1978). Tetrahedral hydration of ions in solution. **Nature**. 273: 135-136.
- Misra, V. K. and Draper, D. E. (1999). The interpretation of Mg^{2+} binding isotherms for nucleic acids using poisson-boltzmann theory. **Journal of Molecular Biology**. 294: 1135-1147.
- Møller, K. B., Rey, R., Masia, M. and Hynes, J. T. (2005). On the coupling between molecular diffusion and solvation shell exchange. **The Journal of Chemical Physics**. 122: 114508.
- Neilson, G. W. and Skipper, N. (1985). K^+ coordination in aqueous solution. **Chemical Physics Letters**. 114: 35-38.
- Newsome, J. R., Neilson, G. W. and Enderby, J. E. (1980). Lithium ions in aqueous solution. **Journal of Physics C: Solid State Physics**. 13: L923.

- Novikov, A. G., Rodnikova, M. N., Savostin, V. V. and Sobolev, O. V. (1999). The study of hydration effects in aqueous solutions of LiCl and CsCl by inelastic neutron scattering. **Journal of Molecular Liquids**. 82: 83-104.
- Obst, S. and Bradaczek, H. (1996). Molecular dynamics study of the structure and dynamics of the hydration shell of alkaline and alkaline-earth metal cations. **The Journal of Physical Chemistry**. 100: 15677-15687.
- Öhrn, A. and Karlström, G. (2004). A combined quantum chemical statistical mechanical simulation of the hydration of Li^+ , Na^+ , F^- , and Cl^- . **The Journal of Physical Chemistry B**. 108: 8452-8459.
- Ohtaki, H. and Radnai, T. (1993). Structure and dynamics of hydrated ions. **Chemical Reviews**. 93: 1157-1204.
- Ohtomo, N. and Arakawa, K. (1979). Neutron diffraction study of aqueous ionic solutions. I. Aqueous solutions of lithium chloride and caesium chloride. **Bulletin of the Chemical Society of Japan**. 52: 2755-2759.
- Ohtomo, N. and Arakawa, K. (1980). Neutron diffraction study of aqueous ionic solutions. II. Aqueous solutions of sodium chloride and potassium chloride. **Bulletin of the Chemical Society of Japan**. 53: 1789-1794.
- Petit, L., Vuilleumier, R., Maldivi, P. and Adamo, C. (2008). *Ab initio* molecular dynamics study of a highly concentrated LiCl aqueous solution. **Journal of Chemical Theory and Computation**. 4: 1040-1048.
- Phiel, C. J., Wilson, C. A., Lee, V. M.-Y. and Klein, P. S. (2003). Lithium inhibits amyloid production. **Nature**. 423: 435-439.
- Pye, C. C., Rudolph, W. and Poirier, R. A. (1996). An *ab initio* investigation of lithium ion hydration. **The Journal of Physical Chemistry**. 100: 601-605.

- Ramaniah, L. M., Bernasconi, M. and Parrinello, M. (1999). *Ab initio* molecular-dynamics simulation of K^+ solvation in water. **The Journal of Chemical Physics**. 111: 1587-1591.
- Rasaiah, J. C., Noworyta, J. P. and Koneshan, S. (2000). Structure of aqueous solutions of ions and neutral solutes at infinite dilution at a supercritical temperature of 683 K. **Journal of the American Chemical Society**. 122: 11182-11193.
- Rempe, S. B., Asthagiri, D. and Pratt, L. R. (2004). Inner shell definition and absolute hydration free energy of $K^+(aq)$ on the basis of quasi-chemical theory and *ab initio* molecular dynamics. **Physical Chemistry Chemical Physics**. 6: 1966-1969.
- Rempe, S. B., Pratt, L. R., Hummer, G., Kress, J. D., Martin, R. L. and Redondo, A. (2000). The hydration number of Li^+ in liquid water. **Journal of the American Chemical Society**. 122: 966-967.
- Rode, B. M., Schwenk, C. F. and Tongraar, A. (2004). Structure and dynamics of hydrated ions-new insights through quantum mechanical simulations. **Journal of Molecular Liquids**. 110: 105-122.
- Rodgers, M. T. and Armentrout, P. B. (1997). Collision-induced dissociation measurements on $Li^+(H_2O)_n$, $n = 1-6$: The first direct measurement of the Li^+-OH_2 bond energy. **The Journal of Physical Chemistry A**. 101: 1238-1249.
- Rudolph, W., Brooker, M. H. and Pye, C. C. (1995). Hydration of lithium ion in aqueous solutions. **The Journal of Physical Chemistry**. 99: 3793-3797.

- Singh, U. C. and Kollman, P. A. (1986). A combined *ab initio* quantum mechanical and molecular mechanical method for carrying out simulations on complex molecular systems: Applications to the $\text{CH}_3\text{Cl} + \text{Cl}^-$ exchange reaction and gas phase protonation of polyethers. **Journal of Computational Chemistry**. 7: 718-730.
- Skipper, N. T. and Neilson, G. W. (1989). X-ray and neutron diffraction studies on concentrated aqueous solutions of sodium nitrate and silver nitrate. **Journal of Physics: Condensed Matter**. 1: 4141.
- Smirnov, P. R. and Trostin, V. N. (2006). Structure of the nearest surrounding of the Li^+ ion in aqueous solutions of its salts. **Russian Journal of General Chemistry**. 76: 175-182.
- Smirnov, P. R. and Trostin, V. N. (2007). Structures of the nearest surroundings of the K^+ , Rb^+ , and Cs^+ ions in aqueous solutions of their salts. **Russian Journal of General Chemistry**. 77: 2101-2107.
- Spangberg, D. and Hermansson, K. (2004). Many-body potentials for aqueous Li^+ , Na^+ , Mg^{2+} , and Al^{3+} : Comparison of effective three-body potentials and polarizable models. **The Journal of Chemical Physics**. 120: 4829-4843.
- Spangberg, D., Rey, R., Hynes, J. T. and Hermansson, K. (2003). Rate and mechanisms for water exchange around $\text{Li}^+(\text{aq})$ from MD simulations. **The Journal of Physical Chemistry B**. 107: 4470-4477.
- Sripa, P., Tongraar, A. and Kerdcharoen, T. (2013). "Structure-Making" ability of Na^+ in dilute aqueous solution: An ONIOM-XS MD simulation study. **The Journal of Physical Chemistry A**. 117: 1826-1833.

- Svensson, M., Humbel, S., Froese, R. D. J., Matsubara, T., Sieber, S. and Morokuma, K. (1996). ONIOM: A multilayered integrated MO + MM method for geometry optimizations and single point energy predictions. A test for Diels–Alder reactions and $\text{Pt}(\text{P}(\text{t-Bu})_3)_2 + \text{H}_2$ oxidative addition. **The Journal of Physical Chemistry**. 100: 19357-19363.
- Tanaka, M. and Aida, M. (2004). An *ab initio* MO study on orbital interaction and charge distribution in alkali metal aqueous solution: Li^+ , Na^+ , and K^+ . **Journal of Solution Chemistry**. 33: 887-901.
- Thaomola, S., Tongraar, A. and Kerdcharoen, T. (2012). Insights into the structure and dynamics of liquid water: A comparative study of conventional QM/MM and ONIOM-XS MD simulations. **Journal of Molecular Liquids**. 174: 26-33.
- Tongraar, A., Liedl, K. R. and Rode, B. M. (1998a). Born–Oppenheimer *ab initio* QM/MM dynamics simulations of Na^+ and K^+ in water: From structure making to structure breaking effects. **The Journal of Physical Chemistry A**. 102: 10340-10347.
- Tongraar, A., Liedl, K. R. and Rode, B. M. (1998b). The hydration shell structure of Li^+ investigated by Born–Oppenheimer *ab initio* QM/MM dynamics. **Chemical Physics Letters**. 286: 56-64.
- Tongraar, A. and Rode, B. M. (2004). Dynamical properties of water molecules in the hydration shells of Na^+ and K^+ : *Ab initio* QM/MM molecular dynamics simulations. **Chemical Physics Letters**. 385: 378-383.
- Tongraar, A., T-Thienprasert, J., Rujirawat, S. and Limpijumnong, S. (2010). Structure of the hydrated Ca^{2+} and Cl^- : Combined X-ray absorption

- measurements and QM/MM MD simulations study. **Physical Chemistry Chemical Physics**. 12: 10876-10887.
- Wanprakhon, S., Tongraar, A. and Kerdcharoen, T. (2011). Hydration structure and dynamics of K^+ and Ca^{2+} in aqueous solution: Comparison of conventional QM/MM and ONIOM-XS MD simulations. **Chemical Physics Letters**. 517: 171-175.
- Warshel, A. and Levitt, M. (1976). Theoretical studies of enzymic reactions: Dielectric, electrostatic and steric stabilization of the carbonium ion in the reaction of lysozyme. **Journal of Molecular Biology**. 103: 227-249.
- White, J. A., Schwegler, E., Galli, G. and Gygi, F. (2000). The solvation of Na^+ in water: First-principles simulations. **The Journal of Chemical Physics**. 113: 4668-4673.
- Yamanaka, K., Yamagami, M., Takamuku, T., Yamaguchi, T. and Wakita, H. (1993). X-ray diffraction study on aqueous lithium chloride solution in the temperature range 138-373 K. **The Journal of Physical Chemistry**. 97: 10835-10839.
- Zhou, J., Lu, X., Wang, Y. and Shi, J. (2002). Molecular dynamics study on ionic hydration. **Fluid Phase Equilibria**. 194-197: 257-270.

CHAPTER II

QUANTUM CHEMISTRY

2.1 Introduction to quantum chemistry

Quantum mechanics are commonly used for studying fundamental behavior of matter at the molecular scale, *i.e.*, through the understanding of electron behaviors. In this respect, the energy and some properties of a molecule can be derived from wavefunction, which can be obtained by solving the *Schrödinger equation* (Schrödinger, 1926). Consequently, many chemical problems can be solved by applying quantum chemistry, especially for the understanding of chemical bonding, spectral phenomena, molecular reactivity and various other fundamental chemical problems.

2.2 Schrödinger equation

The principle of quantum mechanics starts with the Schrödinger equation, describing the atom system. Schrödinger has obtained an equation by taking the time-independent wavefunction equation, which can be written as

$$\hat{H}\Psi = E\Psi, \quad (2.1)$$

where \hat{H} is the *Hamiltonian operator*, which corresponds to the kinetic energy, \hat{T} , and potential energy, \hat{V} , of the system. The *Hamiltonian operator* is usually shown in

atomic units.

$$\hat{H} = \hat{T} + \hat{V}, \quad (2.2)$$

where

$$\hat{T} = -\frac{\hbar^2}{2m} \nabla^2, \quad (2.3)$$

and thus,

$$\hat{H} = -\frac{\hbar^2}{2m} \nabla^2 + \hat{V}, \quad (2.4)$$

where ∇^2 is the *Laplacian operator*, which can be defined as

$$\nabla^2 = \frac{\partial^2}{\partial x^2} + \frac{\partial^2}{\partial y^2} + \frac{\partial^2}{\partial z^2}. \quad (2.5)$$

In general, many-electron Schrödinger equation cannot be solved exactly, even for a simple two electron system such as helium atom or hydrogen molecule. With regard to this point, some approximations have been introduced to provide practical use of this method.

2.3 The variation method

Since the Schrödinger equation for a many-body system cannot be solved exactly, one strategy in the QM calculations is to guess a suitable form of ψ , and then

optimize by using the variation principle. Regarding the variation principle, a trial wavefunction, Φ , is a function of the appropriate electronic and nuclear coordinates to be operated upon by the Hamiltonian. Once a set of the normal wavefunctions, ψ_i , is completely defined, the function Φ can be written in terms of a linear combination of the ψ_i ,

$$\Phi = \sum_i c_i \psi_i, \quad (2.6)$$

where the individual ψ_i and coefficients c_i are unknown. Then, the normality of Φ imposes a constraint on the coefficients, deriving from

$$\begin{aligned} \int \Phi^2 dr = 1 &= \int \sum_i c_i \psi_i \sum_j c_j \psi_j dr \\ &= \sum_{ij} c_i c_j \int \psi_i \psi_j dr \\ &= \sum_{ij} c_i c_j \delta_{ij} \\ &= \sum_i c_i^2. \end{aligned} \quad (2.7)$$

Then, the energy associated with wavefunction (Φ) can be considered as

$$\begin{aligned} \int \Phi H \Phi dr &= \int (\sum_i c_i \psi_i) H (\sum_j c_j \psi_j) dr \\ &= \sum_{ij} c_i c_j \int \psi_i H \psi_j dr \end{aligned}$$

$$\begin{aligned}
&= \sum_{ij} c_i c_j E_j \delta_{ij} \\
&= \sum_i c_i^2 E_i.
\end{aligned} \tag{2.8}$$

After that, combining the results from equation (2.7) and (2.8) as

$$\int \Phi H \Phi dr - E_0 \int \Phi^2 dr = \sum_i c_i^2 (E_i - E_0). \tag{2.9}$$

In general, the coefficients are assumed to be real numbers, thus, c_i^2 and the result of $(E_i - E_0)$ must be greater than or equal to zero. Therefore,

$$\int \Phi H \Phi dr - E_0 \int \Phi^2 dr \geq 0 \tag{2.10}$$

or

$$\frac{\int \Phi H \Phi dr}{\int \Phi^2 dr} \geq E_0. \tag{2.11}$$

According to equation (2.11), the quality of wavefunctions for describing the ground state of a system can be achieved by their associated energies according to the statement that the better wavefunction will give the lower energy. In general, the guess of the trial wavefunction can be constructed in any manner, which determined the quality by the integral in equation (2.11).

2.4 Born-Oppenheimer approximation

For N particle system, the *Hamiltonian operator* (\hat{H}) takes into account five contributions to the total energy of a system, namely the kinetic energies of the electrons (\hat{T}_e) and nuclei (\hat{T}_n), the attraction of the electrons to the nuclei (\hat{V}_{en}), and the inter-electronic (\hat{V}_{ee}) and inter-nuclear (\hat{V}_{nn}) repulsions, as shown in equations (2.12) and (2.13),

$$\hat{H} = \hat{T}_e + \hat{T}_n + \hat{V}_{en} + \hat{V}_{ee} + \hat{V}_{nn}, \quad (2.12)$$

$$\hat{H} = -\sum_{i=1}^N \frac{1}{2} \nabla_i^2 - \sum_{A=1}^M \frac{1}{2M_A} \nabla_A^2 - \sum_{i=1}^N \sum_{A=1}^M \frac{Z_A}{r_{ij}} + \sum_{i=1}^N \sum_{j>i}^N \frac{1}{r_{ij}} + \sum_{A=1}^M \sum_{B>A}^M \frac{Z_A Z_B}{R_{AB}}, \quad (2.13)$$

where i and j represent electrons, A and B represent nuclei, M is the mass of nucleus, Z is the atomic number, r and R are the distances between particles.

The “*Born-Oppenheimer approximation*” (Born and Oppenheimer, 1927) can further be used to simplify the Schrödinger equation. Hence, the equation can be separated into electronic and nuclear terms. Since the nuclei are much heavier than electrons, *i.e.*, they move much more slowly, one can consider the electrons in a molecule to move with respect to the field of fixed nuclei (Szabo and Ostlund, 1989). By this approximation, the kinetic energy of the nuclei can be neglected and the last term in equation (2.13), the repulsion of nuclei, can be considered as a constant. The remaining terms in equation (2.13) are called the electronic Hamiltonian or Hamiltonian describing the motion of N electrons in the field of M point charges,

$$\hat{H}_{elec} = -\sum_{i=1}^N \frac{1}{2} \nabla_i^2 - \sum_{i=1}^N \sum_{A=1}^M \frac{Z_A}{r_{ij}} + \sum_{i=1}^N \sum_{j>i}^N \frac{1}{r_{ij}} + \sum_{A=1}^M \sum_{B>A}^M \frac{Z_A Z_B}{R_{AB}}. \quad (2.14)$$

2.5 Molecular orbital theory

The molecular orbital theory is applied for determining molecular structure. A molecular orbital is a region in which an electron can be found in a molecule. In general, the molecular orbital can be described by wavefunction of the electron in a molecule, in particular a spatial distribution ($|\psi_i(r)|^2$) of an electron and energy of up to two electrons within it. A complete wavefunction for an electron consists of a molecular orbital and a spin function (α and β), which can be defined as a *spin orbital* ($\chi(x)$), where x indicates both space and spin coordinates. Therefore, a spatial orbital can be formed into two different spin orbitals as

$$\chi(x) = \begin{cases} \psi(r)\alpha(\omega) \\ \psi(r)\beta(\omega). \end{cases} \quad (2.15)$$

For N -electron wavefunction, the Hamiltonian of a simple system, which contains non-interacting electrons, can be defined as

$$H = \sum_{i=1}^N h(i), \quad (2.16)$$

where $h(i)$ is the operator that describes the kinetic and potential energies of electron i .

Then, a set of spin orbitals ($\chi_j(x)$) will be added to the operator;

$$h(i)\chi_j(x_i) = \varepsilon_j \chi_j(x_i). \quad (2.17)$$

Here, the wavefunction is a simple product of spin orbital wavefunction for each electron,

$$\Psi^{HP}(x_1, x_2, \dots, x_N) = \chi_i(x_1)\chi_j(x_2) \cdots \chi_k(x_N). \quad (2.18)$$

The above equation can be written as

$$H\Psi^{HP} = E\Psi^{HP}, \quad (2.19)$$

where E is the sum of the spin orbital energies of each spin orbitals in Ψ^{HP} ,

$$E = \varepsilon_i + \varepsilon_j + \cdots + \varepsilon_k. \quad (2.20)$$

The wavefunction of the form in equation (2.18) is called a *Hartree product*, in which the electron-one can be described by the spin orbital χ_i , electron-two can be described by the spin orbital χ_j , etc. However, this wavefunction does not allow the antisymmetry principle.

With regard to the antisymmetry principle, the electron-one is put in χ_i and electron-two in χ_j as

$$\Psi_{12}^{HP}(x_1, x_2) = \chi_i(x_1)\chi_j(x_2). \quad (2.21)$$

In the opposite way, putting electron-one in χ_j and electron-two in χ_i gives

$$\Psi_{21}^{HP}(x_1, x_2) = \chi_i(x_2)\chi_j(x_1). \quad (2.22)$$

Then, the appropriate linear combination of these two Hartree products can be written as

$$\Psi(x_1, x_2) = 2^{-1/2}(\chi_i(x_1)\chi_j(x_2) - \chi_i(x_2)\chi_j(x_1)), \quad (2.23)$$

where the factor $2^{-1/2}$ is a normalization factor and the minus sign insures that $\Psi(x_1, x_2)$ is antisymmetric with respect to the interchange of the coordinates of electrons one and two. From equation (2.23), the wavefunction will be disappeared if both electrons occupy the same spin orbital, *i.e.*, according to the *Pauli exclusion principle*. The antisymmetric wavefunction can be rewritten in terms of a determinant,

$$\Psi(x_1, x_2) = 2^{-1/2} \begin{vmatrix} \chi_i(x_1) & \chi_j(x_1) \\ \chi_i(x_2) & \chi_j(x_2) \end{vmatrix}, \quad (2.24)$$

which is called a *Slater determinant* (Slater, 1929). For an N -electron system, the generalization is

$$\Psi(x_1, x_2, \dots, x_N) = (N!)^{-1/2} \begin{vmatrix} \chi_i(x_1) & \chi_j(x_1) & \cdots & \chi_k(x_1) \\ \chi_i(x_2) & \chi_j(x_2) & \cdots & \chi_k(x_2) \\ \vdots & \vdots & \ddots & \vdots \\ \chi_i(x_N) & \chi_j(x_N) & \cdots & \chi_k(x_N) \end{vmatrix}, \quad (2.25)$$

where $(N!)^{-1/2}$ is the normalization factor.

2.6 The LCAO-MO approach and basis sets

The molecular orbitals can be built from the atomic orbitals according to a so-called *linear combination of atomic orbitals to molecular orbitals* (LCAO-MO) method. The formula can be expressed as

$$\psi_i = \sum_{\mu=1}^N C_{\mu i} \phi_{\mu}, \quad (2.26)$$

where $C_{\mu i}$ are the molecular orbital expansion coefficients, ϕ_{μ} is known as *basis set* and N is the number of atomic basis function.

The common types of basis function, or called *atomic orbital*, used in the electronic structure calculations are *Slater type orbitals* (STOs) (Slater, 1930) and *Gaussian type orbitals* (GTOs) (Boys, 1950).

The formalism of the STOs can be presented as

$$\psi(n, l, m_l; r, \theta, \phi) = N r^{n_{\text{eff}} - 1} e^{-Z_{\text{eff}} \rho / n_{\text{eff}}} Y_{lm_l}(\theta, \phi), \quad (2.27)$$

where n , l , and m_l are the quantum numbers referring to principal, angular momentum and magnetic, respectively, N is the normalization constant and Y_{lm_l} is a spherical harmonic. The STOs screening constants are calculated for small model molecules using rigorous self-consistent field methods, and then being generated for use with actual molecules of interest. Z_{eff} is the effective nuclear charge, while the effective principal quantum number (n_{eff}) is related to the true principal quantum (n) by the mapping of

$$n \rightarrow n_{eff} : 1 \rightarrow 1.2 \rightarrow 2.3 \rightarrow 3.4 \rightarrow 3.7 \rightarrow 4.0 \rightarrow 4.2,$$

in which the value of ρ equal r/a_0 , where a_0 is *Bohr radius*.

The STOs are usually applied for atomic and diatomic system. However, the STOs do not satisfy in the case of two-electron integral problem. With regard to this point, the feasible basis function is *Gaussian type orbitals* (GTOs), which are function of the form

$$\theta_{ijk}(r_1 - r_c) = (x_1 - x_c)^i (y_1 - y_c)^j (z_1 - z_c)^k e^{-\alpha|r_1 - r_c|^2}, \quad (2.28)$$

where (x_c, y_c, z_c) are the Cartesian coordinates of the center of the Gaussian function at r_c , (x_1, y_1, z_1) are the Cartesian coordinates of an electron at r_1 , i, j and k are non-negative integers and α is a positive exponent. The advantage of GTOs is that the product of two Gaussians at different centers is equivalent to a single Gaussian function centered at a point between the two centers. Therefore, the two-electron

integral problem on three and four or more different atomic centers can be reduced to integrals over two different centers. However, it is known that the GTO gives an inferior representation of the orbitals at the atomic nuclei. Considering for 1s-orbital (cf. Figure 2.1), the STO type has a *cusp* at the atomic nucleus while a GTO does not. In this respect, the larger basis must be used to achieve the accuracy comparable to that obtained from STOs.

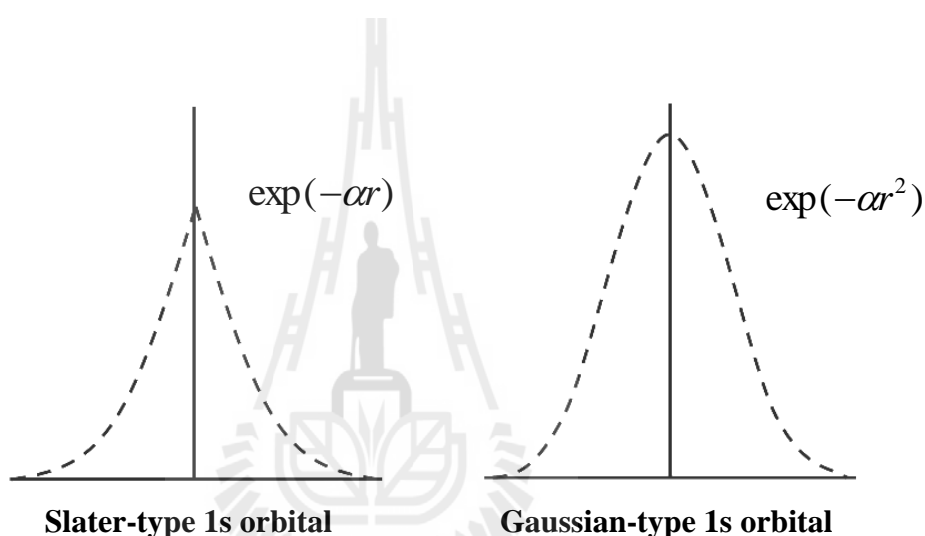


Figure 2.1 The Slater-type and Gaussian-type for 1s orbital.

To create a molecular orbital, a set of parameters applied to the basis function, called as *basis set*, is required. In general, the smallest number of function possible for constructing the molecular orbital is called a *minimum basis set*. The improvement of the basis set can be made by replacing two basis functions into each basis function in the minimal basis set, called as *double zeta (DZ)*. The larger basis set is a *triple zeta (TZ)*, where three basis functions are used to represent each of the minimal basis sets. The compromise between the DZ and TZ basis sets is a *split valence (SV)* basis set, in

which each valence atomic orbital is represented by two basis functions while each core orbital is represented by a single basis function.

Since 1969, Pople and coworkers (Hehre, Stewart, and Pople, 1969) have designed the basis set by expanding the STO in terms of n primitive Gaussians, called as STO- n G basis set. The primitive Gaussian has been derived for $n = 2-6$. However, the STO-3G basis set is a widely used minimal basis set. In Figure 2.2, the STO-3G basis set partially represents the *cusp* of s-type orbital at the atomic nuclei.

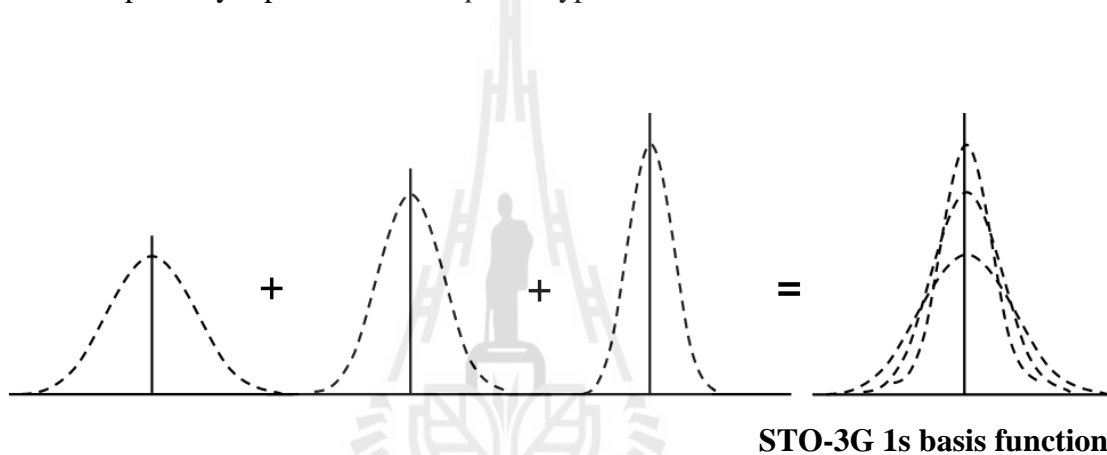


Figure 2.2 The STO-3G basis set representing the desired STO.

Pople and coworkers have also applied the split valence for having flexibility in the basis set, designed as $k-nlm$ G basis set. The first parameter (k) indicates the number of primitives used in the contracted core, while the two values (nl) refer to a split valence, and three values (nlm) refer to a triple split valence, such as 6-311G. For the triple split valence basis, the core orbitals are a contraction of six primitives and the valence split into three functions, represented by three, one and one primitive GTOs. The Pople's style basis sets may include diffuse and/or polarization functions. The diffuse function can be denoted as + or ++ before the G. In this respect, the first +

indicates one set of diffuse s- and p-function adding on heavy atoms and the second + refers to the inclusion of diffuse s-function for hydrogen atom. The polarization function can be put after the G, which separates designation for heavy and hydrogen atoms. For example, 6-31+G(d) basis set refers to a split valence with additional diffuse sp-functions and a single d-type polarization function only on heavy atoms. The largest standard Pople style basis set is 6-311++G(3df,3pd). Alternatively, the polarization function can be replaced with * notation, for example, the 6-311G* basis set is identical to 6-311G(d) and 6-311G** basis set is identical to 6-311G(d,p).

Since several GTOs are often grouped together, the *contracted Gaussian function* has been applied to *Dunning-Huzinaga* (DZ) basis set (Dunning, 1970; Dunning, 1971; Huzinaga, 1965). The DZ basis set can be made by a contraction such as the (9s5p) primitive GTO to [4s,2p]. The contraction scheme is 6,1,1,1 for s-functions and 4,1 for the p-functions. The development of basis set by Dunning and coworker for recovering the correlation energy of the valence electrons is known as the *correlation consistent* (cc) basis sets. The general formulation can be written as cc-pVnZ, where $n = D$ for double zeta, T for triple zeta, Q for quadruple zeta, 5 for quintuple zeta or 6 for sextuple zeta.

For the treatment of systems involving a large number of core electrons, these require a number of basis functions. However, since the deep core electrons are not much important in a chemical reaction, leading to an approximation by replacing the core electrons with analytical functions, called as an *Effective core potential* (ECP) (Collins, Schleyer, Binkley and Pople, 1976) or *Pseudopotentials* (Aqvist and Warshel, 1993). In several cases, such basis set is reasonably accurate and efficient, representing the combined nuclear-electronic core to the remaining electrons.

2.7 Basis Set Superposition Error (BSSE)

In the calculations of molecular energies using atomic basis sets, especially for weak interactions, an error occurs due to the use of basis functions on adjacent molecules (Davidson and Chakravorty, 1994). The results are regarded as “*Basis Set Superposition Error* (BSSE)” (Boys and Bernardi, 1970). The BSSE causes overestimation of the attractive contribution to the interaction energy and consequently provides an illegitimate increase of binding energy in a molecule. As a consequence, this may lead to less accurate results regarding to molecular geometry optimization and molecular charge distribution. The BSSE can be calculated with the help of *ghost* atoms. In this respect, the amount of BSSE can be estimated using *Counterpoise Procedure* (CP) (Boys and Bernardi, 1970). The counterpoise correction is the energy lowering of single monomer in the presence of *ghost* basis functions located at the position of the atomic centers of that monomer, but without additional nuclear charges or electrons. The correction for BSSE in the molecular calculations with medium and small basis sets can result in values of interaction energies which are fairly close to those obtained by using more expensive and large basis sets. However, it should be realized that the counterpoise method will not provide effective improvement of the results if the atomic basis sets are very poor. The counterpoise procedure has been used as a standard tool of theoretical chemistry although some researchers have raised serious doubts on the usefulness of this procedure (Schwenke and Truhlar, 1986; Schwenke and Truhlar, 1987). The counterpoise correction can be very reasonable for the estimation of weak electronic interaction energies with small basis sets at Hartree-Fock level of accuracy. However, this approach has failed for the

estimation of strong electronic interaction energies even if with up to date basis sets, as demonstrated by a study of cyclic hydrogen fluoride trimer (Liedl, 1998).

2.8 Hartree-Fock method

By solving the Schrödinger equation, some approximations are mandatory. According to the variation method, the form of wavefunction is guessed, called the trial wavefunction. For N -electron system, a trial wavefunction can be written as

$$\Psi = \chi_1(1)\chi_2(2)\dots\chi_N(N), \quad (2.29)$$

where $\chi_i(i)$ is the spin orbitals of the i -th electron, and then the trial wavefunction can be expressed in the form of Slater determinant to ensure the antisymmetry upon the interchange of electron coordinates,

$$\Psi = \frac{1}{\sqrt{N!}} \begin{vmatrix} \chi_1(1) & \chi_2(1) & \cdots & \chi_N(1) \\ \chi_1(2) & \chi_2(2) & \cdots & \chi_N(2) \\ \vdots & \vdots & \ddots & \vdots \\ \chi_1(N) & \chi_2(N) & \cdots & \chi_N(N) \end{vmatrix}, \quad (2.30)$$

The spin orbital χ_i is the product of a spatial function or molecular orbital, ψ_i , and a spin function, α or β called as spin up and spin down, respectively. The electronic spin is quantized by $\pm 1/2$; $+1/2$ spin defines α -electron and $-1/2$ spin defines β -spin.

The spin orbital can be written as

$$\chi_i = \psi_i(x_i, y_i, z_i)\alpha(\sigma_i), \quad (2.31)$$

or

$$\chi_i = \psi_i(x_i, y_i, z_i)\beta(\sigma_i). \quad (2.32)$$

The set of spin orbital must have orthonormal properties which defined by

$$\int \chi_i^* \chi_j d\tau = \delta_{ij} \begin{cases} 0 & i \neq j \\ 1 & i = j. \end{cases} \quad (2.33)$$

According to the variation method, the best sets of spin orbital correspond to the one that give the lowest expectation value of energy. Consequently, the appropriate sets of spin orbital can be solved from the HF equation,

$$\hat{F}_i(1)\psi_i(1) = \varepsilon_i\psi_i(1). \quad (2.34)$$

In this respect, the solution of HF equation are set of eigenvalue, $\{\varepsilon_i\}$, and eigenfunction, $\{\psi_i(1)\}$, which corresponds to the lowest energy. By means of the HF method, the Hamiltonian operator considers that each electron individually move in the average field of all other electrons in the molecule. This is the basis of the self-consistent field (SCF) procedure. For closed-shell systems (all electrons spin-paired, two per occupied orbital), the formalism is well known as restricted Hartree-Fock

(RHF). The Hamiltonian operator for one-electron is called Fock operator, \hat{F} , which can be defined for each electron j as

$$\hat{F}(1) = \hat{H}^{core}(1) + \sum_{j=1}^{N/2} (2\hat{J}_j(1) - \hat{K}_j(1)), \quad (2.35)$$

where $\hat{H}^{core}(1)$ is the core Hamiltonian operator,

$$\hat{H}^{core}(1) = -\frac{1}{2}\nabla_1^2 - \sum_{A=1}^{N/2} \frac{Z_A}{r_{1A}}, \quad (2.36)$$

where \hat{J}_j is Coulomb operator representing the classical repulsion between two electron distributions (*i.e.*, interaction potential of electron j with all of the other electrons), which can be defined as

$$\hat{J}_j(1)\chi_i(1) = \left[\int d\tau_2 \chi_j(2) \frac{1}{r_{12}} \chi_j(2) \right] \chi_i(1), \quad (2.37)$$

and \hat{K}_j is exchange operator representing the exchange function according to the fact that the two electrons exchange their positions corresponds to Pauli's principle. The exchange of electrons in two-spin orbitals can be defined as

$$\hat{K}_j(1)\chi_i(1) = \left[\int d\tau_2 \chi_j(2) \frac{1}{r_{12}} \chi_i(2) \right] \chi_j(1). \quad (2.38)$$

The total energy of the system can be obtained from the summation of energy of each electron,

$$\sum_i^{n/2} \varepsilon_i = \sum_i^{n/2} \langle \chi_i(1) | \hat{F}(1) | \chi_i(1) \rangle. \quad (2.39)$$

In general, the HF wavefunction is not complicate, *i.e.*, when applies for atom. However, it becomes more complicate for molecule since there is more than one center. As a consequence, Roothaan-Hall equation has been proposed to write the one-electron molecular wavefunction in terms of atomic wavefunction or basis functions based on the concept of the LCAOs, as shown in equation (2.26). Then, the HF equation can be written as

$$\hat{F}_i(1) \sum_{\nu=1}^N c_{\nu} \phi_{\nu} = \varepsilon_i \sum_{\nu=1}^N c_{\nu} \phi_{\nu}. \quad (2.40)$$

The above equation can be solved easily by converting it into a matrix problem, *i.e.*, multiply on the left hand side by an integration term,

$$\sum_{\nu=1}^N c_{\nu} \int \phi_{\mu}(1) \hat{F}_i \phi_{\nu}(1) d\nu_1 = \varepsilon_i \sum_{\nu=1}^N c_{\nu} \int \phi_{\mu}(1) \phi_{\nu}(1) d\nu_1, \quad (2.41)$$

and then

$$\sum_{\nu=1}^N \hat{F}_{\mu\nu} c_{\nu i} = \varepsilon_i \sum_{\nu=1}^N S_{\mu\nu} c_{\nu i}, \quad (2.42)$$

or

$$\sum_{\nu=1}^N (\hat{F}_{\mu\nu} - \varepsilon_i S_{\mu\nu}) c_{\nu i} = 0, \quad \mu = 1, 2, 3, \dots, N. \quad (2.43)$$

The above equation is called the Roothaan-Hall equation, where $S_{\mu\nu}$ is the overlap matrix,

$$S_{\mu\nu} = \int dv_1 \phi_{\mu}(1) \phi_{\nu}(1). \quad (2.44)$$

The expression for each element $\hat{F}_{\mu\nu}$ of Fock matrix elements for a closed-shell system of N electrons becomes

$$\hat{F}_{\mu\nu} = \hat{H}_{\mu\nu}^{core} + \sum_{\lambda=1}^N \sum_{\sigma=1}^N P_{\lambda\sigma} \left[\langle \mu\nu | \lambda\sigma \rangle - \frac{1}{2} \langle \mu\lambda | \nu\sigma \rangle \right], \quad (2.45)$$

where $\hat{H}_{\mu\nu}^{core}$ is a one electron integral that can be written as

$$\hat{H}_{\mu\nu}^{core} = \int dv_1 \phi_{\mu}(1) H^{core}(1) \phi_{\nu}(1), \quad (2.46)$$

in which

$$\hat{H}^{core}(1) = -\frac{1}{2}\nabla^2 - \sum_{A=1}^M \frac{Z_A}{|r_1 - R_A|}. \quad (2.47)$$

Here, Z_A is the atomic number of atom A . $P_{\sigma\lambda}$ is the density matrix,

$$P_{\sigma\lambda} = 2 \sum_i^{N/2} c_{\lambda i} c_{\sigma i}. \quad (2.48)$$

According to Eq. (2.45), $\langle \mu\nu | \lambda\sigma \rangle$ refers to coulomb integral (two electron repulsion integral) and $\langle \mu\lambda | \nu\sigma \rangle$ represents exchange integral. Then, the total energy of a molecule can be expressed as

$$E_{molecule} = E_{elec} + E_{nuc}, \quad (2.49)$$

where E_{elec} and E_{nuc} are electronic energies of the system and nuclear repulsion, respectively,

$$E_{elec} = \frac{1}{2} \sum_{\mu=1}^N \sum_{\nu=1}^N P_{\mu\nu} (F_{\mu\nu} + H_{\mu\nu}^{core}), \quad (2.50)$$

and

$$E_{nuc} = \sum_{A=1}^N \sum_{B=1}^N \frac{Z_A Z_B}{R_{AB}}. \quad (2.51)$$

2.9 Electron correlation

It is known that motions of electrons are correlated and they tend to repel each electron to give a lower energy. According to the HF method, each electron moves in the static electric field created by all of the other electrons in the system. On the other hand, the electron cannot see other electrons during the HF calculations. Thus, the significant deficiency of the HF method is that it fails to adequately treat the correlation between motions of electrons. The effects of electron correlation are usually neglected in the Hamiltonian in the previous section. This leads to limitation of the HF energy calculations. The difference between HF and exact (non-relativistic) energies is the correlation energy,

$$E_{exact} = E_{HF} + E_{correlation}. \quad (2.52)$$

In several cases, the neglect of electron correlation effects can lead to some anomaly of qualitative information. As a consequence, the Ψ and E cannot be used to correctly predict atomic properties without accounting for electron correlation.

The electron correlation methods calculate the coefficient in front of the other determinants in different way, such as *configuration interaction* (CI) (Sherrill and Schaefer Iii, 1999), *many-body perturbation* (MP) (Møller and Plesset, 1934), *coupled cluster* (CC) (Bartlett, 1989) and *density function theory* (DFT).

2.10 References

- Aqvist, J. and Warshel, A. (1993). Simulation of enzyme reactions using valence bond force fields and other hybrid quantum/classical approaches. **Chemical Reviews**. 93: 2523-2544.
- Bartlett, R. J. (1989). Coupled-cluster approach to molecular structure and spectra: A step toward predictive quantum chemistry. **The Journal of Physical Chemistry**. 93: 1697-1708.
- Born, M. and Oppenheimer, J. R. (1927). On the quantum theory of molecule. **Annalen der Physik**. 84: 457.
- Boys, S. F. (1950). Electronic wavefunctions. I. A general method of calculation for the stationary states of any molecular system. **Proceedings of the Royal Society of London. Series A. Mathematical and Physical Sciences**. 200: 542-554.
- Boys, S. F. and Bernardi, F. (1970). The calculation of small molecular interactions by the differences of separate total energies. Some procedures with reduced errors. **Molecular Physics**. 19: 553-566.
- Collins, J. B., Schleyer, P. v. R., Binkley, J. S. and Pople, J. A. (1976). Self-consistent molecular orbital methods. XVII. Geometries and binding energies of second-row molecules. A comparison of three basis sets. **The Journal of Chemical Physics**. 64: 5142-5151.
- Davidson, E. R. and Chakravorty, S. J. (1994). A possible definition of basis set superposition error. **Chemical Physics Letters**. 217: 48-54.

- Dunning, T. H. J. (1970). Gaussian basis functions for use in molecular calculations. I. Contraction of (9s5p) atomic basis sets for the first-row atoms. **The Journal of Chemical Physics**. 53: 2823-2833.
- Dunning, T. H. J. (1971). Gaussian basis functions for use in molecular calculations. III. Contraction of (10s6p) atomic basis sets for the first-row atoms. **The Journal of Chemical Physics**. 55: 716-723.
- Hehre, W. J., Stewart, R. F. and Pople, J. A. (1969). Self-consistent molecular-orbital methods. I. Use of gaussian expansions of slater-type atomic orbitals. **The Journal of Chemical Physics**. 51: 2657-2664.
- Huzinaga, S. (1965). Gaussian-type functions for polyatomic systems. I. **The Journal of Chemical Physics**. 42: 1293-1302.
- Liedl, K. R. (1998). Dangers of counterpoise corrected hypersurfaces. Advantages of basis set superposition improvement. **The Journal of Chemical Physics**. 108: 3199-3204.
- Møller, C. and Plesset, M. S. (1934). Note on an approximation treatment for many-electron systems. **Physical Review**. 46: 618-622.
- Schrödinger, E. (1926). Quantisierung als eigenwertproblem. **Annalen der Physik**. 385: 437-490.
- Sherrill, C. D. and Schaefer Iii, H. F. (1999). The configuration interaction method: Advances in highly correlated approaches. **Advances in Quantum Chemistry**. 34: 143-269.
- Slater, J. C. (1929). The theory of complex spectra. **Physical Review**. 34: 1293-1322.
- Slater, J. C. (1930). Atomic shielding constants. **Physical Review**. 36: 57-64.

Szabo, A. and Ostlund, N. S. (1989). **Modern quantum chemistry: Introduction to advanced electronic structure theory**. New York: McGraw-Hill.



CHAPTER III

MOLECULAR DYNAMICS SIMULATIONS

3.1 Introduction to molecular dynamics (MD) simulations

In terms of computer simulations, Monte Carlo (MC) and molecular dynamics (MD) are two well-known techniques for studying molecular systems. For the treatment of condensed-phase systems, MD technique is more preferential than MC since it can provide not only the structural data, but also the dynamics details, *e.g.*, providing the information related to time dependent behaviors of the system under investigations.

By the MD technique, the simulation starts with reading in the starting configurations, velocities, accelerations and forces. The starting configuration can be obtained either from a random configuration or a lattice. Each particle in the system will be moved with respect to force from neighboring particles. According to Newton's Equation of motion, $F = ma$, the trajectories cannot be directly obtained from this equation. In this respect, the time integration algorithms will be used to obtain time-dependent trajectories, *i.e.*, a new set of coordinates, velocities and forces will be predicted and corrected. The energy of the system can be obtained from molecular mechanics (MM) or quantum mechanics (QM) calculations. The force of each atom can be obtained from the derivative of the energy with respect to the change in the atom's position. Each particle will be moved by their new force to the new configurations. This process will be repeated until the system reaches its

equilibrium. Once the system reaches its equilibrium, the coordinates, velocities, accelerations, forces and so on of all particles will be collected for further analysis with respect to the structure and dynamics details. The scheme of MD simulation is shown in Figure 3.1.



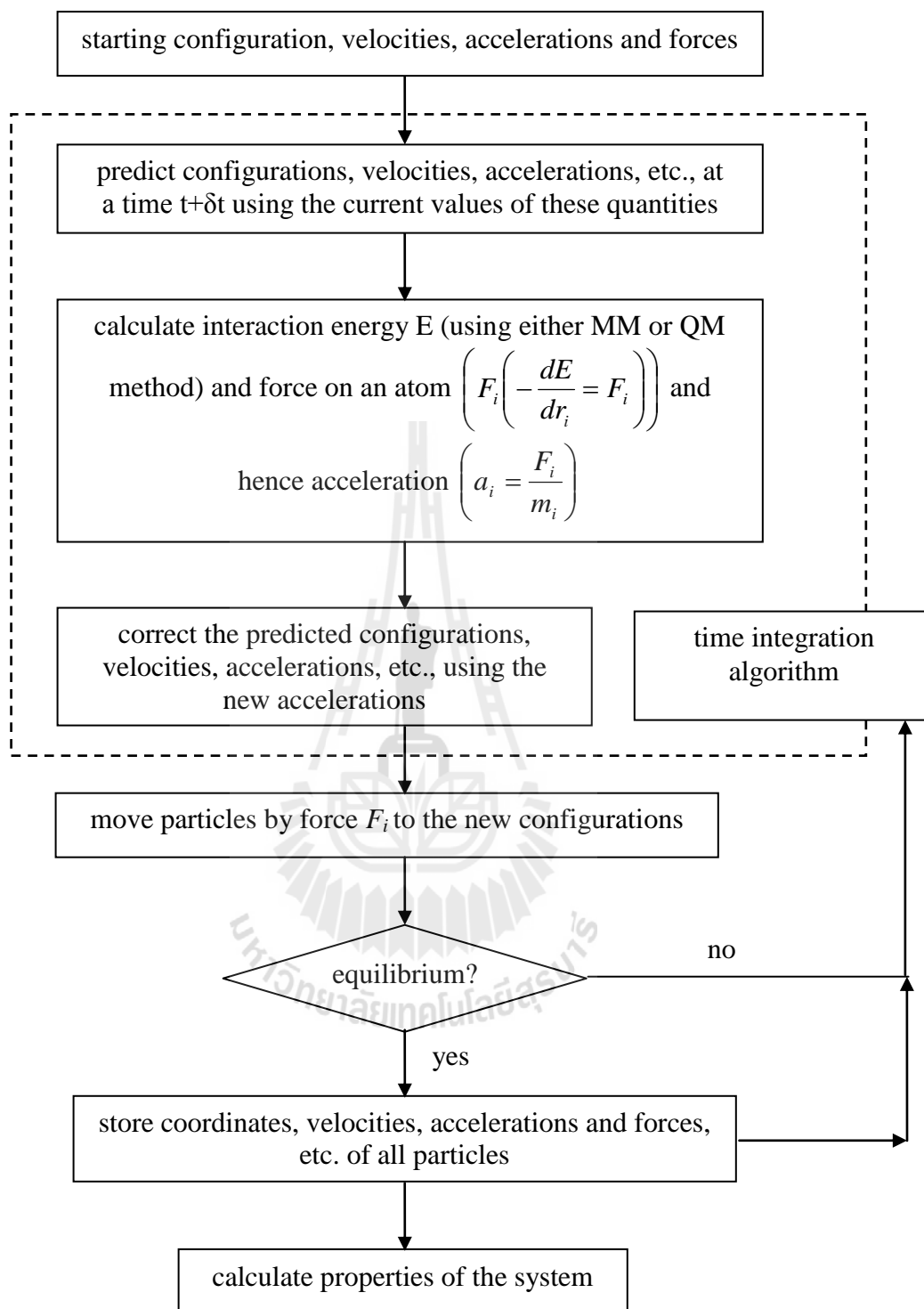


Figure 3.1 The scheme of molecular dynamics simulation.

3.2 Intermolecular potentials

According to the MM-based MD simulations, the interactions of particles in the system are usually described by means of intermolecular potentials. The potential energy function is the total intermolecular interaction energy comprising all of the pair, three-body, four-body up to N-body interactions,

$$V_{total} = \sum V(i, j) + \sum V(i, j, k) + \dots + \sum V(i, j, k, \dots, N). \quad (3.1)$$

However, most of earlier simulation works had neglected the higher order interactions (three, four, ..., N-body), *i.e.*, they are assumed to converge rather slowly and the terms tend to have alternating signs (Kistenmacher, Popkie and Clementi, 1974). Hence, only the pair interaction has been used to describe the intermolecular interaction of the system, known as pairwise additive approximation. The pair potential functions can be constructed from experimental data. However, a popular way is to construct them with respect to *ab initio* calculations.

3.3 Many-body interactions

In several cases, the pairwise additive approximations may not adequate, *i.e.*, the contributions of many-body interactions are significant and these terms must be taken into account in order to achieve sufficient agreement with experimental binding enthalpies. The influence of many-body interactions is defined by the difference of the *ab initio* interactions and the interactions that calculated on the basis of pairwise additive approximations. To estimate the influence of many-body contributions, for

example, in the case of $M(H_2O)_n^+$ complex, the *ab initio* interaction energy of the complex can be computed using supermolecular approach as,

$$\Delta E_{ab} = E(M(H_2O)_n^+) - E(M^+) - nE(H_2O), \quad (3.2)$$

and the pair interaction energy can be obtained from

$$\begin{aligned} \Delta E_{pair} = & \sum_i^n [E(M^+ - H_2O^i) - E(M^+) - E(H_2O)] \\ & + \sum_{j>i}^n [E(H_2O^i - H_2O^j) - 2E(H_2O)] \end{aligned} \quad (3.3)$$

In this respect, the interaction energy difference ΔE_{diff} , and the percentage of them with respect to pair potential, $\% E$, can be calculated by

$$\Delta E_{diff} = \Delta E_{ab} - \Delta E_{pair}, \quad (3.4)$$

and

$$\% E = \frac{\Delta E_{diff}}{abs(\Delta E_{pair})} \times 100. \quad (3.5)$$

3.4 Time interaction algorithms

The MD technique solves the Newton's equation of motion for atom by taking small step in time and using approximate numerical methods to predict all its future positions and velocity. A collection of position is known as a trajectory. The approximate numerical method employed by one time step is known as an integration algorithm. All the integration algorithms assume that the positions, velocities and accelerations can be expressed by a *Taylor series expansion*,

$$r(t + \delta t) = r(t) + v(t)\delta t + \frac{1}{2} a(t)\delta t^2 + \frac{1}{6} b(t)\delta t^3 + \frac{1}{24} c(t)\delta t^4 + \dots \quad (3.6)$$

$$v(t + \delta t) = v(t) + a(t)\delta t + \frac{1}{2} b(t)\delta t^2 + \frac{1}{6} c(t)\delta t^3 + \dots \quad (3.7)$$

$$a(t + \delta t) = a(t) + b(t)\delta t + \frac{1}{2} c(t)\delta t^2 + \dots \quad (3.8)$$

$$b(t + \delta t) = b(t) + c(t)\delta t + \dots, \quad (3.9)$$

where r is the position, v is the velocity (the first derivative of the position with respect to time), a is the acceleration (the second derivative), b is the third derivative, and so on.

Many integration algorithms have been developed for integrating the equations of motion. Two popular integration algorithms are the *Verlet algorithm* (Verlet, 1967) and the *Predictor-corrector algorithm* (Gear, 1971).

3.4.1 Verlet algorithm

The Verlet algorithm uses the positions and accelerations at time t and positions from the previous step, $r(t - \delta t)$, to calculate the new position at $t + \delta t$. The following relationships between these quantities and the velocities at time t would be of the form

$$r(t + \delta t) = r(t) + v(t)\delta t + \frac{1}{2}a(t)\delta t^2 \quad (3.10)$$

$$r(t - \delta t) = r(t) - v(t)\delta t + \frac{1}{2}a(t)\delta t^2. \quad (3.11)$$

The summation of equations (3.10) and (3.11) yields

$$r(t + \delta t) = 2r(t) - r(t - \delta t) + a(t)\delta t^2 \quad (3.12)$$

Note that the velocities of the Verlet algorithm do not explicitly appear in the equations. In practice, the velocities can be calculated by dividing the difference in positions at time $t + \delta t$ and $t - \delta t$ by $2\delta t$ as

$$v(t) = [r(t + \delta t) - r(t - \delta t)] / 2\delta t. \quad (3.13)$$

In addition, the velocities can be obtained at the half-step ($t + \frac{1}{2}\delta t$) as

$$v(t + \frac{1}{2}\delta t) = [r(t + \delta t) - r(t)] / \delta t. \quad (3.14)$$

However, the deficiency of the Verlet algorithm is that the calculation of the velocities cannot be obtained unless the positions at the next step are known. Thus, it is not a self-starting algorithm. With regard to this point, some variants of the Verlet algorithm have been developed. For example, the *leap-frog* algorithm (Hockney, 1970), which uses the following expansions,

$$r(t + \delta t) = r(t) + v(t + \frac{1}{2} \delta t) \delta t, \quad (3.15)$$

$$v(t + \frac{1}{2} \delta t) = v(t - \frac{1}{2} \delta t) + a(t) \delta t. \quad (3.16)$$

By this scheme, the velocities $v(t + \frac{1}{2} \delta t)$ are firstly calculated from the velocities at time $(t - \frac{1}{2} \delta t)$, and the accelerations at time t . Then, the positions at time $t + \delta t$ are deduced from the velocities just calculated together with the positions at time t using equation (3.15). The velocities at time t can be calculated from

$$v(t) = \frac{1}{2} \left[v(t + \frac{1}{2} \delta t) + v(t - \frac{1}{2} \delta t) \right]. \quad (3.17)$$

The advantage of this algorithm is that the velocities are explicitly calculated. However, some disadvantages exist, such as they are not calculated at the same time as the positions.

An even better implementation of such algorithm is the *velocity Verlet* algorithm (Swope, Andersen, Berens and Wilson, 1982), which gives positions, velocities and accelerations at the same time,

$$r(t + \delta t) = r(t) + v(t)\delta t + \frac{1}{2}a(t)\delta t^2, \quad (3.18)$$

$$v(t + \delta t) = v(t) + \frac{1}{2}[a(t) + a(t + \delta t)]\delta t. \quad (3.19)$$

Another integration method is the Beeman's algorithm (Beeman, 1976), which is related to the Verlet method, and can be expressed as

$$r(t + \delta t) = r(t) + v(t)\delta t + \frac{2}{3}a(t)\delta t^2 - \frac{1}{6}a(t - \delta t)\delta t^2, \quad (3.20)$$

$$v(t + \delta t) = v(t) + \frac{1}{3}a(t)\delta t + \frac{5}{6}a(t)\delta t - \frac{1}{6}a(t - \delta t)\delta t. \quad (3.21)$$

The Beeman's algorithm uses a more accurate expression for the velocities and gives better energy conservation. However, the performance of this algorithm is more complicate, as well as more expensive.

3.4.2 Predictor-corrector algorithm

The predictor-corrector algorithm consists of three basic steps. First, the new positions, velocities, accelerations and higher-order terms are predicted according to the Taylor expansion, as shown in equations (3.6)-(3.9). Second, the forces are then evaluated at the new positions to give the accelerations, $a(t + \delta t)$. These accelerations are compared with the accelerations predicted from the Taylor

series expansion ($a^c(t + \delta t)$). The difference between the predicted and the calculated accelerations is used to correct the positions, velocities, etc., according to equations (3.22)-(3.26).

$$\Delta a(t + \delta t) = a^c(t + \delta t) - a^p(t + \delta t). \quad (3.22)$$

Then,

$$r^c(t + \delta t) = r^p(t + \delta t) + c_0 \Delta a(t + \delta t), \quad (3.23)$$

$$v^c(t + \delta t) = v^p(t + \delta t) + c_1 \Delta a(t + \delta t), \quad (3.24)$$

$$a^c(t + \delta t) = a^p(t + \delta t) + c_2 \Delta a(t + \delta t), \quad (3.25)$$

$$b^c(t + \delta t) = b^p(t + \delta t) + c_3 \Delta a(t + \delta t), \quad (3.26)$$

where the superscript p represents the predicted values, r and v stand for the complete set of positions and velocities, respectively, a represents the accelerations and b denotes all the third time derivatives of r .

3.5 Periodic boundary conditions

The boundary effects or surface effects are often found in the computer simulation using small system size. The interactions between particles and the wall reflect in wrong properties of bulk. This problem can be solved by using the periodic boundary (PB) conditions. By the PB conditions, the particles in the box are replicated in all directions to give a periodic array, which can be represented in Figure 3.2.

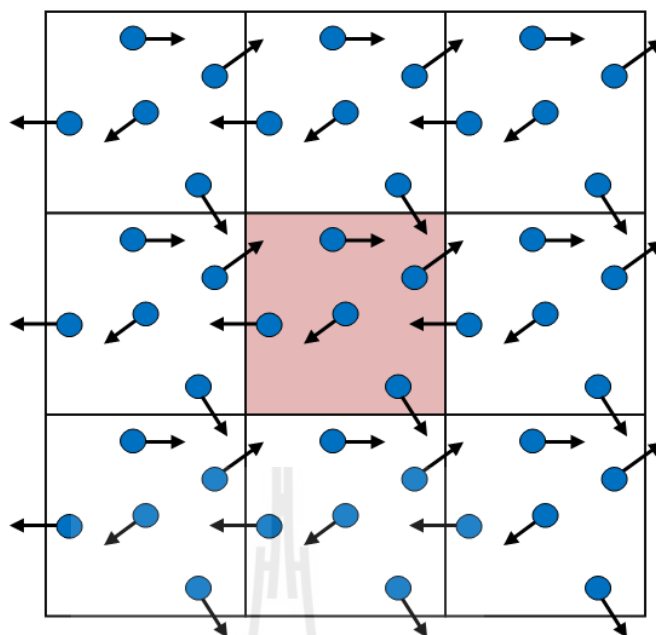


Figure 3.2 The periodic boundary conditions in two dimensions.

The concept of the periodic boundary conditions is that the coordinates of the particles in the image boxes can be computed by adding or subtracting integral multiples of the box sides. If a particle leaves the box during the simulation, it is replaced by an image particle that enters from the opposite side at the same time, as illustrated in Figure 3.2. By this scheme, the number of particles within the central box remains constant.

3.6 Cut-off and minimum image convention

In earlier MC and MD studies, *i.e.*, most of which relied on the MM-based models, one of the very time-consuming of the simulations is the calculation of the non-bond energies and forces. The simple way of reducing the expense is to use a cut-off and to apply the minimum image convention. The minimum image convention is a

common form of the PB condition, in which each atom interacts with only its neighboring atoms in the system. The energies and forces are computed with respect to the closest atom or image, as shown in Figure 3.3.

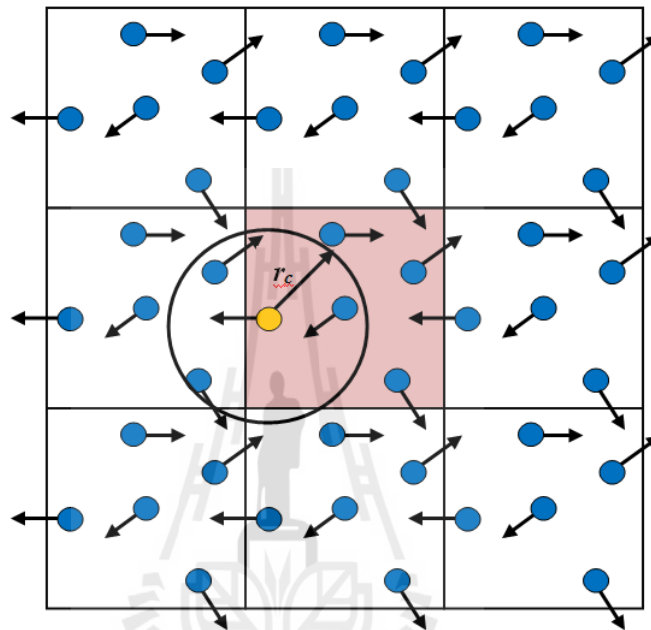


Figure 3.3 The spherical cut-off and the minimum image convention.

By using the cut-off, the interactions between all pairs of atoms that are further apart from the cut-off value are set to zero. In this regard, the cut-off distance should not be greater than half of the length of their image. However, the use of cut-off leads to a serious problem in the simulation, as can be seen in Figure 3.4

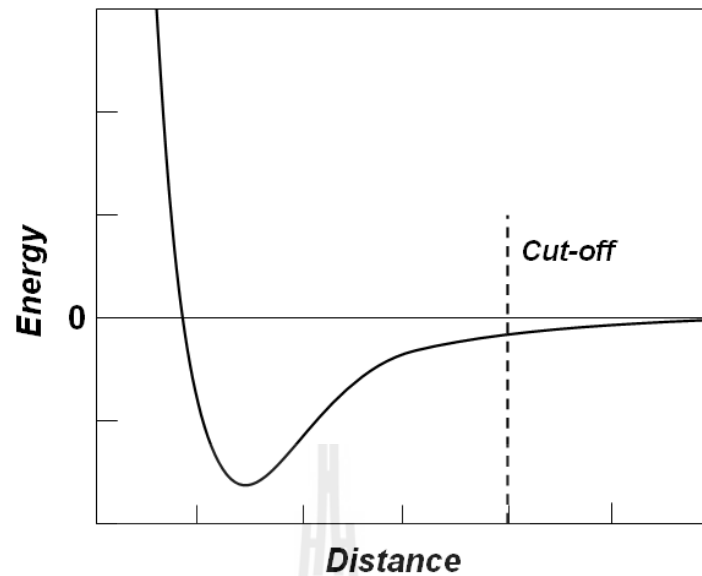


Figure 3.4 A discontinuity of cut-off.

According to the use of cut-off limit, this reflects in the discontinuity in both the potential energy and the force after the cut-off value, as depicted in Figure 3.4.

This problem can be solved by *shifted potential function* by an amount V_c ,

$$V'(r) = \begin{cases} V(r) - V_c & \text{if } r \leq r_c \\ 0 & \text{if } r > r_c \end{cases}, \quad (3.27)$$

where r_c is the cut-off distance and V_c corresponds to the value of the potential at the cut-off distance. In this respect, although the energy conservation can be improved by the shifted potential, the discontinuity in the force with the shifted potential still exists. At the cut-off distance, since the force will have a finite value, a suitable shifted potential would be of the form

$$V'(r) = \begin{cases} V(r) - V_c - \left(\frac{dV(r)}{dr} \right)_{r=r_c} (r - r_c) & \text{if } r \leq r_c \\ 0 & \text{if } r > r_c \end{cases} . \quad (3.28)$$

However, the application of shifted potential is not easy for inhomogeneous systems containing many different types of atom. An alternative way is to eliminate discontinuities in the energy and force by using a *switching function*. The switched potential ($V^{SF}(r)$) is related to the true potential ($V(r)$) as

$$V'(r) = V(r)S(r). \quad (3.29)$$

Some switching functions are applied to the entire range of the potential up to the cut-off point. In general, the switching function has a value of 1 at $r = 0$ and a value of 0 at $r = r_c$, while the switching function values between two cut-offs are varied. The example of a switching function applied to the Lennard-Jones potential is given in Figure 3.5.

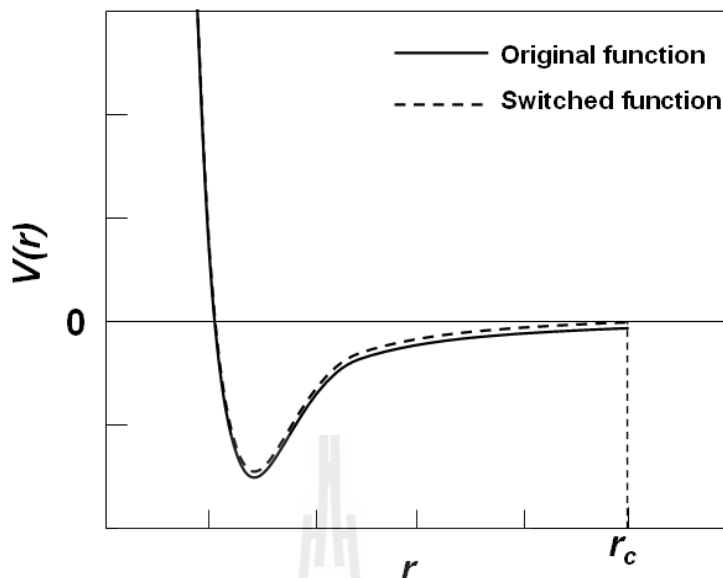


Figure 3.5 The effect of a switching function applied on the Lennard-Jones potential.

3.7 Non-bonded neighbor lists

In practice, the use of cut-off and minimum image convention is not actually reduces the time in the simulation since all the non-bonded distances must firstly be calculated and checked whether it is inside or outside the cut-off distance. A useful technique for solving this problem is to use the *non-bonded neighbor list*. The first non-bonded neighbor list has been proposed by Verlet (Verlet, 1967). As depicted in Figure 3.6, the Verlet neighbor list stores all atoms within the cut-off distance (the solid circle (r_c)) and atoms are slightly further away than the cut-off distance (the dashed circle (r_m)). The neighbor list will frequently be updated throughout the simulation. With regard to this point, the distance used to calculate each atom's neighbors should be slightly larger than the actual cut-off distance in order to ensure

that the atoms outside the cut-off will not move closer than the cut-off distance before the neighbor list is updated again.

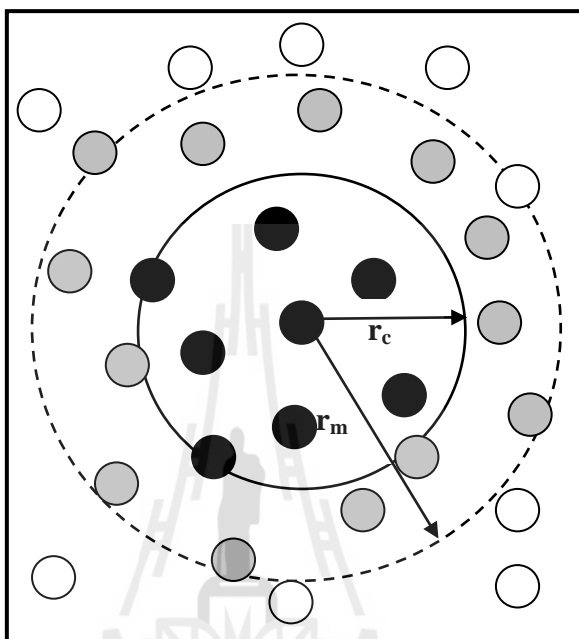


Figure 3.6 The non-bonded neighbor list.

3.8 Long-range interactions

Since the charge-charge interactions in range greater than half of the box length still has significance, the neglect of long-range interactions of cut-off may introduce serious errors in the simulation. There are two common methods used for the treatment of long-range forces. The first one is Ewald summation (Ewald, 1921), computing the interaction energy of ionic crystals by including the interaction of the particle with all the other of periodic systems. The potential energy of the Ewald summation can be expressed as

$$V = \frac{1}{2} \sum'_{|\mathbf{n}|=0} \sum_{i=1}^N \sum_{j=1}^N \frac{q_i q_j}{4\pi\epsilon_0 |r_{ij} + \mathbf{n}|}, \quad (3.30)$$

where the prime on the first summation indicates that the series does not include the interaction $i = j$ for $\mathbf{n} = 0$, q_i and q_j are charges and \mathbf{n} is a cubic lattice point. The Ewald summation method is the most correct way to accurately include all the effects of long-range forces in the computer simulation. However, this method is rather expensive to implement since the equation (3.30) converges extremely slowly. Another method for the treatment of long-range interactions is to apply the *reaction field method* (Foulkes and Haydock, 1989). This method constructs the sphere around the molecule with a radius equal to the cut-off distance. All interactions within the sphere are calculated explicitly, while those outside of the sphere are modeled as a homogeneous medium of dielectric constant (ϵ_s). The electrostatic field due to the surrounding dielectric is given by

$$E_i = \frac{2(\epsilon_s - 1)}{\epsilon_s + 1} \left(\frac{1}{r_c^3} \right) \sum_{j: r_{ij} \leq r_c} \mu_j, \quad (3.31)$$

where μ_j are the dipoles of the neighboring molecules that are located within the cut-off distance (r_c) of the molecules i . The interaction between molecule i and the reaction field equals to $E_i \cdot \mu_i$.

3.9 Research methodology

3.9.1 Conventional QM/MM MD technique

According to the conventional QM/MM MD scheme (B. M. Rode, Schwenk, Hofer and Randolph, 2005; Bernd M. Rode, Schwenk and Tongraar, 2004; Xenides, Randolph and Rode, 2005), the system is partitioned into two parts, namely QM and MM regions.

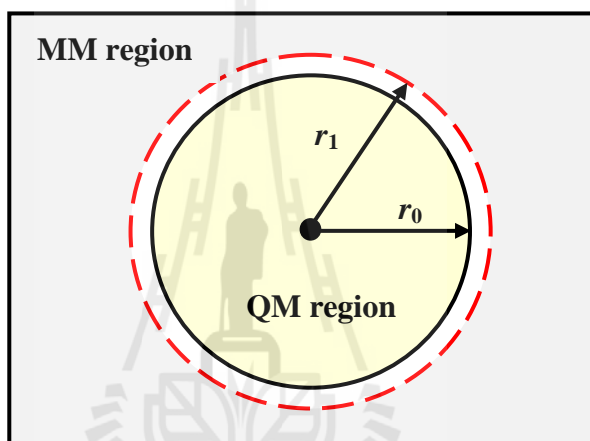


Figure 3.7 System's partition.

For example, for a system of aqueous solution containing an alkali metal ion, the QM region refers to a sphere which contains a central ion and its nearest-neighbor waters, which is treated by quantum mechanics, and the MM part corresponds to the bulk waters, which is described by MM force fields. The total interaction energy of the system is defined as

$$E_{total} = \langle \Psi_{QM} | \hat{H} | \Psi_{QM} \rangle + E_{MM} + E_{QM-MM} , \quad (3.32)$$

where $\langle \Psi_{QM} | \hat{H} | \Psi_{QM} \rangle$ denotes the interactions within the QM region, and E_{MM} and E_{QM-MM} represent the interactions within the MM and between the QM and MM regions, respectively. Note that the E_{MM} and E_{QM-MM} terms are described by classical MM force fields. The total force of the system is described by

$$F_{tot} = F_{MM}^{sys} + (F_{QM}^{QM} - F_{MM}^{QM}), \quad (3.33)$$

where F_{MM}^{sys} , F_{QM}^{QM} and F_{MM}^{QM} are the MM force of the total system, the QM force in the QM region and the MM force in the QM region, respectively. In this respect, the F_{MM}^{QM} term accounts for the coupling between the QM and MM regions. During the QM/MM simulations, forces acting on each particle in the system are switched according to which region the solvent molecule was entering or leaving the QM region and is defined as

$$F_i = S_m(r)F_{QM} + (1 - S_m(r))F_{MM}, \quad (3.34)$$

where F_{QM} and F_{MM} are the quantum mechanical and molecular mechanical forces, respectively. $S_m(r)$ is the smoothing function (Brooks, Bruccoleri, Olafson, States, Swaminathan and Karplus, 1983), described by

$$\begin{aligned}
S_m(r) &= 1, & \text{for } r \leq r_0, \\
S_m(r) &= \frac{(r_1^2 - r^2)^2 (r_1^2 + 2r^2 - 3r_0^2)}{(r_1^2 - r_0^2)^3}, & \text{for } r_0 < r \leq r_1, \\
S_m(r) &= 0, & \text{for } r > r_1,
\end{aligned} \tag{3.35}$$

where r_0 and r_1 are the distances characterizing the start and the end of the QM region, respectively, and applied within an interval of 0.2 Å to ensure a continuous change of forces at the transition between QM and MM regions.

3.9.2 QM/MM MD based on ONIOM-XS technique

A schematic diagram of the ONIOM-XS method (Kerdcharoen and Morokuma, 2002) is given in Figure 3.8. With regard to the ONIOM-XS MD technique, the system is divided into a high-level (QM) sphere, *i.e.* a sphere which contains the ion and its surrounding water molecules, and the “low-level” MM region, *i.e.* the bulk water. A thin switching shell located between the QM and MM subsystems is introduced in order to smooth the transition due to the solvent exchange.

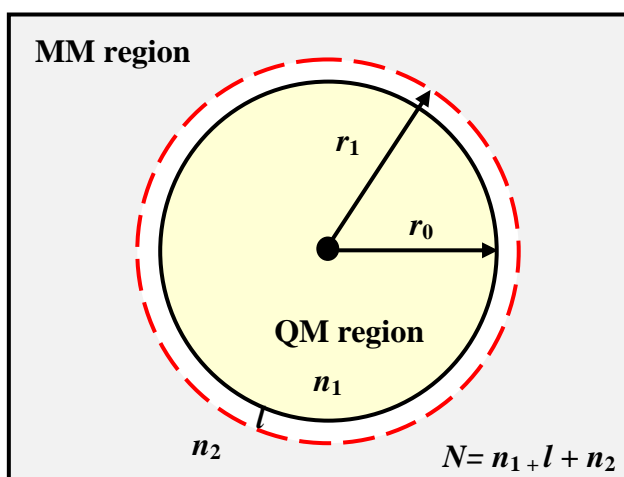


Figure 3.8 Schematic diagram of the ONIOM-XS method (Kerdcharoen and Morokuma, 2002).

Given n_1 , l and n_2 as number of particles in the QM region, the switching shell and the MM region, respectively, and $N = n_1 + l + n_2$ is the total number of particles, the potential energy term can be written by equations (3.36) and (3.37) based on the ONIOM extrapolation scheme (Svensson, Humbel, Froese, Matsubara, Sieber and Morokuma, 1996). If the switching layer is included into the high-level QM sphere, the energy expression is defined as

$$E^{\text{ONIOM}}(n_1 + l; N) = E^{\text{QM}}(n_1 + l) - E^{\text{MM}}(n_1 + l) + E^{\text{MM}}(N). \quad (3.36)$$

If the switching layer is considered as part of the “low-level” MM region, the energy expression can be written as

$$E^{\text{ONIOM}}(n_1; N) = E^{\text{QM}}(n_1) - E^{\text{MM}}(n_1) + E^{\text{MM}}(N). \quad (3.37)$$

Then, the potential energy of the entire system is taken as a hybrid between both energy terms (3.36) and (3.37),

$$E^{\text{ONIOM-XS}}(\{r_l\}) = (1 - \bar{s}(\{r_l\})) \cdot E^{\text{ONIOM}}(n_1 + l; N) + \bar{s}(\{r_l\}) \cdot E^{\text{ONIOM}}(n_1; N), \quad (3.38)$$

where $\bar{s}(\{r_l\})$ is an average over a set of switching functions for individual exchanging particle in the switching shell $s_i(x_i)$ (Tasaki, McDonald and Brady, 1993),

$$\bar{s}(\{r_l\}) = \frac{1}{l} \sum_{i=1}^l s_i(x_i). \quad (3.39)$$

The switching function $s_i(x_i)$ in equation (3.39) is written in a polynomial form as

$$s_i(x_i) = 6 \left(x_i - \frac{1}{2} \right)^5 - 5 \left(x_i - \frac{1}{2} \right)^3 + \frac{15}{8} \left(x_i - \frac{1}{2} \right) + \frac{1}{2}, \quad (3.40)$$

where $x_i = ((r_i - r_0)/(r_1 - r_0))$, and r_0 and r_1 are the radius of inner and outer surfaces of the switching shell, respectively, and r_i is the distance between the center of mass of the exchanging particle and the center of the QM sphere. Then, the gradient of the energy can be written as

$$\begin{aligned}
\nabla_R E^{ONIOM-XS}(\{r_l\}) &= (1 - \bar{s}(\{r_l\})) \cdot \nabla_R E^{ONIOM}(n_l + l; N) + \bar{s}(\{r_l\}) \\
&\cdot \nabla_R E^{ONIOM}(n_1; N) + \frac{1}{(r_1 - r_0)} \nabla \bar{s}(\{r_l\}) \\
&\cdot (E^{ONIOM}(n_1; N) - E^{ONIOM}(n_1 + l; N)).
\end{aligned} \tag{3.41}$$

3.10 Research procedures

3.10.1 Construction of pair potential functions

The pair potential functions for describing ion-water interactions were newly constructed. The 2354, 2424 and 2682 HF interaction energy points for various Li^+ - H_2O , Na^+ - H_2O and K^+ - H_2O configurations, respectively, obtained from Gaussian03 calculations (Frisch et al., 2005), using the DZP basis set (Dunning and Hay, 1977) for water and Li^+ and the LANL2DZ basis set (Check, Faust, Bailey, Wright, Gilbert and Sunderlin, 2001; Hay and Wadt, 1985) for Na^+ and K^+ , were fitted to the analytical forms of

$$\Delta E_{\text{Li}^+-\text{H}_2\text{O}} = \sum_{i=1}^3 \left(\frac{A_{ic}}{r_{ic}^4} + \frac{B_{ic}}{r_{ic}^5} + C_{ic} \exp(-D_{ic} r_{ic}) + \frac{q_i q_c}{r_{ic}} \right), \tag{3.42}$$

$$\Delta E_{\text{Na}^+-\text{H}_2\text{O}} = \sum_{i=1}^3 \left(\frac{A_{ic}}{r_{ic}^4} + \frac{B_{ic}}{r_{ic}^8} + C_{ic} \exp(-D_{ic} r_{ic}) + \frac{q_i q_c}{r_{ic}} \right), \tag{3.43}$$

$$\Delta E_{\text{K}^+-\text{H}_2\text{O}} = \sum_{i=1}^3 \left(\frac{A_{ic}}{r_{ic}^4} + \frac{B_{ic}}{r_{ic}^6} + C_{ic} \exp(-D_{ic} r_{ic}) + \frac{q_i q_c}{r_{ic}} \right), \tag{3.44}$$

where A , B , C and D are the fitting parameters (see Table 3.1), r_{ic} denotes the distances between the ion and the i -th atom of water, and q_i and q_c are the atomic net

charges. The charge values for all ions were set to 1.0 and for O and H of water were set to -0.6598 and 0.3299, respectively.

Table 3.1 Optimized parameters of the analytical pair potentials for the interaction of water with Li^+ , Na^+ and K^+ . (interaction energies in kcal mol^{-1} and distances in \AA)

	<i>A</i>	<i>B</i>	<i>C</i>	<i>D</i>
Li-O	-1050.70523	1157.41401	5931.628	2.9058482
Li-H	-69.95421	131.67480	15.710	0.7012464
Na-O	-663.20896	967.45544	28536.783	3.2925018
Na-H	148.86809	605.89247	-7143.015	3.5661953
K-O	-1808.22101	11173.26863	-36489.438	3.7078857
K-H	649.72461	-485.33410	-581.534	1.6453366

3.10.2 Effects of many-body interactions

The results of many-body effects in $\text{Li}^+(\text{H}_2\text{O})_n$, $\text{Na}^+(\text{H}_2\text{O})_n$, $\text{K}^+(\text{H}_2\text{O})_n$ complexes, where $n = 1, 2, 3, 4$ and 6 , as obtained from QM calculations at HF, CCSD, MP2, B3LYP levels of accuracy using DZP basis set for H_2O and Li^+ , and LANL2DZ basis set for Na^+ and K^+ are given in Tables 3.2-3.4.

Table 3.2 Optimized geometries and corresponding many-body effects for $\text{Li}^+(\text{H}_2\text{O})_n$ complexes, as obtained by various QM methods using DZP basis set. (distances, angles and energies are in Å, degree and kcal.mol^{-1} , respectively)

Method	n	$r_{\text{Li-O}}$	$r_{\text{O-H}}$	\angle_{HOH}	ΔE_{ab}	ΔE_{pair}	ΔE_{diff}	$\%E_{nbd}$
HF	1	1.87	0.9505	106.5	-37.2	-37.2	-	-
	2	1.89	0.9494	106.7	-70.1	-72.2	2.1	2.9
	3	1.92	0.9480	106.9	-95.7	-102.9	7.3	7.1
	4	1.97	0.9468	107.1	-113.9	-128.7	14.7	11.4
	6	2.17	0.9462	107.7	-130.6	-160.1	29.5	18.4
B3LYP	1	1.86	0.9714	105.8	-39.7	-39.7	-	-
	2	1.88	0.9702	106.0	-74.8	-77.4	2.6	3.4
	3	1.90	0.9688	105.6	-102.1	-111.7	9.6	8.6
	4	1.96	0.9679	106.3	-122.0	-141.6	19.7	13.9
	6	2.17	0.9710	107.8	-147.1	-184.0	36.9	20.0
MP2	1	1.88	0.9693	105.3	-37.8	-37.8	-	-
	2	1.90	0.9683	105.4	-71.8	-73.8	2.0	2.7
	3	1.93	0.9670	105.6	-99.0	-106.6	7.5	7.1
	4	1.97	0.9661	105.7	-119.5	-135.2	15.8	11.7
	6	2.16	0.9679	106.6	-146.2	-177.7	31.5	17.8
CCSD	1	1.88	0.9678	105.4	-37.5	-37.5	-	-
	2	1.90	0.9668	105.5	-71.1	-73.1	1.9	2.6
	3	1.92	0.9657	105.7	-98.2	-105.5	7.3	6.9
	4	1.97	0.9648	105.8	-118.5	-133.8	15.3	11.4
	6	2.15	0.9663	106.6	-147.5	-174.7	27.2	15.6

Table 3.3 Optimized geometries and corresponding many-body effects for $\text{Na}^+(\text{H}_2\text{O})_n$ complexes, as obtained by various QM methods using DZP basis set for H_2O and LANL2DZ basis set for Na^+ . (distances, angles and energies are in Å, degree and kcal.mol^{-1} , respectively)

Method	n	$r_{\text{Na-O}}$	$r_{\text{O-H}}$	\angle_{HOH}	ΔE_{ab}	ΔE_{pair}	ΔE_{diff}	$\%E_{\text{nbd}}$
HF	1	2.28	0.9486	105.9	-26.2	-26.2	-	-
	2	2.29	0.9648	106.1	-50.4	-51.1	0.8	1.5
	3	2.31	0.9473	106.3	-70.5	-73.8	3.2	4.4
	4	2.34	0.9466	106.5	-86.9	-93.8	6.9	7.4
	6	2.44	0.9450	106.7	-105.4	-122.5	17.1	14.0
B3LYP	1	2.27	0.9698	104.9	-26.8	-26.8	-	-
	2	2.28	0.9692	105.0	-51.7	-52.4	0.8	1.5
	3	2.30	0.9684	105.1	-72.3	-75.8	3.6	4.7
	4	2.33	0.9679	105.4	-89.3	-96.8	7.6	7.8
	6	2.42	0.9668	105.3	-110.1	-105.9	20.6	15.8
MP2	1	2.29	0.9675	104.5	-26.3	-26.3	-	-
	2	2.30	0.9670	104.6	-50.8	-51.5	0.7	1.4
	3	2.32	0.9664	104.8	-71.5	-74.7	3.2	4.3
	4	2.35	0.9658	104.9	-88.7	-95.8	7.1	7.4
	6	2.44	0.9648	104.9	-110.4	-128.7	18.4	14.3
CCSD	1	2.29	0.9661	104.6	-26.0	-26.0	-	-
	2	2.30	0.9657	104.7	-50.2	-50.9	0.7	1.4
	3	2.32	0.9651	104.9	-70.7	-73.8	3.1	4.3
	4	2.35	0.9646	105.1	-87.8	-94.6	6.9	7.3
	6	2.44	0.9637	105.0	-109.2	-127.0	17.8	14.0

Table 3.4 Optimized geometries and corresponding many-body effects for $K^+(H_2O)_n$ complexes, as obtained by various QM methods using DZP basis set for H_2O and LANL2DZ basis set for K^+ . (distances, angles and energies are in Å, degree and kcal.mol⁻¹, respectively)

Method	n	r_{K-O}	r_{O-H}	\angle_{HOH}	ΔE_{ab}	ΔE_{pair}	ΔE_{diff}	% E_{nbd}
HF	1	2.68	0.9477	105.5	-18.4	-18.4	-	-
	2	2.71	0.9475	105.6	-35.5	-35.9	0.5	1.3
	3	2.73	0.9469	105.8	-50.5	-52.0	1.5	2.8
	4	2.76	0.9464	106.0	-63.4	-66.4	2.9	4.4
	6	2.82	0.9454	106.6	-79.3	-90.1	10.8	12.0
B3LYP	1	2.65	0.9690	104.3	-19.4	-18.5	-	-
	2	2.67	0.9686	104.4	-37.5	-36.2	0.5	1.2
	3	2.69	0.9682	104.6	-53.5	-52.5	1.5	2.8
	4	2.71	0.9679	104.8	-67.7	-67.5	3.2	4.5
	6	2.78	0.9671	105.2	-88.7	-93.2	8.9	9.1
MP2	1	2.69	0.9667	103.8	-18.5	-18.5	-	-
	2	2.71	0.9664	103.9	-35.8	-36.2	0.4	1.1
	3	2.73	0.9661	104.1	-51.2	-52.5	1.3	2.6
	4	2.76	0.9657	104.2	-64.7	-67.5	2.8	4.1
	6	2.81	0.9650	104.7	-85.7	-93.2	7.5	8.1
CCSD	1	2.69	0.9655	104.0	-18.3	-18.3	-	-
	2	2.71	0.9653	104.1	-55.4	-35.8	0.5	1.3
	3	2.73	0.9650	104.2	-50.6	-51.9	1.5	2.8
	4	2.76	0.9646	104.4	-63.9	-66.7	2.9	4.4
	6	2.81	0.9640	104.8	-84.7	-92.0	7.3	8.0

As can be seen in Tables 3.2-3.4, it is apparent that the many-body effects are relevant to the strength of ion-ligand interactions, *i.e.*, the stronger ion-ligand interactions will produce larger amount of errors regarding the many-body interactions. The increase of number of ligands in the ion-ligand clusters results in an increase of many-body effects. In this study, the assumption of pairwise additive approximations leads to the errors of 18.4%, 14.0% and 12.0% for the $\text{Li}^+(\text{H}_2\text{O})_6$, $\text{Na}^+(\text{H}_2\text{O})_6$, and $\text{K}^+(\text{H}_2\text{O})_6$ complexes, respectively. From these values, it could be expected that the non-additive interactions are significant and are not negligible for studying the behaviors of the Li^+ , Na^+ and K^+ hydrates. These observations clearly confirm the need for more accurate simulation techniques, in particular the QM-based simulation approaches, for the treatment of such systems.

3.10.3 Selection of method and basis set

In this work, since the correlated QM calculations, even at the simple MP2-level, are still beyond our current computational feasibility, the HF method using the DZP basis set (Dunning and Hay, 1977) for water and Li^+ and LANL2DZ basis set (Boys and Bernardi, 1970; Check, Faust, Bailey, Wright, Gilbert and Sunderlin, 2001; Hay and Wadt, 1985) for Na^+ and K^+ have been employed in the present ONIOM-XS MD studies. The reliability of the HF method and the quality of the basis sets have been verified by comparing the HF results with those obtained by other QM methods, as shown in Figures 3.9 and 3.10. Comparing to the CCSD results, the HF method reveals an underestimation of the interaction energies, while an overestimation is observed in the B3LYP calculations. As can be seen in Figure 3.10, while the HF calculations show slight elongation of the ion-water distances, *i.e.*, compared to the

MP2 and CCSD data, the B3LYP method significantly predicts relatively short ion-water distances. With regard to the B3LYP results, it could be demonstrated that the implement of this method may lead to too rigidity of the ion-water complexes, as well as to the too slow dynamics properties of the ion hydrates.

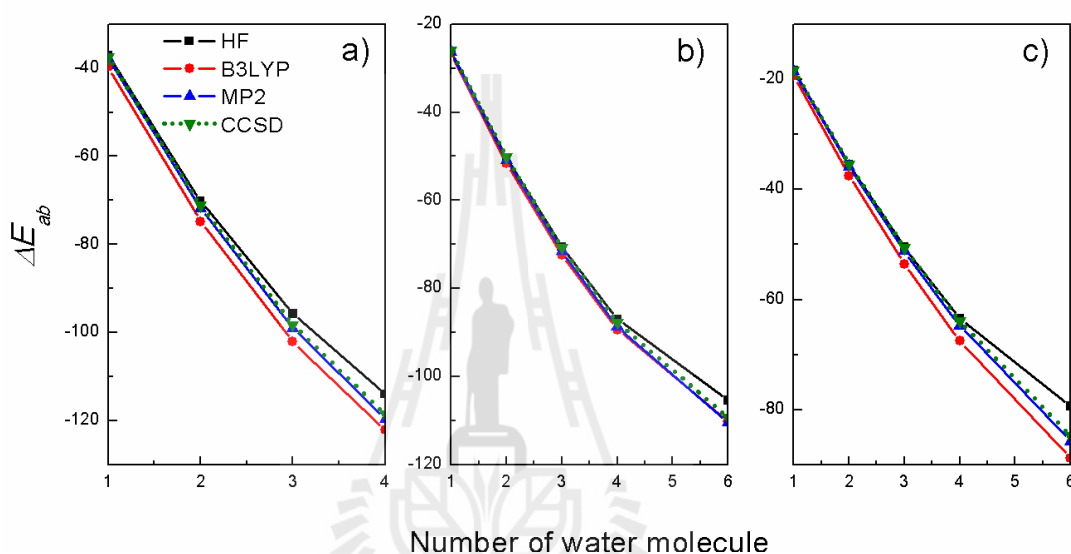


Figure 3.9 The *ab initio* interaction energies of a) $\text{Li}^+(\text{H}_2\text{O})_n$ complex, where $n = 1-4$, b) $\text{Na}^+(\text{H}_2\text{O})_n$ and c) $\text{K}^+(\text{H}_2\text{O})_n$ complexes, where $n = 1-6$, as obtained by various QM methods (HF, B3LYP, MP2 and CCSD) using DZP basis set for H_2O and Li^+ , and LANL2DZ basis set for Na^+ and K^+ , respectively. (energies are in $\text{kcal}\cdot\text{mol}^{-1}$)

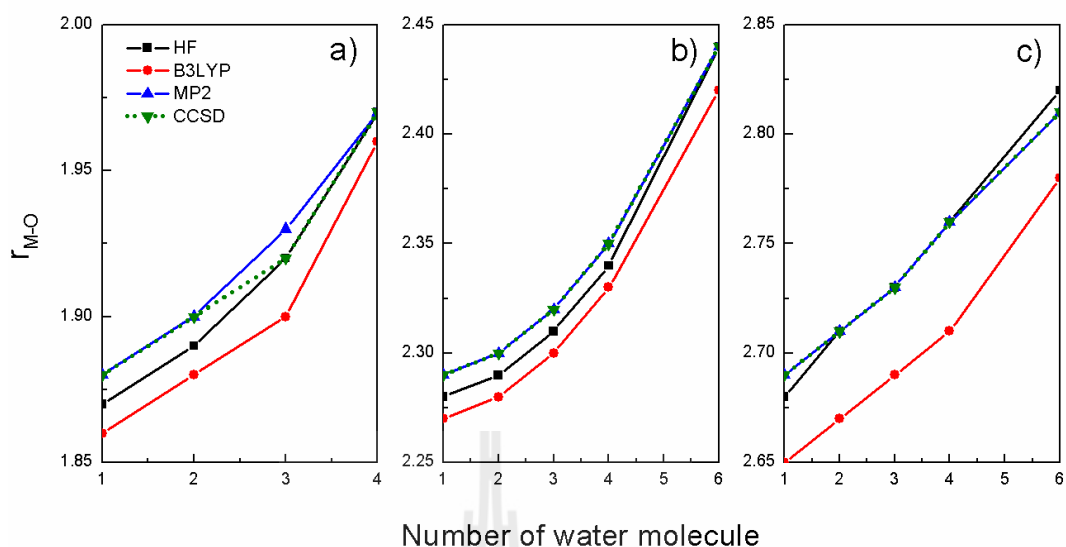


Figure 3.10 M-O distance of the optimized geometries of a) $\text{Li}^+(\text{H}_2\text{O})_n$ complex, where $n = 1-4$, b) $\text{Na}^+(\text{H}_2\text{O})_n$ and c) $\text{K}^+(\text{H}_2\text{O})_n$ complexes, where $n = 1-6$, as obtained by various QM methods (HF, B3LYP, MP2 and CCSD) using DZP basis set for H_2O and Li^+ , and LANL2DZ basis set for Na^+ and K^+ , respectively. (distances are in Å)

Figure 3.11 displays some essential structural parameters of the optimized ion-water complexes, as obtained by the HF calculations using different basis sets. It is apparent that the use of medium-size basis set, like the DZP, could provide results in good accord with those obtained by the calculations using larger 6-311++G(d,p) and AUG-cc-pVDZ basis sets. In general, the use of larger basis set can provide more reliable simulation results. In practice, however, the use of large basis sets is still beyond our current computational facilities (cf. Figures 3.12-3.14). In this study, the selection of the DZP basis set for water and Li^+ and the LANL2DZ basis set for Na^+ and K^+ is assumed to be good enough to achieve a sufficiently level of accuracy in the simulations.

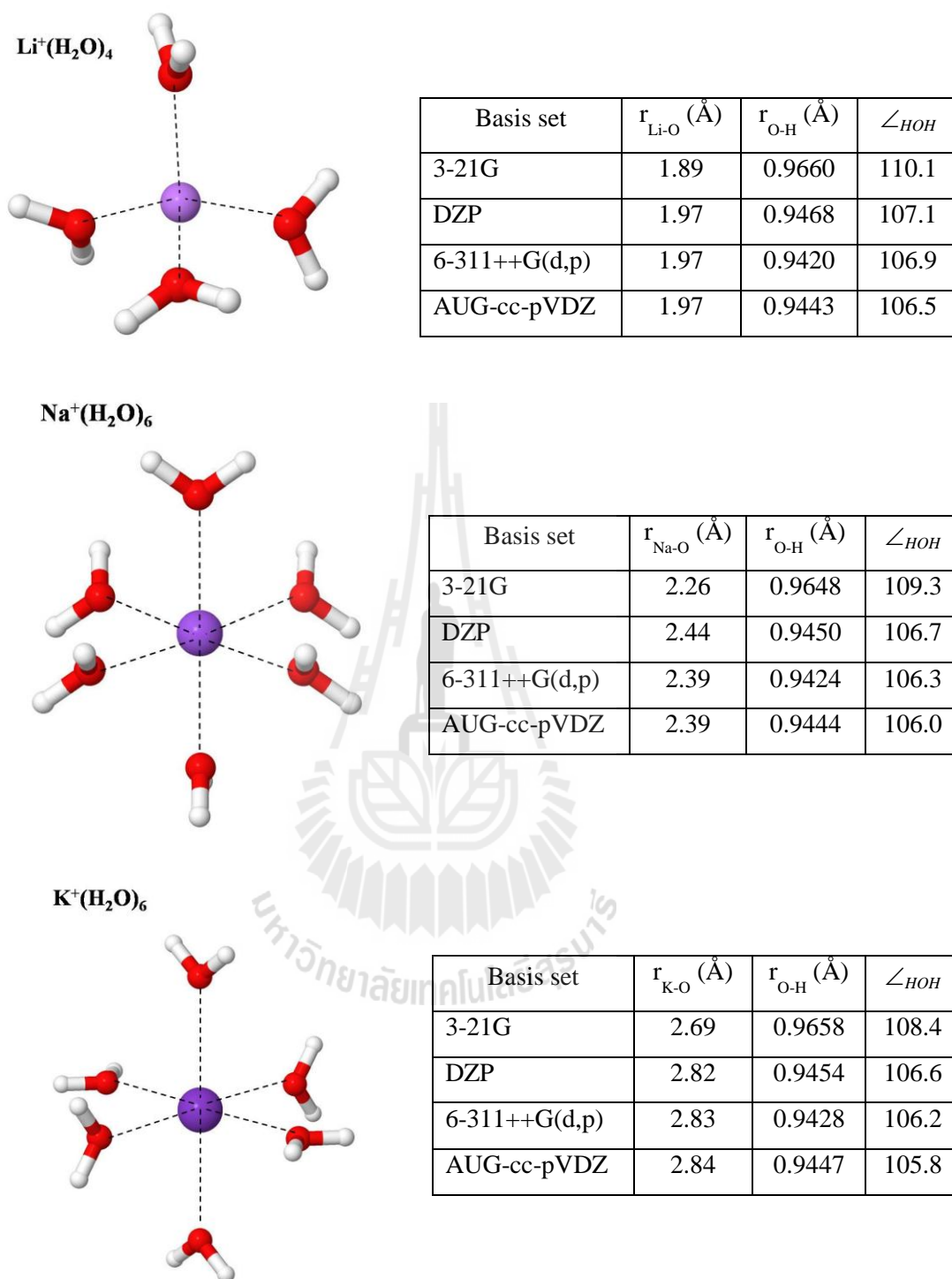


Figure 3.11 Optimized geometries of $\text{Li}^+(\text{H}_2\text{O})_4$, $\text{Na}^+(\text{H}_2\text{O})_6$ and $\text{K}^+(\text{H}_2\text{O})_6$ complexes, as obtained by the HF calculations using different basis sets (3-21G, DZP, 6-311++G(d,p) and AUG-cc-pVDZ). (distances and angles are in Å and degree, respectively)

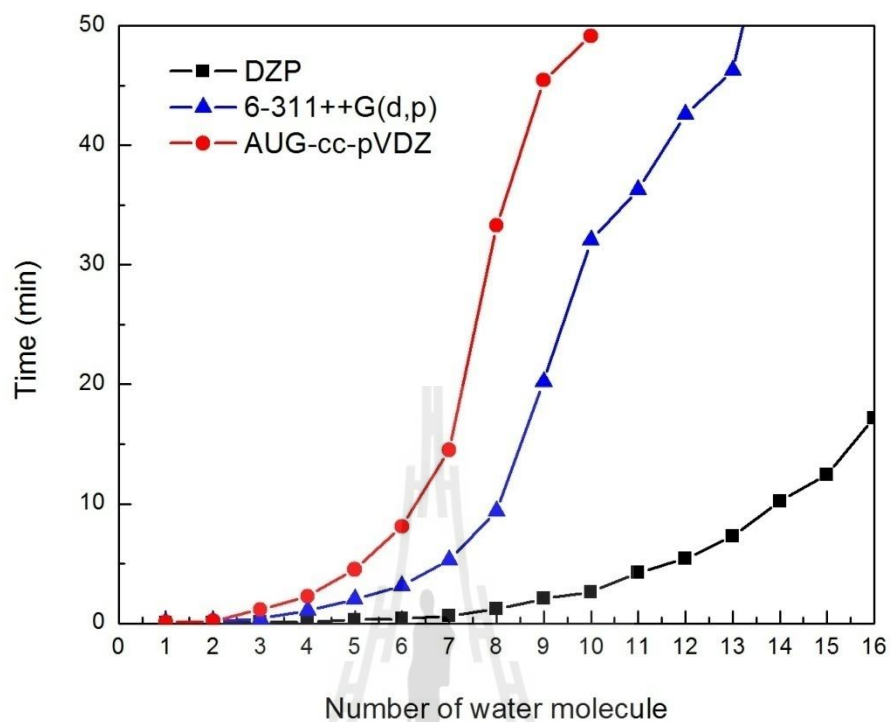


Figure 3.12 Requirements of CPU times for HF force calculations of $\text{Li}^+(\text{H}_2\text{O})_n$ complexes, where $n=1-16$, using DZP, 6-311++G(d,p) and AUG-cc-pVDZ basis sets. All QM calculations were performed on CCRL cluster.

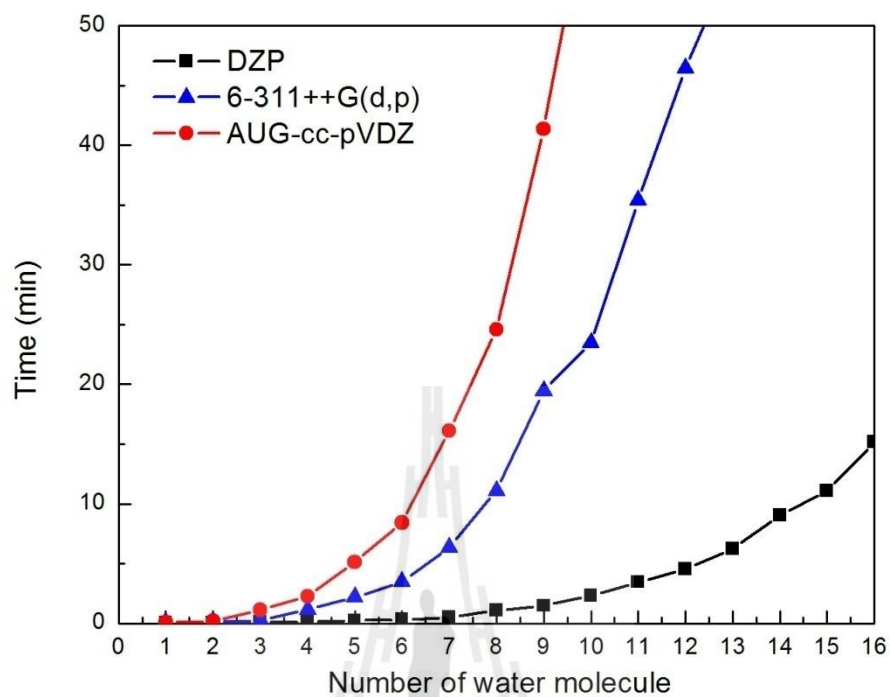


Figure 3.13 Requirements of CPU times for HF force calculations of $\text{Na}^+(\text{H}_2\text{O})_n$ complex, where $n=1-16$, using DZP, 6-311++G(d,p) and AUG-cc-pVDZ basis sets for H_2O and LANL2DZ basis set for Na^+ . All QM calculations were performed on CCRL cluster.

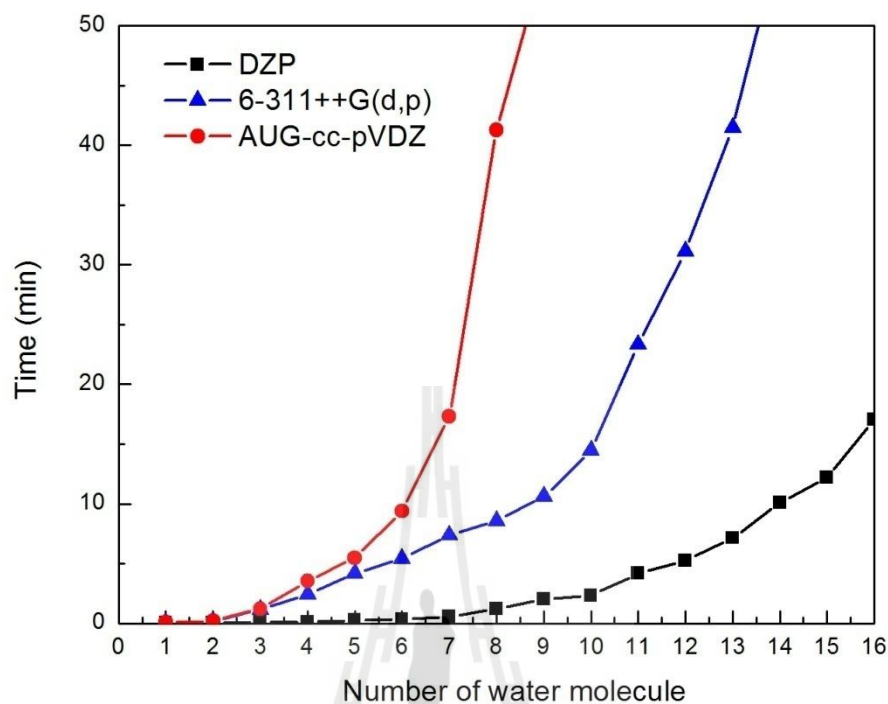


Figure 3.14 Requirements of CPU times for HF force calculations of $K^+(H_2O)_n$ complex, where $n=1-16$, using DZP, 6-311++G(d,p) and AUG-cc-pVDZ basis sets for H_2O and LANL2DZ basis set for K^+ . All QM calculations were performed on CCRL cluster.

3.10.4 Simulation details

All ONIOM-XS MD simulations were carried out in a canonical ensemble (NVT) at 298 K with periodic boundary conditions. The periodic box, with a box length of 18.19 Å, contains one ion (Li^+ , Na^+ or K^+) and 199 water molecules, which corresponds to the experimentally observed density of pure water. The QM size, with radius of 4.2 Å, is employed. The reaction-field method (Adams, Adams

and Hills, 1979) was employed for the treatment of long-range interactions. The Newtonian equations of motions were treated by a general predictor-corrector algorithm. The time step size was set to 0.2 fs, allowing for the explicit movement of the hydrogen atoms of water molecules. For each ONIOM-XS MD simulation, the system was initially equilibrated by performing the simulations for 25,000 steps, follows by 200,000 time steps to collect configurations every 10th step.

3.11 Determination of system's properties

3.11.1 Structural properties

The structural properties of the hydrated ions will be analyzed in terms of radial distribution functions (RDFs) and their corresponding integration numbers, together with the analyses of angular distribution functions (ADFs) and orientations of water molecules surrounding the ion. A typical RDF can be expressed as

$$g_{\alpha\beta}(r) = N_{\alpha\beta}(r) / (4\pi r^2 \Delta r \rho_{\beta}), \quad (3.45)$$

where $N_{\alpha\beta}(r)$ is the average number of β sites located in the shell $(r, r+\Delta r)$ centered on site α , and $\rho_{\beta} = \frac{N_{\beta}}{V}$ is the average number density of β sites in the system.

The corresponding integration number of RDF is defined as

$$n_{\alpha\beta}(r) = 4\pi\rho_{\beta} \int_0^r g_{\alpha\beta}(r')r'^2 dr' . \quad (3.46)$$

3.11.2 Dynamical properties

The dynamical properties will be analyzed through mean residence times (MRTs) and self-diffusion coefficient (D). The mobility of water molecules surrounding the ion can be interpreted through the D value, which can be calculated from their center-of-mass velocity autocorrelation functions (VACFs) using the Green-Kubo relation,

$$D = \frac{1}{3} \lim_{t \rightarrow \infty} \int_0^t C_v(t) dt. \quad (3.47)$$

The MRT data was calculated using the direct method (Hofer, Tran, Schwenk and Rode, 2004), being the product of the average number of water molecules in the first shell with the duration of the simulations, divided by the observed number of exchange events lasting a given time interval t^* .

$$MRT(\tau) = \frac{CN \times t_{sim}}{N_{ex}} \quad (3.48)$$

where CN is the average coordination number, t_{sim} is the simulation time and N_{ex} is the number of exchange events. With regard to the “direct” method, it has been suggested that a t^* value of 0.0 ps is suitable for the estimation of hydrogen bond lifetimes, while a t^* value of 0.5 ps is recommended as a good measure for water exchange processes (Hofer, Tran, Schwenk and Rode, 2004).

Exchange mechanism of ligands around metal ions can be assigned into five types: an associative exchange (A), presence of high coordination number intermediate leading to an increasing volume of the hydration shell. In contrast, if an intermediate of reduced coordination number, the mechanism process is called dissociative exchange (D). The interchange mechanism (I), prefers the complex that has incoming and outgoing molecule at the same time, which can be subdivided into two classes depending on the exchange as associative-like (I_a) or dissociative-like (I_d) mechanisms (Helm and Merbach, 1999), as can be seen in Figure 3.15.

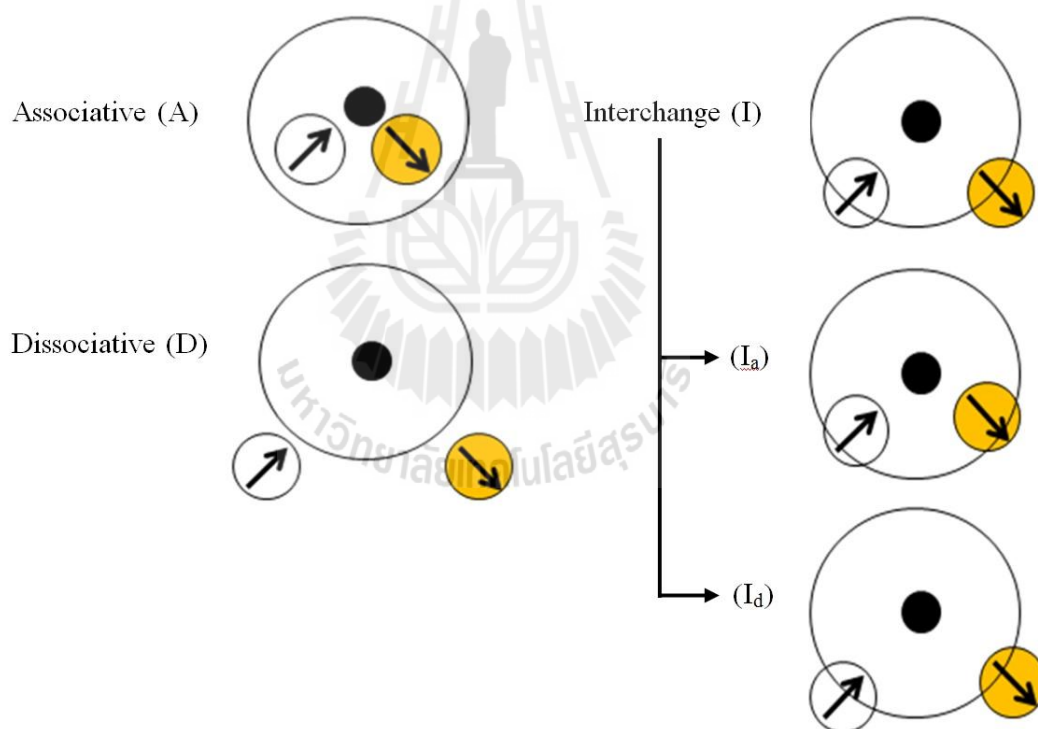




Figure 3.15 Definition of mechanism of ligand exchange process;  is external solvent molecule;  is leaving solvent molecule.

3.12 References

- Adams, D. J., Adams, E. M. and Hills, G. J. (1979). The computer simulation of polar liquids. **Molecular Physics**. 38: 387-400.
- Beeman, D. (1976). Some multistep methods for use in molecular dynamics calculations. **Journal of Computational Physics**. 20: 130-139.
- Brooks, B. R., Bruccoleri, R. E., Olafson, B. D., States, D. J., Swaminathan, S. and Karplus, M. (1983). CHARMM: A program for macromolecular energy, minimization, and dynamics calculations. **Journal of Computational Chemistry**. 4: 187-217.
- Check, C., Faust, T., Bailey, J., Wright, B., Gilbert, T. and Sunderlin, L. (2001). Addition of polarization and diffuse functions to the LANL2DZ basis set for P-Block elements. **The Journal of Physical Chemistry A**. 105: 8111-8116.
- Dunning, T. H. and Hay, P. J. (1977). **Methods of electronic structure theory**.
- Ewald, P. P. (1921). Die berechnung optischer and elektrostatischer gitterpotentiale. **Annalen der Physik**. 369: 253-287.
- Foulkes, W. M. C. and Haydock, R. (1989). Tight-binding models and density-functional theory. **Physical Review B**. 39: 12520-12536.
- Frisch, M. J., Trucks, G. W., Schlegel, H. B., Scuseria, G. E., Robb, M. A., Cheeseman, J. R., Zakrzewski, V. G., Montgomery, J. A., Stratmann, R. E., Burant, J. C., Dapprich, S., Millam, J. M., Daniel, A. D., Kudin, K. N., Strain, M. C., Farkas, O., Tomasi, J., Barone, V., Mennucci, B., Pomelli, C., Adamo, C., Clifford, S., Ochterski, J., Petersson, G. A., P.Y. Ayala, Q. C., Morokuma, K., Salvador, P., Foresman, Cioslowski, J., Ortiz, J. V., Baboul, A. G., Stefanov, B. B., Liu, G., Liashenko, A., Piskorz, P., Komaromi, I., Gomperts,

- R., Martin, R. L., Fox, D. J., T. Keith, M. A. A. L., Peng, C. Y., Nanayakkara, A., Gill, B. J., Chen, W., Gonzalez, C., Pople, J. A. (2005). Gaussian 03 (Revision D.1) [Computer Software]. Wallingford, CT, USA: Gaussian.
- Gear, C. W. (1971). **Numerical initial value problems in ordinary differential equations**. Englewood Cliffs, N.J.: Prentice-Hall.
- Hay, P. J. and Wadt, W. R. (1985). *Ab initio* effective core potentials for molecular calculations. Potentials for the transition metal atoms Sc to Hg. **The Journal of Chemical Physics**. 82: 270-283.
- Helm, L. and Merbach, A. E. (1999). Water exchange on metal ions: Experiments and simulations. **Coordination Chemistry Reviews**. 187: 151-181.
- Hockney, R. W. (1970). The potential calculation and some applications. **Methods in Computational Physics**. 9: 136-211.
- Hofer, T. S., Tran, H. T., Schwenk, C. F. and Rode, B. M. (2004). Characterization of dynamics and reactivities of solvated ions by *ab initio* simulations. **Journal of Computational Chemistry**. 25: 211-217.
- Kerdcharoen, T. and Morokuma, K. (2002). ONIOM-XS: An extension of the ONIOM method for molecular simulation in condensed phase. **Chemical Physics Letters**. 355: 257-262.
- Kistenmacher, H., Popkie, H. and Clementi, E. (1974). Study of the structure of molecular complexes. VIII. Small clusters of water molecules surrounding Li^+ , Na^+ , K^+ , F^- , and Cl^- ions. **The Journal of Chemical Physics**. 61: 799-815.
- Rode, B. M., Schwenk, C. F., Hofer, T. S. and Randolph, B. R. (2005). Coordination and ligand exchange dynamics of solvated metal ions. **Coordination Chemistry Reviews**. 249: 2993-3006.

- Rode, B. M., Schwenk, C. F. and Tongraar, A. (2004). Structure and dynamics of hydrated ions-new insights through quantum mechanical simulations. **Journal of Molecular Liquids**. 110: 105-122.
- Svensson, M., Humbel, S., Froese, R. D. J., Matsubara, T., Sieber, S. and Morokuma, K. (1996). ONIOM: A multilayered integrated MO + MM method for geometry optimizations and single point energy predictions. A test for Diels–Alder reactions and Pt(P(t-Bu)₃)₂ + H₂oxidative addition. **The Journal of Physical Chemistry**. 100: 19357-19363.
- Swope, W. C., Andersen, H. C., Berens, P. H. and Wilson, K. R. (1982). A computer simulation method for the calculation of equilibrium constants for the formation of physical clusters of molecules: Application to small water clusters. **The Journal of Chemical Physics**. 76: 637-649.
- Tasaki, K., McDonald, S. and Brady, J. W. (1993). Observations concerning the treatment of long-range interactions in molecular dynamics simulations. **Journal of Computational Chemistry**. 14: 278-284.
- Verlet, L. (1967). Computer "Experiments" on classical fluids. I. Thermodynamical properties of Lennard-Jones molecules. **Physical Review**. 159: 98-103.
- Xenides, D., Randolph, B. R. and Rode, B. M. (2005). Structure and ultrafast dynamics of liquid water: A quantum mechanics/molecular mechanics molecular dynamics simulations study. **The Journal of Chemical Physics**. 122: 174506.
- Xenides, D., Randolph, B. R. and Rode, B. M. (2006). Hydrogen bonding in liquid water: An *ab initio* QM/MM MD simulation study. **Journal of Molecular Liquids**. 123: 61-67.

CHAPTER IV

RESULTS AND DISCUSSION

4.1 “Structure-making” ability of Li^+ in aqueous solution : A comparative study of conventional QM/MM and ONIOM-XS MD simulations

The ONIOM-XS MD technique has been developed in order to improve the methodical drawbacks of the conventional QM/MM MD framework. To verify the reliability of the ONIOM-XS MD technique, the hydration structure and dynamics of Li^+ in aqueous solution will be firstly investigated by means of the conventional QM/MM and ONIOM-XS MD simulations. The results obtained by the two QM/MM-based MD simulation types will be compared and discussed with respect to the important treatment of the ONIOM-XS method for describing the “structure-making” ability of Li^+ in aqueous solution.

The structural properties of the hydrated Li^+ are explained in terms of Li-O and Li-H RDFs and their corresponding integration numbers, as depicted in Figure 4.1, comparing the results as obtained by the conventional QM/MM and ONIOM-XS MD simulations. Based on the two QM/MM-based MD simulations, the features of the first Li-O peaks are almost identical, *i.e.*, showing a well-defined first hydration shell with the maxima centered at 1.96 and 1.93 Å, respectively. The shape and height of the first Li-O and Li-H RDFs reveal a clear “structure-making” ability of Li^+ in

aqueous solution, *i.e.*, the ability by which the ion can order the HB structure of its surrounding waters to form its specific Li^+ -water complexes. In this study, it should be clarified at the beginning that all discussion with respect to the “structure-making” and “structure-breaking” abilities of ions in water assumes a sufficiently dilute aqueous solution, *i.e.*, the solution in which the influences of either counter-ion or ion-pairing are negligible. With regard to the Li-O and Li-H RDFs in Figure 4.1, the first hydration shell of Li^+ is not completely separated from the outer region, indicating that some water exchange processes can take place between these two regions. Integrations up to the first minimum of the conventional QM/MM and ONIOM-XS MD’s Li-O RDFs yield the average coordination numbers of 4.1 and 4.2, respectively. Note that the details with respect to the first hydration shell of Li^+ are close to those reported in the recent QM/MM MD (Hannes H. Loeffler, Mohammed, Inada and Funahashi, 2003; H. H. Loeffler and Rode, 2002) and CP-MD (Lyubartsev, Laasonen and Laaksonen, 2001) studies. Regarding the two QM/MM-based MD results, the observed similarity of the first Li-O and Li-H RDFs is understandable since most of the particles embedded within the first hydration shell of Li^+ are treated by the similar QM forces. In this respect, since the ONIOM-XS MD technique has been proposed in order to improve the forces of QM particles according to immediate exchanges of particles between the QM and MM regions, a significant difference between the conventional QM/MM and ONIOM-XS MD results is expected to be found at the region nearby the QM-MM boundary. Interestingly, it has been demonstrated that the differences between the conventional QM/MM and ONIOM-XS MD simulations are more visible for the situation where the number of ligands that are crossing the QM-MM boundary is large, *i.e.*, a system where ion-water interactions are weak and water

molecules surrounding the ion are labile (Sripa, Tongraar and Kerdcharoen, 2013; Wanprakhon, Tongraar and Kerdcharoen, 2011). In this work, the remarkable difference between the conventional QM/MM and ONIOM-XS MD results appears at the region beyond the first hydration shell of Li^+ . As can be seen in Figure 4.1a, the recognizable second peak of the ONIOM-XS MD's Li-O RDF is located at a shorter distance of 3.71 Å, compared to the corresponding value of 3.95 Å obtained by the conventional QM/MM MD simulation. This observed difference clearly implies an important treatment of the ONIOM-XS MD technique in obtaining a more reliable description of the Li^+ hydrate.



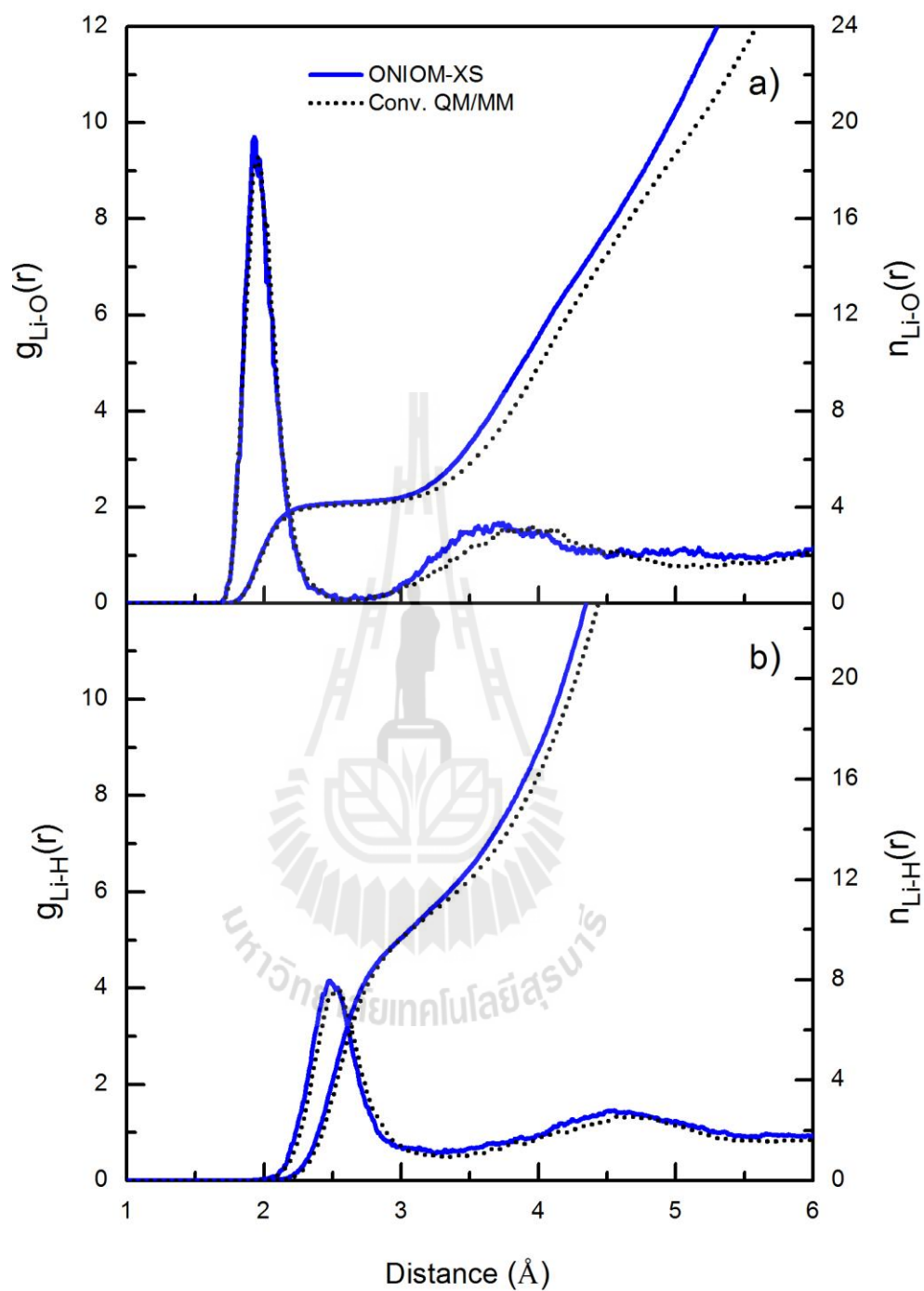


Figure 4.1 a) Li-O and b) Li-H RDFs and their corresponding integration numbers, as obtained by the conventional QM/MM and ONIOM-XS MD simulations.

Figure 4.2 shows the probability distributions of the coordination number of Li^+ , calculated up to first minimum of the Li-O RDFs. In both the conventional QM/MM and ONIOM-XS MD simulations, the Li^+ clearly favors a coordination number of 4, followed by 5 in smaller amounts. However, the probability distributions of the 4-fold and 5-fold coordinated complexes obtained by the two QM/MM-based MD techniques are significantly different, being of 90.7 and 9.2 %, and of 75.2 and 23.9%, respectively. Interestingly, the ONIOM-XS MD results clearly reveal that the hydration structure of the Li^+ is somewhat flexible and that, besides the prevalent $\text{Li}^+(\text{H}_2\text{O})_4$ species, the $\text{Li}^+(\text{H}_2\text{O})_5$ complex could more frequently be formed in aqueous solution.

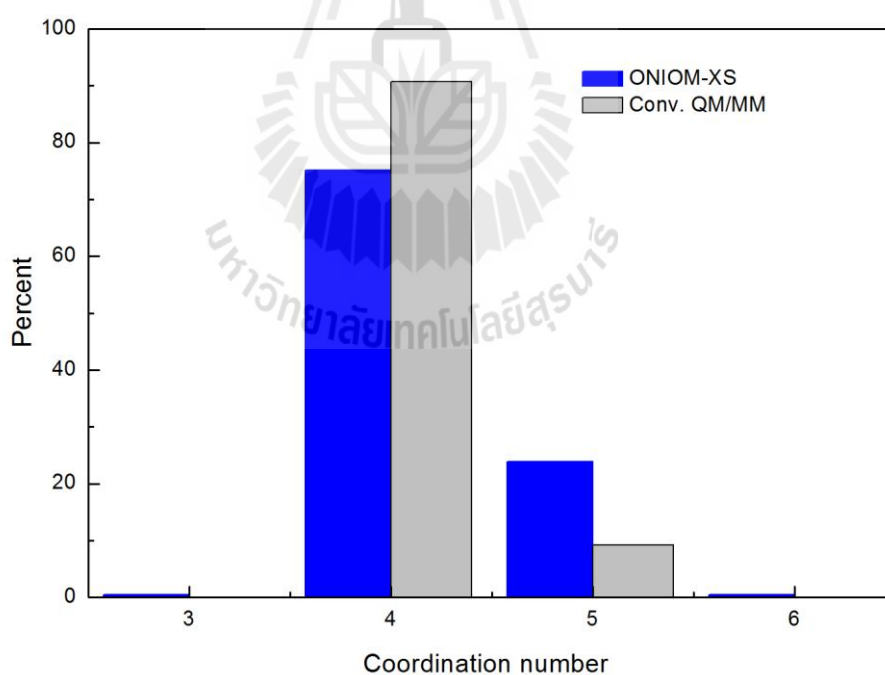


Figure 4.2 Distributions of the coordination number of Li^+ , calculated within the first minimum of the Li-O RDFs, as obtained by the conventional QM/MM and ONIOM-XS MD simulations.

The flexibility of the Li^+ hydration can be described by the distributions of the O---Li---O angle, as shown in Figure 4.3. By means of the ONIOM-XS MD simulation, as compared to the conventional QM/MM MD results, the observed broader distributions of the O---Li---O angle clearly indicate a higher flexibility of the hydrated Li^+ . In particular, as can be seen in Figure 4.3, a recognizable shoulder between 150° and 180° corresponds to a higher probability of finding the arrangement with respect to the 5-fold coordinated complexes. Consequently, these observed differences could further be expected to reflect in different dynamics details of the ligands surrounding the Li^+ .

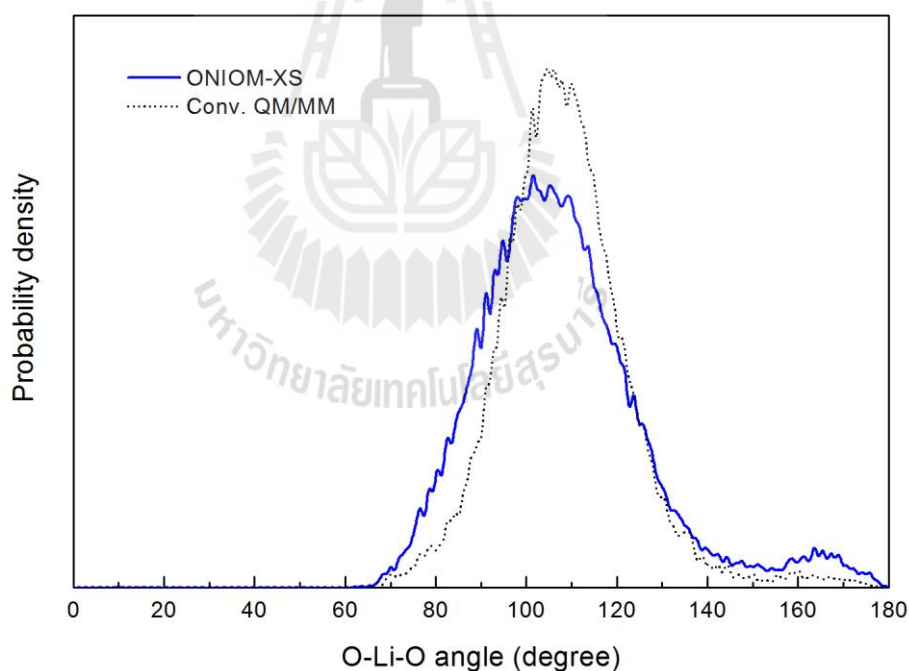


Figure 4.3 Distributions of the O---Li---O angle, calculated within the first minimum of the Li-O RDFs, as obtained by the conventional QM/MM and ONIOM-XS MD simulations.

The dynamical properties of the Li^+ hydrate can be visualized through the plots of time dependence of the Li-O distance and number of first-shell waters, as depicted in Figures 4.4 and 4.5 for the conventional QM/MM and ONIOM-XS MD simulations, respectively. In the ONIOM-XS MD simulation, as compared to the conventional QM/MM MD results, water molecules surrounding the Li^+ are more labile, showing more frequent exchanges of water molecules between those in the hydration shell of Li^+ and the bulk. Consequently, this leads to a higher probability of finding $\text{Li}^+(\text{H}_2\text{O})_5$ or even $\text{Li}^+(\text{H}_2\text{O})_3$ species. In this respect, it is observed that the most favorable $\text{Li}^+(\text{H}_2\text{O})_4$ species can temporarily convert back and forth to the lower probability $\text{Li}^+(\text{H}_2\text{O})_5$ complexes, or even to a less favorable $\text{Li}^+(\text{H}_2\text{O})_3$ formation. For example, at the simulation time of 4.2 ps, an arrangement of the 5-fold coordinated complex is temporarily formed, *i.e.*, one water molecule from the outer region (labeled in “green”) transiently approaches as close as 2.2 Å to the Li^+ , forming an $\text{Li}^+(\text{H}_2\text{O})_4(\text{H}_2\text{O})$ intermediate. At the simulation times of 8.7 and 17.3 ps, the $\text{Li}^+(\text{H}_2\text{O})_5$ intermediates are formed according to associative (A) exchange processes, *i.e.*, a new (fifth) water molecule from the outer region (labeled in “blue” and “green”, respectively) comes into the first hydration shell of Li^+ , and then, one of water molecules from the initial hydration shell is repelled. Interestingly, other intermediates, such as the $\text{Li}^+(\text{H}_2\text{O})_3$ species, also exist in aqueous solution (*e.g.*, at the simulation time of 2.1 ps, in which one first-shell water molecule is found to temporarily move as far as 1 Å away from its optimal distance).

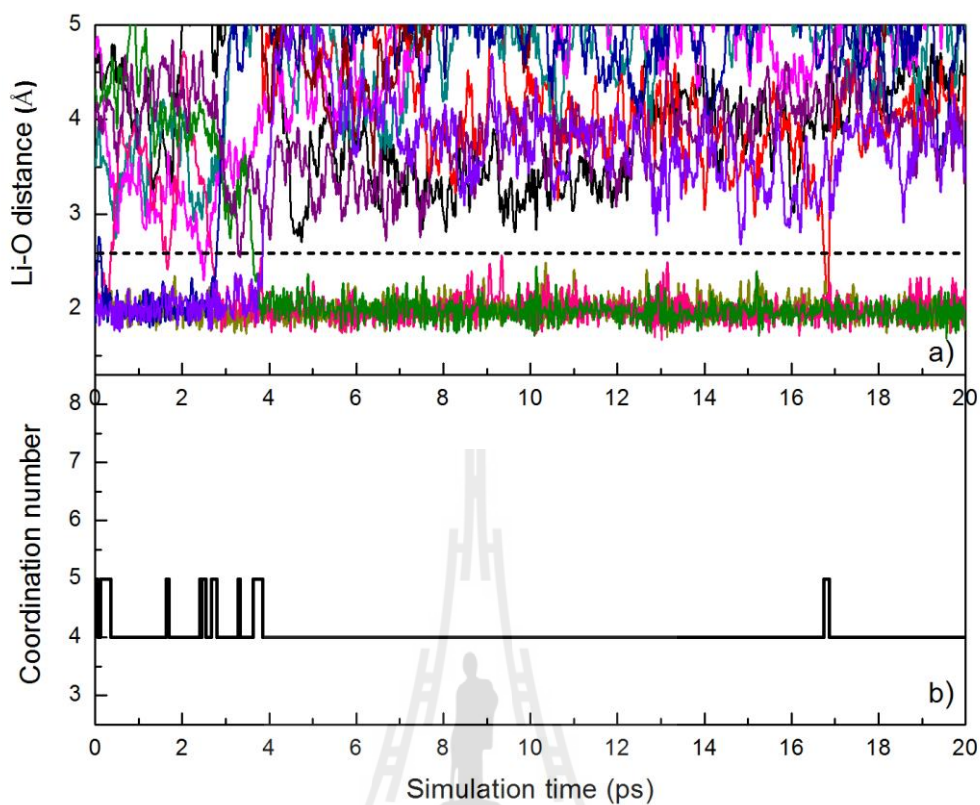


Figure 4.4 Time dependence of a) Li^+ -O distance and b) number of first-shell waters, as obtained from first 20 ps of the conventional QM/MM MD simulation. In Figure 4.4a), the dash line parallel to the x-axis indicates the first minimum of the Li-O RDF.

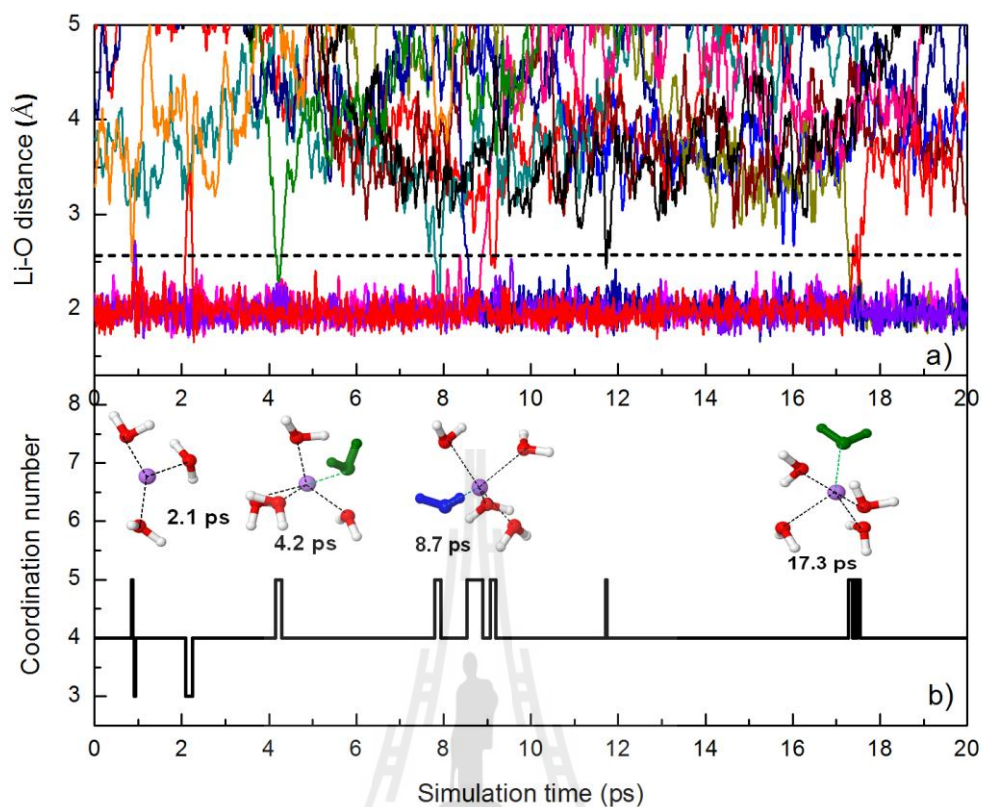


Figure 4.5 Time dependence of a) Li^+ -O distance and b) number of first-shell waters, as obtained from first 20 ps of the ONIOM-XS MD simulation. In Figure 4.5a), the dash line parallel to the x-axis indicates the first minimum of the Li-O RDF.

The lability of water molecules in the first hydration shell of Li^+ can be interpreted through the D values of first-shell waters. By the conventional QM/MM and ONIOM-XS MD simulations, the D values for water molecules in the vicinity of Li^+ are estimated to be 1.01×10^{-5} and $1.38 \times 10^{-5} \text{ cm}^2.\text{s}^{-1}$, respectively. Apparently, these D values are relatively lower than the corresponding values of 3.23×10^{-5} and $2.73 \times 10^{-5} \text{ cm}^2.\text{s}^{-1}$ of pure water derived by the conventional QM/MM and ONIOM-XS MD techniques (Thaomola, Tongraar and Kerdcharoen, 2012), respectively. This indicates that water molecules in the first hydration shell of Li^+ are well attached to the ion, showing a clear “structure-making” ability of Li^+ in water. Comparing the conventional QM/MM and ONIOM-XS MD results, however, the D values are somewhat different, *i.e.*, the D values of water molecules in the hydration shell of Li^+ are of about 3 and 2 times slower than those of bulk waters, respectively. In this respect, it is apparent that the ONIOM-XS MD simulation reveals the “structure-making” ability of Li^+ which is significantly less than that predicted by the conventional QM/MM MD scheme. With regard to this point, it is worth noting that the correct degree of the lability of the first-shell waters is a crucial factor in determining the reactivity of Li^+ in aqueous solution. Interestingly, the ONIOM-XS MD results clearly suggest that the “structure-making” ability of this ion is not too strong. Regarding the Li-O RDF in Figure 4.1a, the less pronounced second peak clearly supplies information that the effects of Li^+ on the water structure does not propagate beyond the first hydration shell.

The rates of water exchange processes at Li^+ were evaluated through MRTs of the first-shell water molecules. The calculated MRT data for water molecules in the bulk and in the vicinity of Li^+ with respect to t^* values of 0.0 and 0.5 ps are

summarized in Table 4.1, comparing the results as obtained by the conventional QM/MM and ONIOM-XS MD simulations. For both $t^* = 0.0$ and 0.5 ps, the MRT values of water molecules in the hydration shell of Li^+ obtained from both the conventional QM/MM and ONIOM-XS MD simulations are higher than the corresponding values of bulk waters, confirming a clear “structure-making” ability of Li^+ in aqueous solution. By means of the ONIOM-XS MD simulation, however, the ability of Li^+ in ordering the structure of its surrounding waters is significantly weaker than that predicted by the conventional QM/MM MD scheme. According to the data in Table 4.1, the MRT values of water molecules in the vicinity of K^+ derived by the conventional QM/MM and ONIOM-XS MD simulations were found to be quite similar. However, it has been reported that the average coordination number of K^+ and the amount of exchange events are somewhat different (Wanprakhon, Tongraar and Kerdcharoen, 2011). In the case of Ca^{2+} , a significant difference between the two QM/MM-based MD simulations is found for $t^* = 0.5$ ps, in which the ONIOM-XS MD simulation revealed a relatively large number of exchange events (with the smaller MRT value) when compared to those obtained by the conventional QM/MM MD simulation (Wanprakhon, Tongraar and Kerdcharoen, 2011). Recently, the ONIOM-XS MD technique has also been applied for studying the preferential solvation and dynamics of Li^+ in aqueous ammonia solution (Kabbalee, Tongraar and Kerdcharoen, 2015). Of particular interest, as compared to the conventional QM/MM MD study, which predicts a clear water preference with the arrangement of the $\text{Li}^+[(\text{H}_2\text{O})_4][(\text{H}_2\text{O})_4]$ type, the ONIOM-XS MD simulation clearly reveals that this ion can order both water and ammonia molecules to form a preferred $\text{Li}^+[(\text{H}_2\text{O})_3\text{NH}_3][(\text{H}_2\text{O})_{11}(\text{NH}_3)_3]$ complex. In addition, it was observed that the

“structure-making” ability of Li^+ in this solvent mixture is not too strong and that the second solvation of this ion is less structured, implying a small influence of Li^+ in ordering the solvent molecules in this shell. Undoubtedly, the overall observed differences between the two QM/MM-based MD simulations clearly confirm that the use of the more accurate ONIOM-XS MD technique is highly recommended for obtaining more reliable descriptions of the Li^+ hydrates.

Table 4.1 Number of water exchange events (N_{ex}) and mean residence times (MRTs) of water molecules in the bulk and in the vicinity of ions, as obtained by the conventional QM/MM and ONIOM-XS MD simulations.

Ion/solute	CN	t_{sim}	$t^* = 0.0$ ps		$t^* = 0.5$ ps	
			$N_{\text{ex}}^{0.0}$	$\tau_{\text{H}_2\text{O}}^{0.0}$	$N_{\text{ex}}^{0.5}$	$\tau_{\text{H}_2\text{O}}^{0.5}$
Conventional QM/MM MD						
Li^+	4.1	40.0	37	4.43	9	18.22
K^{+*}	7.0	30.0	514	0.41	112	1.87
Ca^{2+*}	7.8	40.0	26	12.00	8	39.00
H_2O^{**}	4.9	40.0	944	0.21	84	2.33
ONIOM-XS MD						
Li^+	4.2	40.0	79	2.13	13	12.92
K^{+*}	6.3	30.0	445	0.42	105	1.80
Ca^{2+*}	7.6	40.0	30	10.13	14	21.71
H_2O^{**}	4.7	30.0	607	0.23	65	2.17

* (Wanprakhon, Tongraar and Kerdcharoen, 2011)

** (Thaomola, Tongraar and Kerdcharoen, 2012)

4.2 ONIOM-XS MD simulations of Na⁺ and K⁺ in aqueous solution : Transition from “structure-making” to “structure-breaking” behaviors

The details with respect to the hydration structures of Na⁺ and K⁺ can be visualized from the plots of M-O and M-H RDFs for M = Li, Na and K, respectively, and their corresponding integration numbers, as depicted in Figure 4.6. Note that the Li-O and Li-H RDFs derived by the ONIOM-XS MD simulation are also given for comparison. For Na⁺, a well-defined first Na-O peak with a maximum centered at 2.35 Å is observed. However, as compared to the Li-O RDF, the first peak of the Na-O RDF is significantly less pronounced. In addition, the non-zero minimum following the first Na-O peak clearly suggests some exchange processes between first-shell waters and water molecules in the outer region. Integration up to the first minimum of the Na-O RDF yields an average coordination number of 5.4. This observed value is in good agreement with the recent ND experiments (Mancinelli, Botti, Bruni, Ricci and Soper, 2007) and AI-MD studies (Ikeda, Boero and Terakura, 2007; Kulik, Marzari, Correa, Prendergast, Schwegler and Galli, 2010; Mancinelli, Botti, Bruni, Ricci and Soper, 2007; White, Schwegler, Galli and Gygi, 2000), which reported the coordination numbers of 5.3 and 5.2, respectively. The second peak of the Na-O RDF is less pronounced, indicating that the influence of Na⁺ beyond the first hydration layer is relatively weak, *i.e.*, only a single layer of Na⁺ hydration is formed. For the aqueous K⁺ solution, the first K-O peak is centered at around 2.78 Å, which corresponds to the average coordination number of 6.5. As compared to the Li-O and Na-O RDFs, the first peak of K-O RDF is rather broad and is not well separated from

the bulk, indicating that water molecules surrounding the ion can easily exchange with bulk waters.

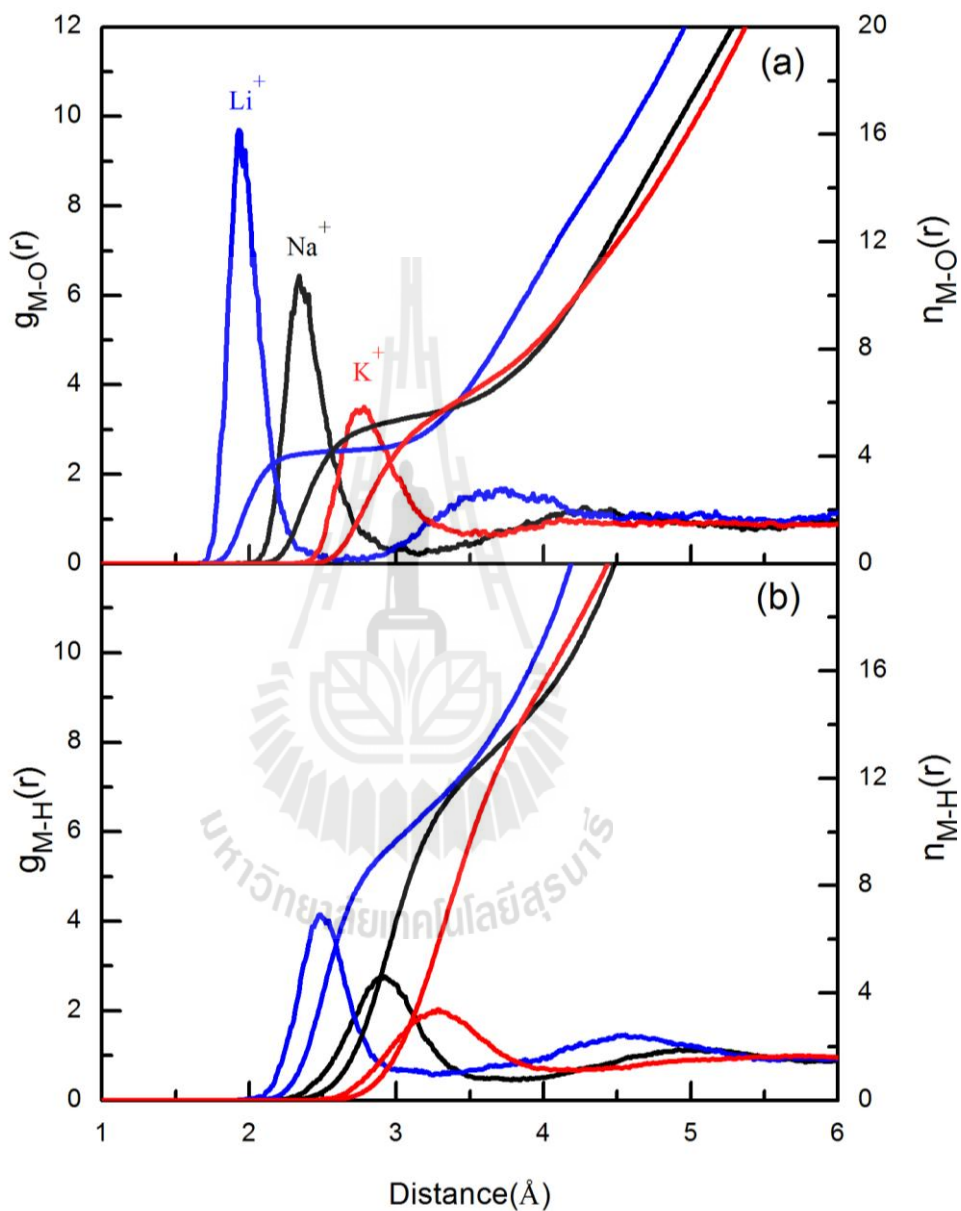


Figure 4.6 a) M–O and b) M–H RDFs and their corresponding integration numbers, as obtained by the ONIOM-XS MD simulations.

According to the present ONIOM-XS MD simulations, the results are in good accord with the interpretation of X-ray absorption spectroscopy (XAS) experiments, which indicated that there is no long-range effect on the HB network of water due to the presence of monovalent cations (Cappa, Smith, Messer, Cohen and Saykally, 2006). With regard to the XAS results, it has been demonstrated that the changes in the XA spectra observed upon addition of monovalent cation halide salts are due mainly to the interactions of water molecules with the halide anions. In addition, according to the recent femtosecond pump-probe spectroscopy study (Bakker, Kropman and Omta, 2005), it has been suggested that the effect of alkali ions on the structure and dynamics of water is limited to the first hydration shell of ions, *i.e.*, the HB network beyond the first-shell is not different from that of bulk water.

Figure 4.7 shows the probability distributions of the coordination number of Li^+ , Na^+ and K^+ , calculated up to first minimum of the M-O RDFs. For Li^+ , it has been shown that this ion clearly favors a coordination number of 4 followed by 5 in smaller amounts, with the probability distributions of 75% and 24%, respectively. For Na^+ , it is apparent that this ion prefers the coordination numbers of 5 and 6, with the probability distributions of 56% and 37%, respectively, whereas the distributions of 4-fold and 7-fold coordinated complexes appear to be quite rare. This supplies information that only $\text{Na}^+(\text{H}_2\text{O})_5$ and $\text{Na}^+(\text{H}_2\text{O})_6$ complexes are the most prevalent species formed in aqueous solution. In the case of K^+ , the distribution of the coordination number is rather broad, varying from 4 to 9. This suggests that a number of different hydrated K^+ complexes can simultaneously be formed in the solution.

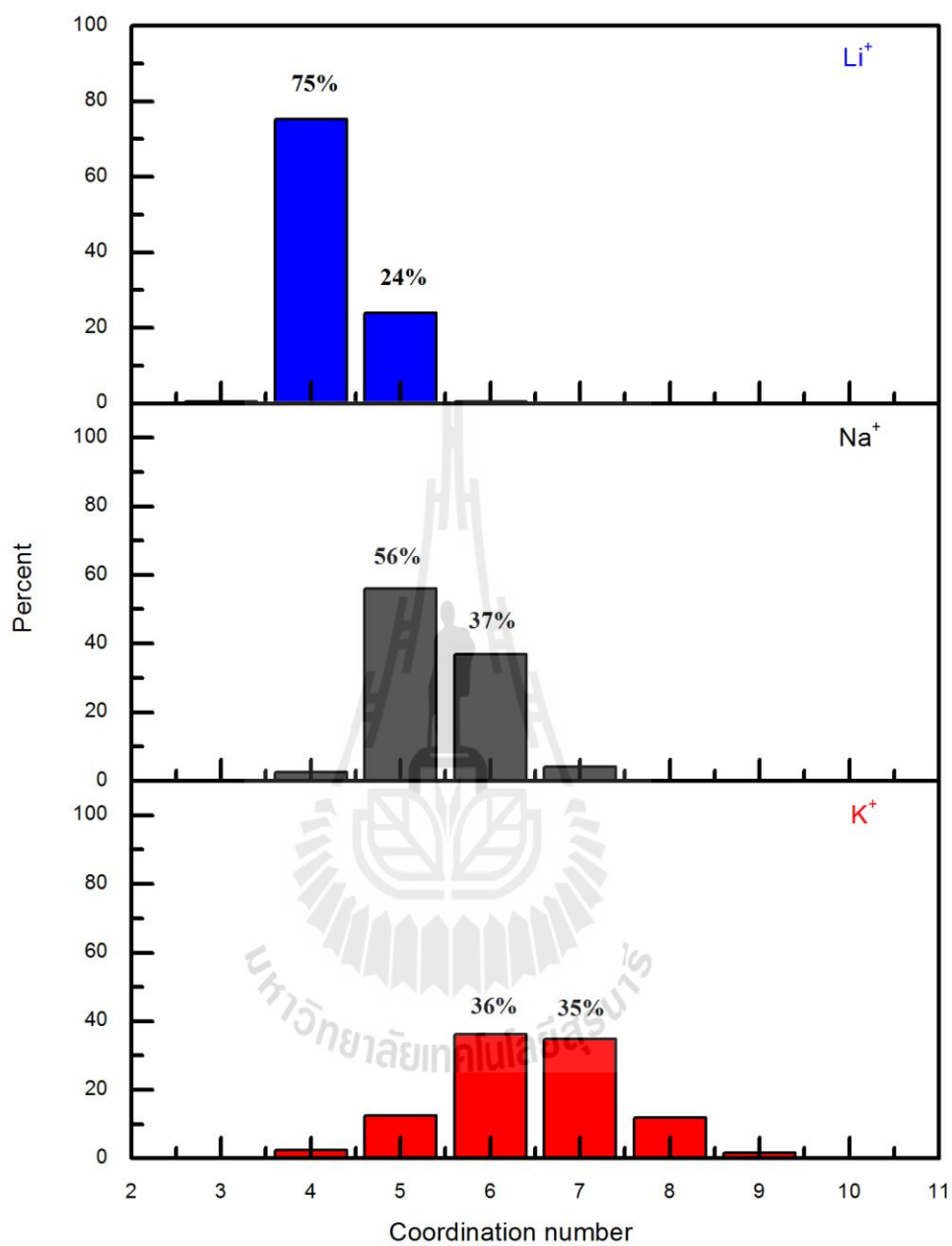
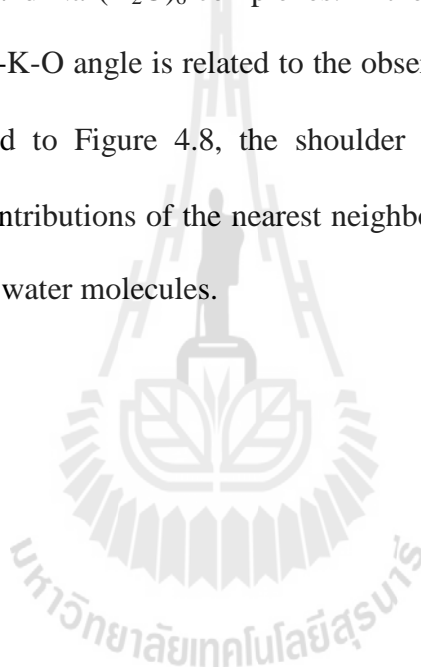


Figure 4.7 Probability distributions of the coordination number of Li^+ , Na^+ and K^+ , calculated up to first minimum of the M-O RDFs.

The flexibility of the hydrated ions can be described by the distributions of O--M--O angles, calculated up to the first minimum of the M-O RDFs, as shown in Figure 4.8. For Li^+ , it has been pointed out that the hydration structure of this ion is arranged with respect to the tetrahedral geometry. For Na^+ , as compared to Li^+ , the hydration shell structure is more flexible, by the pronounced peak between $80\text{-}90^\circ$ and the small shoulders at around $150\text{-}170^\circ$. This corresponds to the arrangements of the observed $\text{Na}^+(\text{H}_2\text{O})_5$ and $\text{Na}^+(\text{H}_2\text{O})_6$ complexes. In the case of K^+ , as compared to Li^+ and Na^+ , the wider O-K-O angle is related to the observed higher flexibility of the K^+ hydrates. With regard to Figure 4.8, the shoulder of the peak at around $40\text{-}60^\circ$ corresponds to the contributions of the nearest neighbor waters that come close to the ion and the first-shell water molecules.



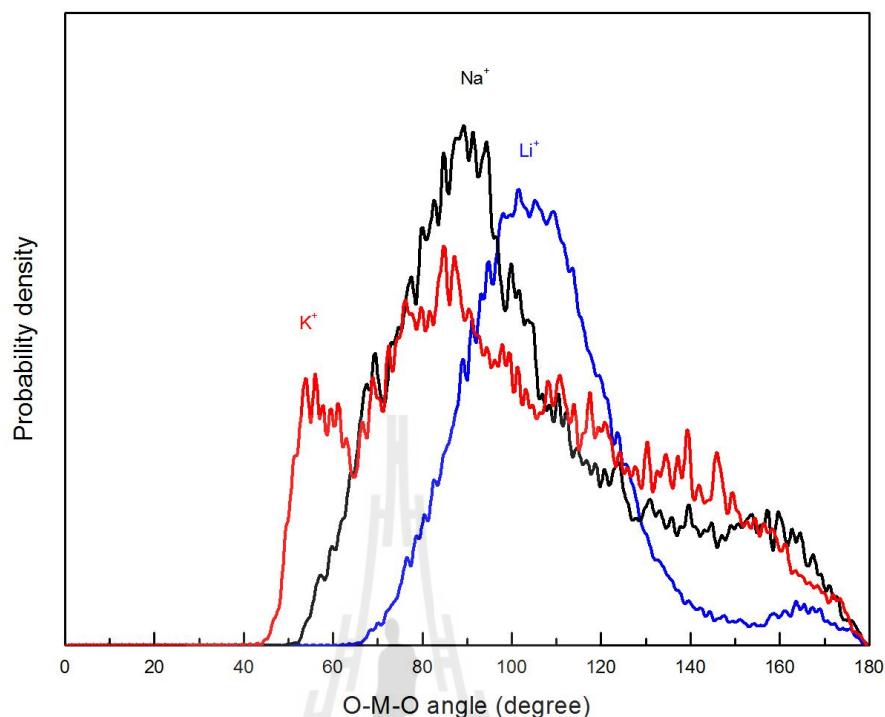


Figure 4.8 Distributions of the O---M---O angle, calculated within first minimum of the M-O RDFs.

Figure 4.9 displays the dipole-oriented arrangements of first-shell water molecules. In this context, the θ angle is defined by the M---O axis and the dipole vector of first-shell water molecules. Regarding the ONIOM-XS MD simulations, it is apparent that water molecules surrounding the ions are arranged with respect to the influence of the ions. However, the observed peaks with maxima at around 130° clearly suggest small influence of the ions in ordering their surrounding water molecules to form their specific hydration structures. In the cases of Li^+ and Na^+ , the ONIOM-XS MD results imply that the “structure-making” effects of these ions in aqueous solution might not be strong, *i.e.*, when compared to those of alkali earth metal ions, such as Ca^{2+} (Wanprakhon, Tongraar and Kerdcharoen, 2011).

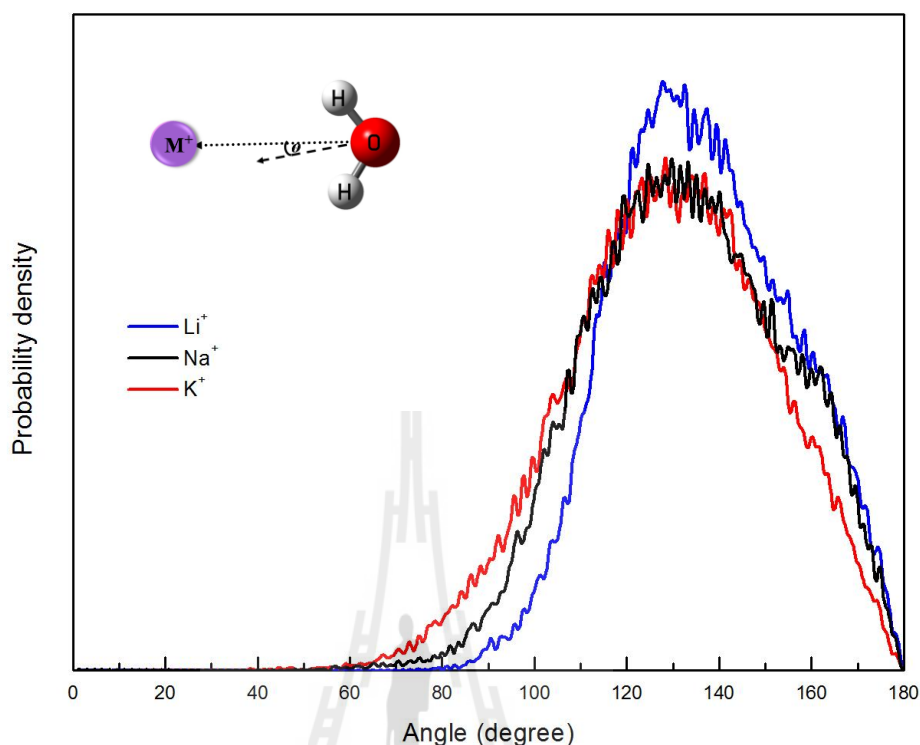
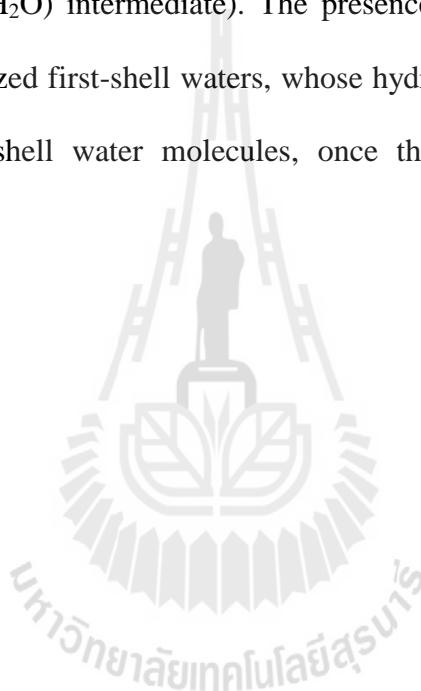


Figure 4.9 Probability distributions of θ angle in the first hydration shells of Li^+ , Na^+ and K^+ , calculated within first minimum of the M-O RDFs.

Figures 4.10 and 4.11 show the plots of time dependences of $\text{M}^+\text{---O}$ distance and number of first-shell waters, as obtained from first 20 ps of the ONIOM-XS MD simulations of Na^+ and K^+ in water, respectively. For Na^+ , it is observed that the structure of the Na^+ hydrates is rather flexible in which the most favorable $\text{Na}^+(\text{H}_2\text{O})_5$ species can convert back and forth to the lower probability $\text{Na}^+(\text{H}_2\text{O})_6$ complexes. This leads to several re-arrangements of the hydrated Na^+ complexes, as well as numerous attempts of first-shell waters to interchange with water molecules in the outer region. For example, at the simulation time of 5.2 ps, the arrangement of $\text{Na}^+(\text{H}_2\text{O})_4(\text{H}_2\text{O})$ complexes ($\text{CN} = 4$) can temporarily be formed, *i.e.*, one first-shell

water molecule (labeled in “green”) moved as far as 1 Å away from its optimal distance but it forms a hydrogen bond to an inner-shell water molecule. In addition, other transition complexes, such as of the types $\text{Na}^+(\text{H}_2\text{O})_5(\text{H}_2\text{O})_2$ and $\text{Na}^+(\text{H}_2\text{O})_6(\text{H}_2\text{O})$ (CN = 7), can transiently be formed (*e.g.*, at the simulation time of 9.1 ps, in which a “green” water molecule from the outer region approaches as close as 3 Å to the Na^+ ion and form hydrogen bonds to some inner-shell water molecules, forming $\text{Na}^+(\text{H}_2\text{O})_6(\text{H}_2\text{O})$ intermediate). The presence of such intermediates can be ascribed to the polarized first-shell waters, whose hydrogen atoms can form hydrogen bonds to the outer-shell water molecules, once they are arranged in a suitable geometrical position.



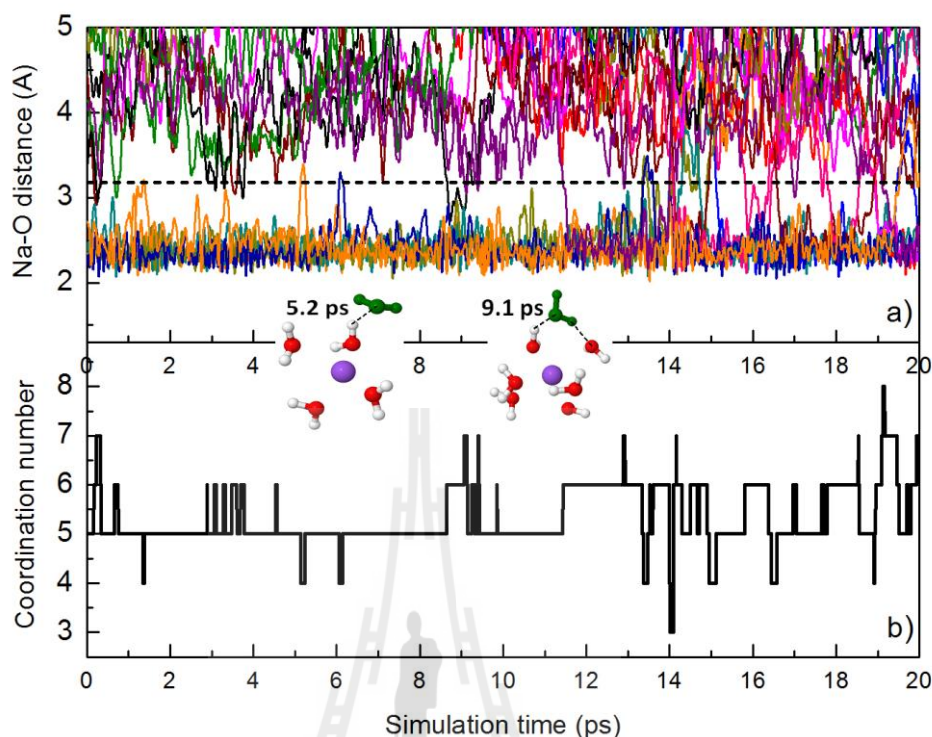


Figure 4.10 Time dependences of a) Na^+ ---O distance and b) number of first-shell waters, as obtained from first 20 ps of the ONIOM-XS MD simulation.

For K^+ (cf. Figure 4.11), it is observed that water molecules in the first hydration shell are rather labile, showing several re-arrangements of the hydrated K^+ complexes, as well as numerous attempts of outer-shell water molecules to interchange with the inner-shell waters. These observed several exchange processes clearly indicate that the K^+ complex is not only more flexible than the Li^+ and Na^+ complexes, but also than the solvent structure itself. In this respect, the K^+ can be considered as a perturbation to its surrounding water environment, reflecting the experimentally observed “structure-breaking” ability of this ion.

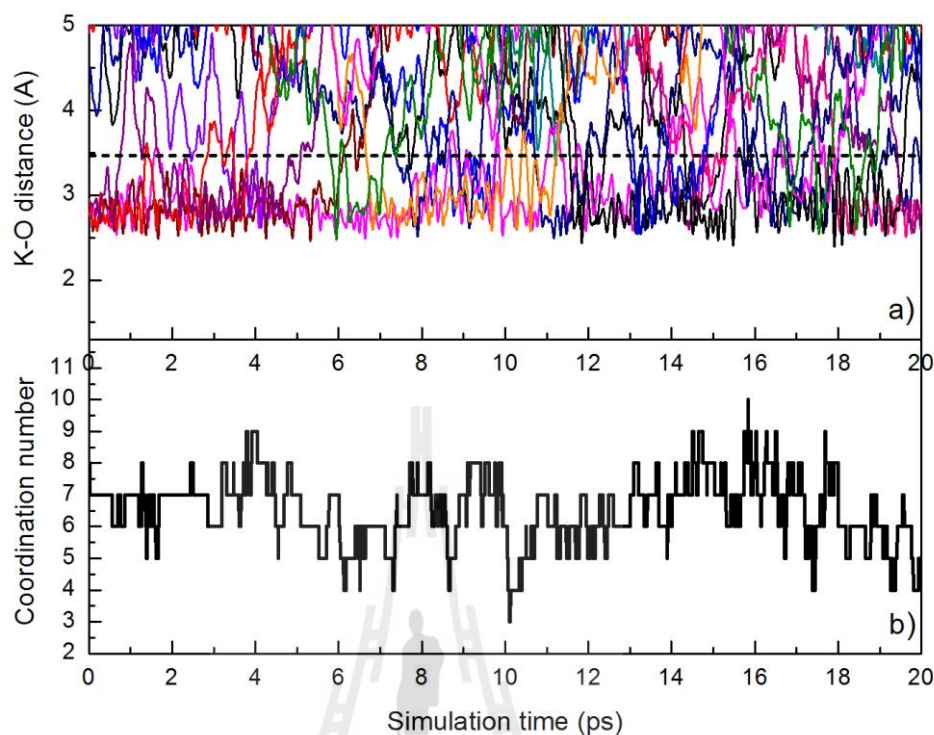


Figure 4.11 Time dependences of a) K^+ ---O distance and b) number of first-shell waters, as obtained from first 20 ps of the ONIOM-XS MD simulation.

Table 4.2 summarizes the D values of water molecules in the bulk and those in the first hydration shells of Li^+ , Na^+ and K^+ , as obtained by the ONIOM-XS MD simulations. In comparison to the D value of pure water (Thaomola, Tongraar and Kerdcharoen, 2012), water molecules in the first hydration shell of Li^+ are well attached to the ion, showing a clear “structure-making” ability of Li^+ in aqueous solution. However, it is worth noting that its “structure-making” ability is less significant than those of alkali earth metal ions, such as Ca^{2+} (Wanprakhon, Tongraar and Kerdcharoen, 2011). For Na^+ , the D value is also larger than the value of pure water, indicating a “structure-making” ability of this ion. As compared to Li^+ ,

however, its “structure-making” ability is relatively weak. In the cases of K^+ , the D value of first-shell waters is comparable to that of bulk water, which corresponds to the “structure-breaking” ability of this ion in water.

Table 4.2 D values of water molecules in the bulk and in the hydration shells of Li^+ , Na^+ and K^+ , as obtained by the ONIOM-XS MD simulations.

Phase	D ($cm^2 \cdot s^{-1}$)
Hydration shell of Li^+	1.38×10^{-5}
Hydration shell of Na^+	1.75×10^{-5}
Hydration shell of K^+	2.14×10^{-5}
Bulk water *	2.73×10^{-5}

* (Thaomola, Tongraar and Kerdcharoen, 2012)

The MRT values of water molecules in the bulk and in the vicinity of Li^+ , Na^+ , K^+ and Ca^{2+} , as obtained by the ONIOM-XS MD simulations, are summarized in Table 4.3. For both $t^* = 0.0$ and 0.5 ps, the MRT values of water molecules in the hydration shell of Li^+ are higher than the corresponding values of bulk waters, confirming a clear “structure-making” ability of Li^+ in aqueous solution. However, as mentioned earlier, the ability of Li^+ in ordering the structure of its surrounding waters is much less than that of a stronger “structure-maker”, like Ca^{2+} (Sripa, Tongraar and Kerdcharoen, 2013; Wanprakhon, Tongraar and Kerdcharoen, 2011). In the case of Na^+ , the MRT values of water molecules in the hydration shell of this ion are also higher than those of bulk waters, showing a “structure-making” ability of Na^+ in

aqueous solution. However, the ability of Na^+ in ordering the structure of its surrounding waters is less than that of Li^+ . In this respect, it could be demonstrated that Na^+ acts as a weak “structure-maker” in aqueous solution. The ONIOM-XS MD results are consistent with the assignment of “structure-makers/breakers” according to Marcus (Marcus, 2009), indicating that Na^+ should be a weak “structure-maker”, *i.e.*, it is considered as a borderline ion dividing “structure-makers” from “structure-breakers”. In terms of thermodynamics evidences, the details with respect to ion hydration entropies can provide a direct connection to ordering effects due to the insertion of ions into bulk water (Beck, 2011; Collins, 2012). For Na^+ , the hydration entropy of this ion analyzed via energetic partitioning of the potential distribution theorem free energy suggested that Na^+ is indeed a weak “structure-maker” and that the effect is relatively local around the ion (Beck, 2011). Very recently, the hydration of Na^+ in aqueous solution has been studied by large angle X-ray scattering (LAXS) and double difference infrared spectroscopy (DDIR), suggesting that this ion is weakly hydrated with only a single shell of water molecules and that it may be a “structure-breaker” even though its interactions with water are stronger than bulk water molecules interacting internally (Mähler and Persson, 2011). In the case of K^+ , the MRT values of first-shell waters are close to the corresponding data for bulk waters, suggesting that K^+ may not be able to form any specific geometrical order of its hydration shell. Thus, this ion can be classified as a “structure-breaker” in aqueous solution.

Table 4.3 Number of water exchange events (N_{ex}) and mean residence times (MRTs) of water molecules in the vicinity of ions and in the bulk, as obtained by ONIOM-XS MD simulations.

Ion/solute	CN	t_{sim}	$t^* = 0.0$ ps		$t^* = 0.5$ ps	
			$N_{ex}^{0.0}$	$\tau_{H_2O}^{0.0}$	$N_{ex}^{0.5}$	$\tau_{H_2O}^{0.5}$
Li ⁺	4.2	40.0	79	2.31	13	12.92
Na ⁺	5.4	41.0	164	1.35	36	6.18
K ⁺	6.5	40.0	557	0.46	107	2.42
H ₂ O *	4.7	30.0	607	0.23	65	2.17
Ca ²⁺ **	7.6	40.0	30	10.13	14	21.71

* (Thaomola, Tongraar and Kerdcharoen, 2012)

** (Wanprakhon, Tongraar and Kerdcharoen, 2011)

More details regarding the dynamics of water molecules in the vicinity of ions can be gained by computing the velocity autocorrelation functions (VACFs) of first-shell waters and their Fourier transformations. In this work, the normal-coordinate analysis developed by Bopp (Bopp, 1986; Spohr, Pálinkás, Heinzinger, Bopp and Probst, 1988) was used for obtaining three quantities Q_2 , Q_1 and Q_3 , which are defined for describing bending vibration, and symmetric and asymmetric stretching vibrations of water molecules, respectively, as depicted in Figure 4.12. By the ONIOM-XS MD technique, since all atomic motions of first-shell water molecules are generated according to QM force calculations, the calculated vibrational spectra are usually scaled by an empirical factor, *i.e.*, an approximate correction for errors in the force constants and for anharmonic effects (Johnson, Irikura, Kacker and Kessel, 2010;

Merrick, Moran and Radom, 2007; Scott and Radom, 1996). With regard to the systematic error of HF frequency calculations, all frequencies obtained by the ONIOM-XS MD simulation were multiplied by an appropriate scaling factor of 0.905 (Scott and Radom, 1996). To reliably illustrate the “structure-making” ability of ions in water, the corresponding Q_1 , Q_2 and Q_3 frequencies obtained from the ONIOM-XS MD simulation of liquid water (Thaomola, Tongraar and Kerdcharoen, 2012) were utilized for comparison. All intramolecular vibrational frequencies (Q_1 , Q_2 and Q_3) of water molecules in the hydration shell of Li^+ , Na^+ , K^+ and in the liquid water are given in Table 4.4. For liquid water, all the bending and stretching vibrational frequencies showed peaks with recognizable shoulders, especially for the symmetric and asymmetric vibrational modes. These observed spectra have been ascribed to the presence of several kinds, with varying strengths, of HBs formed in liquid water (Thaomola, Tongraar and Kerdcharoen, 2012). In the hydration shell of ions, water molecules are less mobilized and are arranged with respect to the influence of the ions, leading to more intense and better defined vibrational frequencies. As compared to liquid water, the bending frequency of first-shell waters shows a clear “red-shift”, *i.e.*, by about $25\text{-}30\text{ cm}^{-1}$, while the symmetric (Q_1) and asymmetric (Q_3) stretching frequencies are mostly found to be exhibited between the main peaks and the shoulders of the respective Q_1 and Q_3 frequencies of liquid water. These observed data are in good accord with the observed “structure-making” and “structure-breaking” abilities of the three ions. In this context, it could be demonstrated that the results obtained by the ONIOM-XS MD simulations can provide more insights into the behaviors of the Li^+ , Na^+ and K^+ hydrates, which are very crucial in order to correctly understand the reactivity of these ions in aqueous solution.

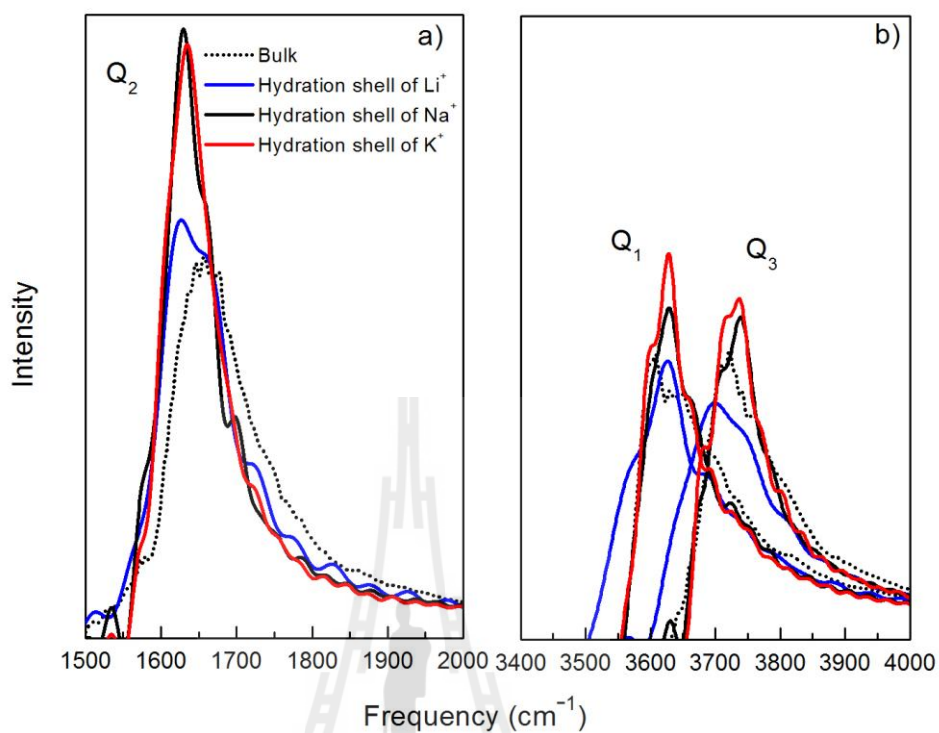


Figure 4.12 Fourier transforms of the hydrogen velocity autocorrelation functions of a) bending vibrations (Q_2) and b) symmetric and asymmetric stretching vibrations (Q_1 and Q_3) of water molecules in the first hydration shells of Li^+ , Na^+ and K^+ and in the bulk.

Table 4.4 Vibrational frequencies of water molecules in the hydration shells of Li^+ , Na^+ , K^+ and in the bulk water. (Q_1 , Q_2 and Q_3 corresponding to symmetric stretching, bending, and asymmetric stretching vibrations, respectively)

Phase	Frequency (cm^{-1})		
	Q_2	Q_1	Q_3
Hydration shell of Li^+	1627	3626	3699
Hydration shell of Na^+	1629	3628	3738
Hydration shell of K^+	1635	3628	3736
Pure water *	1660	3606 (3650)	3720 (3755)

* (Thaomola, Tongraar and Kerdcharoen, 2012)

4.3 References

- Bakker, H. J., Kropman, M. F. and Omta, A. W. (2005). Effect of ions on the structure and dynamics of liquid water. **Journal of Physics: Condensed Matter**. 17: S3215.
- Beck, T. L. (2011). A local entropic signature of specific ion hydration. **The Journal of Physical Chemistry B**. 115: 9776-9781.
- Bopp, P. (1986). A study of the vibrational motions of water in an aqueous CaCl_2 solution. **Chemical Physics**. 106: 205-212.
- Cappa, C. D., Smith, J. D., Messer, B. M., Cohen, R. C. and Saykally, R. J. (2006). Effects of cations on the hydrogenbond network of liquid water: New results from X-ray absorption spectroscopy of liquid microjets. **The Journal of Physical Chemistry B**. 110: 5301-5309.

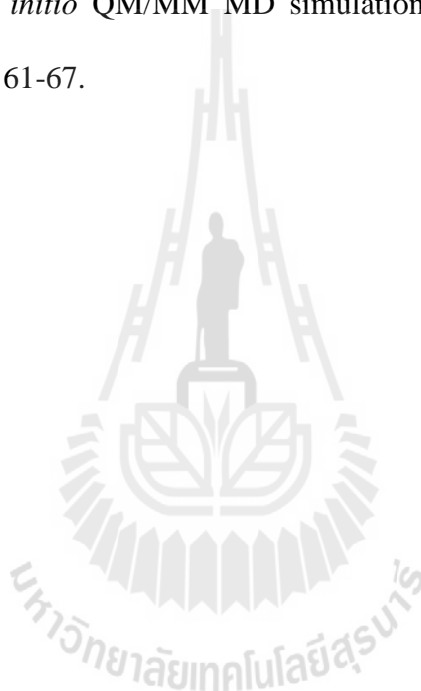
- DeFrees, D. J. and McLean, A. D. (1985). Molecular orbital predictions of the vibrational frequencies of some molecular ions. **The Journal of Chemical Physics**. 82: 333-341.
- Ikeda, T., Boero, M. and Terakura, K. (2007). Hydration of alkali ions from first principles molecular dynamics revisited. **The Journal of Chemical Physics**. 126: 034501-034509.
- Johnson, R. D., Irikura, K. K., Kacker, R. N. and Kessel, R. d. (2010). Scaling factors and uncertainties for *ab initio* anharmonic vibrational frequencies. **Journal of Chemical Theory and Computation**. 6: 2822-2828.
- Kabbalee, P., Tongraar, A. and Kerdcharoen, T. (2015). Preferential solvation and dynamics of Li^+ in aqueous ammonia solution: An ONIOM-XS MD simulation study. **Chemical Physics**. 446: 70-75.
- Kulik, H. J., Marzari, N., Correa, A. A., Prendergast, D., Schwegler, E. and Galli, G. (2010). Local Effects in the X-ray absorption spectrum of salt water. **The Journal of Physical Chemistry B**. 114: 9594-9601.
- Loeffler, H. H. and Rode, B. M. (2002). The hydration structure of the lithium ion. **The Journal of Chemical Physics**. 117: 110-117.
- Loeffler, H. H., Mohammed, A. M., Inada, Y. and Funahashi, S. (2003). Lithium (I) ion hydration: A QM/MM-MD study. **Chemical Physics Letters**. 379: 452-457.
- Lyubartsev, A. P., Laasonen, K. and Laaksonen, A. (2001). Hydration of Li^+ ion. An *ab initio* molecular dynamics simulation. **The Journal of Chemical Physics**. 114: 3120-3126.

- Mähler, J. and Persson, I. (2011). A study of the hydration of the alkali metal ions in aqueous solution. **Inorganic Chemistry**. 51: 425-438.
- Mancinelli, R., Botti, A., Bruni, F., Ricci, M. A. and Soper, A. K. (2007). Perturbation of water structure due to monovalent ions in solution. **Physical Chemistry Chemical Physics**. 9: 2959-2967.
- Merrick, J. P., Moran, D. and Radom, L. (2007). An evaluation of harmonic vibrational frequency scale factors. **The Journal of Physical Chemistry A**. 111: 11683-11700.
- Scott, A. P. and Radom, L. (1996). Harmonic vibrational frequencies: An evaluation of Hartree–Fock, Møller–Plesset, quadratic configuration interaction, density functional theory, and semiempirical scale factors. **The Journal of Physical Chemistry**. 100: 16502-16513.
- Spohr, E., Pálinkás, G., Heinzinger, K., Bopp, P. and Probst, M. M. (1988). A molecular dynamics study of an aqueous SrCl_2 solution. **The Journal of Physical Chemistry**. 92: 6754-6761.
- Sripa, P., Tongraar, A. and Kerdcharoen, T. (2013). “Structure-making” ability of Na^+ in dilute aqueous solution: An ONIOM-XS MD simulation study. **The Journal of Physical Chemistry A**. 117: 1826-1833.
- Thaomola, S., Tongraar, A. and Kerdcharoen, T. (2012). Insights into the structure and dynamics of liquid water: A comparative study of conventional QM/MM and ONIOM-XS MD simulations. **Journal of Molecular Liquids**. 174: 26-33.
- Wanprakhon, S., Tongraar, A. and Kerdcharoen, T. (2011). Hydration structure and dynamics of K^+ and Ca^{2+} in aqueous solution: Comparison of conventional

QM/MM and ONIOM-XS MD simulations. **Chemical Physics Letters**. 517: 171-175.

White, J. A., Schwegler, E., Galli, G. and Gygi, F. (2000). The solvation of Na^+ in water: First-principles simulations. **The Journal of Chemical Physics**. 113: 4668-4673.

Xenides, D., Randolf, B. R. and Rode, B. M. (2006). Hydrogen bonding in liquid water: An *ab initio* QM/MM MD simulation study. **Journal of Molecular Liquids**. 123: 61-67.



CHAPTER V

CONCLUSION

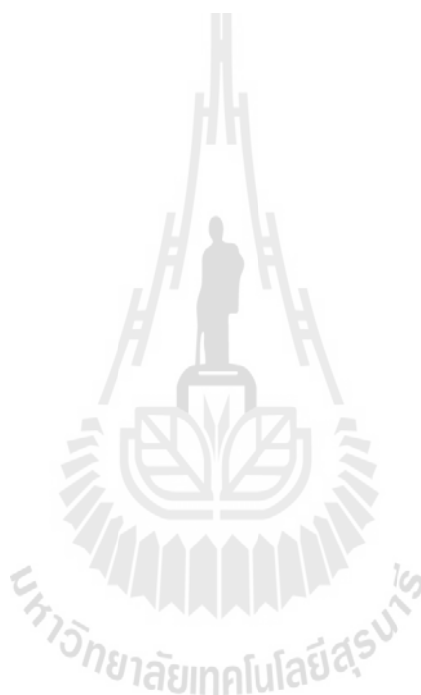
Structural and dynamical properties of alkali metal ions (Li^+ , Na^+ and K^+) in aqueous solution have been investigated by means of ONIOM-XS MD simulations. The region of most interest, *i.e.*, a sphere that includes the ion and its surrounding water molecules, was treated at the HF level of accuracy using the DZP basis set for water and Li^+ , and LANL2DZ basis set for Na^+ and K^+ , whereas the rest of the system was described by classical pair potentials. The HF method and the DZP and LANL2DZ basis sets employed in this work were considered to be good enough to provide reliable data, compromising between the quality of the simulation results and the requirement of the CPU time. In this respect, it should be realized that the instantaneous electron correlation and the charge transfer effects may not be typically well-described by the HF theory, and that the use of the DZP and LANL2DZ basis sets could result in a high basis set superposition error and an exaggeration of the ligand-to-metal charge transfer. In addition, the selected QM size was assumed to be large enough to include most of the many-body contributions and the polarization effects, *i.e.*, at least within the first hydration shell of the ions.

To verify the reliability of the ONIOM-XS MD technique for the study of such condensed phase systems, the hydration structure and dynamics of Li^+ in liquid water were firstly investigated by means of the conventional QM/MM and ONIOM-XS MD simulations. Based on the two QM/MM-based MD techniques, the features of

the first hydration shell of Li^+ are almost identical, showing a well-defined tetrahedral geometry with the average coordination numbers of 4.1 and 4.2, respectively. However, significant differences between the conventional QM/MM and ONIOM-XS MD simulations appear in the detailed analyses of the geometrical arrangement and the dynamics of the Li^+ hydrates. In the course of the ONIOM-XS MD simulation, it was observed that the structure of the hydrated Li^+ is more flexible and that, besides the prevalent $\text{Li}^+(\text{H}_2\text{O})_4$ species, other ion-water complexes, in particular the $\text{Li}^+(\text{H}_2\text{O})_5$, could more frequently be formed in aqueous solution. Together with the analyses on the dynamical data, the ONIOM-XS MD results clearly supply information that the “structure-making” ability of Li^+ in aqueous solution is not too strong. These observed differences clearly confirm the important treatment of the ONIOM-XS MD technique in obtaining more reliable description of this hydrated ion.

Later, the characteristics of Na^+ and K^+ with respect to their “structure-making” and “structure-breaking” abilities in aqueous solution were investigated through the ONIOM-XS MD simulations. For the Na^+ hydration, a distorted octahedral arrangement with the average coordination number of 5.4 is observed. The detailed analyzes of the ONIOM-XS MD trajectories show that Na^+ is able to order the structure of waters in its surroundings, forming two prevalent $\text{Na}^+(\text{H}_2\text{O})_5$ and $\text{Na}^+(\text{H}_2\text{O})_6$ species with the probability distributions of 56% and 37%, respectively. Interestingly, it is observed that these 5-fold and 6-fold coordinated complexes can convert back and forth with some degree of flexibility, leading to frequent rearrangements of the Na^+ hydrates, as well as numerous attempts of inner-shell water molecules to interchange with waters in the outer region. Such phenomenon clearly demonstrates the weak “structure-making” ability of Na^+ in aqueous solution.

In the case of K^+ , the ONIOM-XS MD simulation reveals a distorted octahedral geometry with the average coordination number of 6.5. As compared to Li^+ and Na^+ , the first hydration shell of K^+ is less structured and water molecules surrounding the ion are more labile, showing several re-arrangements of the hydrated K^+ complexes. This implies that K^+ may not be able to form any specific geometrical order of its hydration shell, and thus, this ion can be classified as a “structure-breaker” in aqueous solution.





APPENDICES

APPENDIX A

EXPERIMENTAL AND THEORETICAL

OBSERVATIONS OF Li⁺, Na⁺ and K⁺ IN AQUEOUS

SOLUTION

Table A1 Experimental data for aqueous Li⁺ solutions.

Solute	Molarity (M)	Method	CN	r _{ion-O} (Å)	Year	Ref.
LiCl	2.0	XRD	4	2.17	1980	Palinkas <i>et al.</i>
LiBr	2.1	XRD	4	2.25	1975	Licheri <i>et al.</i>
LiBr	2.29	XRD	4	1.99	1991	Cartailler <i>et al.</i>
LiBr	4.5	XRD	4	2.14	1975	Licheri <i>et al.</i>
LiBr	5.6	XRD	4	2.16	1975	Licheri <i>et al.</i>
LiI	2.2	XRD	6	2.10	1986	Palincas <i>et al.</i>
LiI	2.78	XRD	4-6	2.20	1987	Tamura <i>et al.</i>
LiCl	1.0	ND	4	1.90 ± 0.05	1979	Ohtomo <i>et al.</i>
LiCl	1.0	ND	6.5 ± 1	1.96	1996	Howell <i>et al.</i>
LiCl	2.14	ND	3.7	1.95	1999	Novikov <i>et al.</i>
LiCl	3.57	ND	5.5	1.95	1980	Newsome <i>et al.</i>
LiCl	3.6	ND	6.0 ± 0.04	1.95	1996	Howell <i>et al.</i>
LiCl	9.3	ND	4	2.02	1995	Yamaguchi <i>et al.</i>
LiCl	9.95	ND	3.3	1.95	1980	Newsome <i>et al.</i>
LiCl	14.0	ND	3.2 ± 0.2	1.96	1996	Howell <i>et al.</i>

Table A2 Theoretical observations of Li⁺ in aqueous solutions.

Solute	ion/water ratio	Method	CN	$r_{\text{ion-O}}$ (Å)	Year	Ref.
Li ⁺	1/89	MM MC	4.0	3.88	2004	Öhrn <i>et al.</i>
Li ⁺	1/199	MM MD	6.0	2.06	1998	Tongraar <i>et al.</i>
Li ⁺	1/499	MM MD	4.0	2.05	2006	Loeffler <i>et al.</i>
Li ⁺	1/500	MM MD	4.08	2.03	2006	Lamoureux <i>et al.</i>
Li ⁺	1/255	MM MD	4.4	1.97	2002	Zhou <i>et al.</i>
Li ⁺	1/512	MM MD	4.02	1.96	2003	Spångberg <i>et al.</i>
Li ⁺	1/525	MM MD	4.5	2.0	1996	Obst and Brada
Li ⁺	1/986	MM MD	4.07 ± 0.03	-	2005	Chorny <i>et al.</i>
Li ⁺	1/6	AIMD	4	-	2000	Rempe <i>et al.</i>
Li ⁺	1/32	CPMD	4	1.96	2000	Lyubartsev <i>et al.</i>
Li ⁺	1/63	FPMD	4.0	1.882	2007	Ikeda <i>et al.</i>
Li ⁺	1/199	QM/MM MD	4.1	1.94	1998	Tongraar <i>et al.</i>
Li ⁺	1/499	QM/MM MD	4.0	1.95	2006	Loeffler <i>et al.</i>
Li ⁺	1/499	QM/MM MD	4.3	1.97	2003	Loeffler <i>et al.</i>

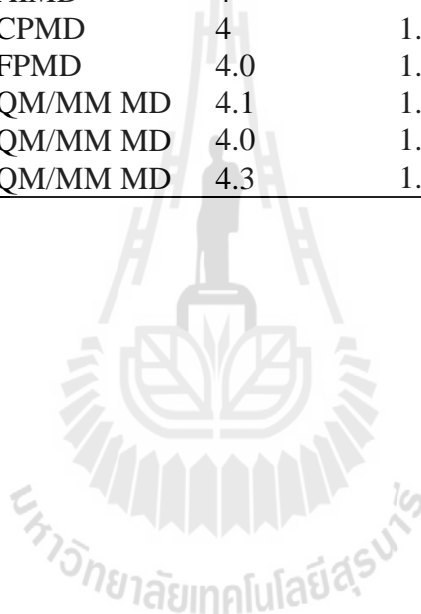


Table A3 Experimental data for aqueous Na⁺ solutions.

Solute	Molarity (M)	Method	CN	$r_{\text{ion-O}}$ (Å)	Year	Ref.
NaCl	1.1	XRD	4.1	2.82	2006	Bondarenko <i>et al.</i>
NaCl	6.167	XRD	4.6	2.39	1998	Kameda <i>et al.</i>
NaNO ₃	3.13	XRD	4.9± 0.1	2.40	1989	Skipper <i>et al.</i>
NaNO ₃	6.01	XRD	6	2.44	1980	Caminiti <i>et al.</i>
NaCl	1.0	ND	8	2.50	1980	Ohtomo <i>et al.</i>
NaCl	1/83	ND	5.3	3.2	2007	Mancinelli <i>et al.</i>
NaCl	0.5	XAS	5.2	-	2010	Kulik <i>et al.</i>



Table A4 Theoretical observations of Na⁺ in aqueous solutions.

Solute	ion/water ratio	Method	CN	$r_{\text{ion-O}}$ (Å)	Year	Ref.
Na ⁺	1/89	MM MC	5.85	4.63	2004	Öhrn and Karlström
Na ⁺	-	MM MC	5.56	2.37	2003	Carrillo-Tripp <i>et al.</i>
Na ⁺	1/255	MM MC	6.0	2.5	2001	Kim
Na ⁺	1/499	MM MD	6.19	2.37	2010	Azam <i>et al.</i>
Na ⁺	1/216	MM MD	6.0	2.233	2003	Grossfield <i>et al.</i>
Na ⁺	1/255	MM MD	6.0	2.37	2002	Zhou <i>et al.</i>
Na ⁺	1/512	MM MD	5.68	2.43	2004	Spangberg <i>et al.</i>
Na ⁺	1/525	MM MD	6.0	2.597	1996	Obst and Bradaczek
Na ⁺	1/986	MM MD	5.72 ± 0.07	-	2005	Chorny <i>et al.</i>
Na ⁺	-	CPMD	5.31	2.50	2008	Megyes <i>et al.</i>
Na ⁺	1/53	CPMD	5.2	2.49	2000	White <i>et al.</i>
Na ⁺	1/32	BOMD	4.8	2.35	2009	Galamba <i>et al.</i>
Na ⁺	1/63	FPMD	5.2 ± 0.1	2.40	2007	Ikeda <i>et al.</i>
Na ⁺	1/199	QM/MM MD	5.6±0.3	2.33	1998	Tongraar <i>et al.</i>
Na ⁺	1/499	QM/MM MD	6.0	2.39	2010	Azam <i>et al.</i>
NaCl	1/499	QM/MM MD	5.5	2.34	2009	Azam <i>et al.</i>
NaCl	1/499	QMCF MD	5.5	2.5	2009	Azam <i>et al.</i>

Table A5 Experimental data for aqueous K⁺ solutions.

Solute	Molarity (M)	Method	CN	r _{ion-O} (Å)	Year	Ref.
KCl	2.0	XRD	6	2.8	1980	Palinkas <i>et al.</i>
KCl	2.4	ND	5.5	2.65	2006	Soper and Weckstrom
KCl	4.0	ND	-	3.1	1985	Neilson and Skipper
K ⁺	1.0	ND	8	2.70 ± 0.1	1980	Ohtomo and Arakawa
K ⁺	2.5	EXAFS	6.1	2.732	2006	Dang <i>et al.</i>

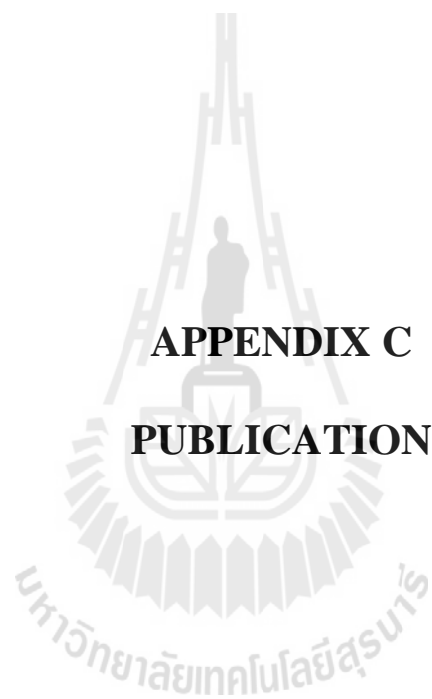
Table A6 Theoretical observations of K⁺ in aqueous solutions.

Solute	ion/water ratio	Method	CN	r _{ion-O} (Å)	Year	Ref.
K ⁺	1/255	MM MC	6.7	2.8	2001	Kim
K ⁺	-	MM MC	7.85	2.79	2003	Carrillo-Tripp <i>et al.</i>
K ⁺	1/499	MM MD	7.9	2.80	2010	Azam <i>et al.</i>
K ⁺	1/500	MM MD	6.90	2.74	2006	Lamoureux <i>et al.</i>
K ⁺	-	MM MD	5.7	2.77	2006	Dang <i>et al.</i>
K ⁺	1/216	MM MD	7.0	2.59	2003	Grossfield <i>et al.</i>
K ⁺	1/255	MM MD	6.1	2.86	2002	Zhou <i>et al.</i>
K ⁺	1/525	MM MD	7.60	2.9	1996	Obst and Bradaczek
K ⁺	1/59	CPMD	6.75	2.81	1999	Ramaniah <i>et al.</i>
K ⁺	1/63	FPMD	5.2 ± 0.1	2.85	2007	Ikeda <i>et al.</i>
K ⁺	1/32	AIMD	4+2	3.0	2004	Rempe <i>et al.</i>
K ⁺	1/199	QM/MM MD	8.3 ± 0.3	2.81	1998	Tongraar <i>et al.</i>
K ⁺	1/499	QM/MM MD	8.8	2.85	2010	Azam <i>et al.</i>
KCl	1/499	QM/MM MD	6.2	2.80	2009	Azam <i>et al.</i>
KCl	1/499	QMCF MD	6.8	2.80	2009	Azam <i>et al.</i>

APPENDIX B

LIST OF PRESENTATIONS

1. Pattrawan Sripa and Anan Tongraar. (March 27-29, 2013). Characteristics of Na^+ and K^+ in aqueous solution: Transition from “structure-making” to “structure-breaking” ability. **International Annual Symposium on Computational Science and Engineering (ANSCSE) 17th**, Khon Kaen University, Thailand.
2. Pattrawan Sripa and Anan Tongraar. (July 23-28, 2013). Local structure and dynamics of Li^+ , Na^+ and K^+ in water: An ONIOM-XS MD simulations study. **The 7th Conference of the Asian Consortium on Computational Materials Science (ACCMS-7)**, Suranaree University of Technology, Nakhon Ratchasima, Thailand.
3. Pattrawan Sripa and Anan Tongraar. (January 8-10, 2014). On the “structure-making” and “structure-breaking” abilities of alkali metal ions (Li^+ , Na^+ and K^+) in aqueous solutions: An ONIOM-XS MD simulations study. **Pure and Applied Chemistry International Conference 2014 (PACCON2014)**, Centara Hotel and Convention Centre, Khon Kaen, Thailand.



APPENDIX C
PUBLICATION

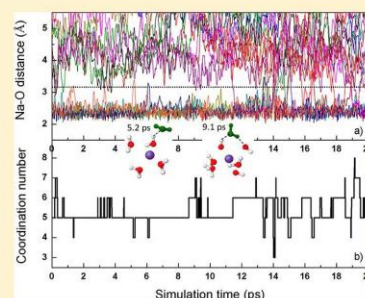
“Structure-Making” Ability of Na⁺ in Dilute Aqueous Solution: An ONIOM-XS MD Simulation Study

Pattawan Sripa,[†] Anan Tongraar,^{*,†} and Teerakiat Kerdcharoen[‡]

[†]School of Chemistry, Institute of Science, Suranaree University of Technology, Nakhon Ratchasima 30000, Thailand

[‡]Department of Physics and NANOTEC Center of Excellence, Faculty of Science, Mahidol University, Bangkok 10400, Thailand

ABSTRACT: An ONIOM-XS MD simulation has been performed to characterize the “structure-making” ability of Na⁺ in dilute aqueous solution. The region of most interest, i.e., a sphere that includes Na⁺ and its surrounding water molecules, was treated at the HF level of accuracy using LANL2DZ and DZP basis sets for the ion and waters, respectively, whereas the rest of the system was described by classical pair potentials. Detailed analyzes of the ONIOM-XS MD trajectories clearly show that Na⁺ is able to order the structure of waters in its surroundings, forming two prevalent Na⁺(H₂O)₅ and Na⁺(H₂O)₆ species. Interestingly, it is observed that these 5-fold and 6-fold coordinated complexes can convert back and forth with some degrees of flexibility, leading to frequent rearrangements of the Na⁺ hydrates as well as numerous attempts of inner-shell water molecules to interchange with waters in the outer region. Such a phenomenon clearly demonstrates the weak “structure-making” ability of Na⁺ in aqueous solution.



1. INTRODUCTION

Detailed knowledge of ions solvated in aqueous electrolyte solution has long been desirable for chemists and biologists to understand the role of these ions in chemical and biological processes.^{1,2} When ions are dissolved in liquid water, the effects of the ions can cause substantial modifications in the local structure and changes in the dynamics of the surrounding water molecules. In this respect, the manners in which ions order the structure of their surrounding waters to form their specific ion–water complexes are strongly related to the strength of ion–water interactions. In general, the terms “structure-makers” and “structure-breakers” have been widely used to describe the effect of different ions in ordering the hydrogen bond (HB) network of surrounding water molecules.³ For example, ions with a small size and high charge density, i.e., the ones that can potentially break the HB networks of their nearest-neighbor waters and can order those water molecules to form well-defined ion–water complexes, are classified as “structure-makers”. In contrast, ions with a large size and low charge density are classified as “structure-breakers”; i.e., they are regarded as causing perturbation of the water HBs. In the case of salt solutions, however, it should be realized that the classification of ions as “structure-makers” or “structure-breakers” could also depend on the salt concentration.

For simple alkali metal ions, Na⁺ is abundant in nature and is known as one of the essential elements that play a vital role for all known life. In particular, the contrasting behavior of Na⁺ in aqueous solution, i.e., compared to K⁺, is of special interest concerning the process of ionic pumps across the cell membrane.⁴ During the past several years, the details with respect to the structure and dynamics of Na⁺ in aqueous solution have been studied intensively, both by experiments

and by theoretical investigations.^{5–24} However, some discrepancies among those results still exist, even for the fundamental properties such as the average coordination number and the mean ion–water distance. For example, experimental observations revealed a large variation of coordination numbers, ranging from 4 to 8,^{5–13} which has been attributed mainly to the concentration dependence and the different experimental methods employed. In addition, it has been demonstrated that the concept of “structure-makers/breakers” is not helpful in understanding the effects of ions on water structure, leading to the ambiguous conclusion that Na⁺ can be classified both as a local “structure-maker” and as a long-range “structure-breaker”.¹² In this regard, because the modifications of the HB water structure in particular at a high salt concentration are due partly to the effect of ion pairing, the concept of “structure-makers/breakers” is probably applicable only for the discussion with respect to very dilute aqueous solutions, i.e., the solution containing a single ion.

Theoretical investigations, especially by means of molecular dynamics (MD) simulations, also predicted different hydration numbers of Na⁺, varying from 4.8 to 7.3.^{14–23} With regard to earlier MD studies,^{14–17,21,22} the observed discrepancies could be ascribed to the use of different molecular mechanical (MM) force fields in describing the system’s interactions; i.e., the quality of the simulation results depends crucially on the quality of the ion–water and water–water potentials employed. By several classical MD simulations, Na⁺ has been classified as a strong “structure-maker”.^{14–16} To obtain more reliable

Received: December 12, 2012

Revised: January 31, 2013

Published: February 18, 2013

simulation results, it has been demonstrated that the “quantum effects” are not negligible and that the inclusion of these effects in the simulations through quantum mechanical calculations is nowadays mandatory for studying such condensed phase systems.²⁴ In terms of ab initio (AI) MD techniques, first-principles (FP-MD)^{18,19} and Born–Oppenheimer (BO-MD)²⁰ simulations have been carried out for Na⁺ in water, providing detailed descriptions on the structure and dynamics of the Na⁺ hydrate. One major advantage of such AI-MD techniques is that the whole system is treated quantum mechanically, most of which are based on the density functional theory (DFT). However, some severe limitations of the AI-MD techniques come from the use of simple generalized gradient approximation (GGA) functionals, such as BLYP and PBE, and of the relatively small system size.²⁵ According to the FP-MD results, a strong discrepancy in determining the behavior of Na⁺ in water is observed, in which the earlier FP-MD simulation¹⁸ has predicted that Na⁺ is a weak “structure-maker”, whereas the later FP-MD work¹⁹ categorized this ion as a weak “structure-breaker”.

An alternative QM-based MD approach is to apply a so-called combined quantum mechanics/molecular mechanics (QM/MM) technique,^{26–28} which treats the active-site region, i.e., a small subsystem that contains most interesting particles, quantum mechanically, whereas the rest of the system is described by classical MM potentials. Recently, a series of QM/MM MD simulations has been performed for the systems of Na⁺ in aqueous solution,^{21–23} revealing results which are also in good accord with previously published experimental and theoretical studies. All QM/MM MD simulations had led to the similar conclusion that Na⁺ showed a clear “structure-making” ability, and that only a single layer of hydration is formed; i.e., the influence of the ion beyond the first hydration shell is definitely very weak. With regard to the QM/MM MD technique, however, a smoothing function is applied only for the exchanging particles that are crossing the QM/MM boundary. Such treatment clearly implies the methodical weakness because an immediate exchange of particles between the QM and MM regions also affects the forces acting on the remaining QM particles. In addition, the conventional QM/MM framework cannot clearly define the energy expression during the solvent exchange process.^{29,30} To solve these problems, a more sophisticated QM/MM MD technique based on the ONIOM-XS method (which will be abbreviated throughout this work as “ONIOM-XS MD”) has been proposed.^{29,30} This technique allows forces on all QM particles to be smoothed during particle exchange and, thus, better defines the system’s energy expression. By the ONIOM-XS MD technique, it is worth noting that both energies and forces can be smoothed, whereas only forces were handled in the conventional QM/MM MD scheme. Recently, the ONIOM-XS MD technique has been successfully applied for various systems, such as Li⁺ and Ca²⁺ in liquid ammonia,^{29,30} K⁺ and Ca²⁺ in aqueous solution,³¹ and pure water.³² Interestingly, it has been demonstrated that the ONIOM-XS MD technique becomes more effective for the situation where the number of ligands that are crossing the QM/MM boundary is large, i.e., a system in which the ion–water interactions are weak and water molecules surrounding the ion are labile.³¹ In this study, the ONIOM-XS MD technique will be applied to investigate the characteristics of Na⁺ hydrate, in particular those related to the “structure-making” ability of Na⁺ in aqueous solution.

2. METHOD

On the basis of the ONIOM-XS MD technique,^{29,30} the system is composed of a “high-level” QM region, i.e., a sphere that contains the Na⁺ ion and its surrounding water molecules, and the remaining “low-level” MM bulk waters. A thin switching layer located between the QM and MM regions is employed to smooth the energy and forces of the combined system according to the solvent exchange. Given n_1 , l , and n_2 as the number of particles in the QM region, the switching layer, and the MM region, respectively, and N as the total number of particles (i.e., $N = n_1 + l + n_2$), the potential energy of the system can be written in two ways with respect to the ONIOM extrapolation scheme.³³ If the switching layer is included into the “high-level” QM sphere, the energy expression is written as

$$E^{\text{ONIOM}}(n_1+l;N) = E^{\text{QM}}(n_1+l) - E^{\text{MM}}(n_1+l) + E^{\text{MM}}(N) \quad (1)$$

If the switching layer is considered as part of the “low-level” MM region, the energy expression is

$$E^{\text{ONIOM}}(n_1;N) = E^{\text{QM}}(n_1) - E^{\text{MM}}(n_1) + E^{\text{MM}}(N) \quad (2)$$

According to eqs 1 and 2, the E^{QM} and E^{MM} terms refer to the interactions derived by means of QM calculations and by the classical MM potentials, respectively. In this respect, the interactions between the QM and MM regions are described by means of MM potentials, and thus, these contributions are already included into the $E^{\text{MM}}(N)$. In practice, when a particle moves into the switching layer (from either the QM or MM region), both eqs 1 and 2 will be evaluated. The potential energy of the entire system is then taken as a hybrid between both energy terms 1 and 2,

$$E^{\text{ONIOM-XS}}(\{r_i\}) = (1 - \bar{s}(\{r_i\})) \cdot E^{\text{ONIOM}}(n_1+l;N) + \bar{s}(\{r_i\}) \cdot E^{\text{ONIOM}}(n_1;N) \quad (3)$$

where $\bar{s}(\{r_i\})$ is an average over a set of switching functions for individual exchanging particles in the switching layer $s_i(x_i)$,

$$\bar{s}(\{r_i\}) = \frac{1}{l} \sum_{i=1}^l s_i(x_i) \quad (4)$$

Basically, the switching function in eq 4 can have any form. In this study, a polynomial expression is employed,

$$s_i(x_i) = 6\left(x_i - \frac{1}{2}\right)^5 - 5\left(x_i - \frac{1}{2}\right)^3 + \frac{15}{18}\left(x_i - \frac{1}{2}\right) + \frac{1}{2} \quad (5)$$

where $x_i = [(r_i - r_0)/(r_1 - r_0)]$, and r_0 and r_1 are the radius of the inner and outer surfaces of the switching shell, respectively, and r_i is the distance between the ion and the oxygen atom of the exchanging water molecule. Note that the above polynomial form and parameter sets were derived to have an S-shape that converges to 0 and 1 at r_0 and r_1 , respectively.²⁹ This polynomial form is preferred over the ST2 switching function³⁴ usually employed in the conventional QM/MM MD scheme because its first and second derivatives are both continuous. Finally, the gradient of the energy can be expressed as

Table 1. Optimized Parameters of the Analytical Pair Potentials for the Interactions of Water with Na⁺ (Interaction Energies in kcal·mol⁻¹ and Distances in Å)

pair	A (kcal mol ⁻¹ Å ⁴)	B (kcal mol ⁻¹ Å ⁸)	D (kcal mol ⁻¹)	D (Å ⁻¹)
Na–O	-663.2089588	967.45544406	28536.783215	3.2925018407
Na–H	148.8680902	605.89247202	-7143.0151207	3.5661952849

$$\begin{aligned} \nabla_{\mathbf{R}} E^{\text{ONIOM-XS}}(\{r_i\}) &= (1 - \bar{s}(\{r_i\})) \cdot \nabla_{\mathbf{R}} E^{\text{ONIOM}}(n_i + l; N) + \bar{s}(\{r_i\}) \cdot \\ &\nabla_{\mathbf{R}} E^{\text{ONIOM}}(n_i; N) + \frac{1}{(r_i - r_0)} \nabla \bar{s}(\{r_i\}) \cdot \\ &(E^{\text{ONIOM}}(n_i; N) - E^{\text{ONIOM}}(n_i + l; N)) \end{aligned} \quad (6)$$

In this work, because the correlated QM calculations, even at the simple MP2-level, are rather too time-consuming for our current computational feasibility, all interactions within the QM region were evaluated by performing ab initio calculations at the Hartree–Fock (HF) level of accuracy using DZP³⁵ and LANL2DZ^{36,37} basis sets for H₂O and Na⁺, respectively. With regard to the fact that the HF method could produce an error due to the neglect of electron correlation effects, it is assumed that the use of this method with sufficiently large QM size and basis sets can achieve a sufficient level of accuracy, compromising between the quality of the simulation results and the requirement of CPU time.²⁴ The DFT methods, such as B3LYP, are not taken into account for this work because these methods often yielded overestimation of the ion–water interactions as well as considerably shorter ion–water distances.^{22,23} For the QM size, a QM radius of 4.2 Å and a switching width of 0.2 Å were chosen, corresponding to the ONIOM-XS parameters r_0 and r_1 of 4.0 and 4.2 Å, respectively. This QM size is considered to be large enough to include most of the many-body contributions and the polarization effects, i.e., at least within the first hydration shell of Na⁺, and the remaining interactions beyond the QM region could be well accounted for by the MM potentials. As can be seen in the next section (cf. Figure 1), the smooth shape of the Na–O radial distribution function (RDF) between 4.0 and 4.2 Å clearly supplies information that transition of water molecules between the QM and MM regions occurs smoothly. For the interactions within the MM and between the QM and MM regions, a flexible BJH–CF2 model, which describes intermolecular³⁸ and intramolecular³⁹ interactions, was employed for water. This flexible water model allows explicit hydrogen movements and, thus, ensures a smooth transition when water molecules move from the QM region with its full flexibility to the MM region and vice versa. The pair potential functions for describing Na⁺–H₂O interactions were newly constructed. The 2424 HF interaction energy points for various Na⁺–H₂O configurations, obtained from Gaussian03⁴⁰ calculations using DZP³⁵ and LANL2DZ^{36,37} basis sets for H₂O and Na⁺, respectively, were fitted to the analytical form of

$$\Delta E_{\text{Na}^+ - \text{H}_2\text{O}} = \sum_{i=1}^3 \left(\frac{A_{ic}}{r_{ic}^4} + \frac{B_{ic}}{r_{ic}^8} + C_{ic} \exp(-D_{ic} r_{ic}) + \frac{q_i q_c}{r_{ic}} \right) \quad (7)$$

where A , B , C , and D are fitting parameters (Table 1), r_{ij} denotes the distances between the ion and the i th atoms of water molecule, and q are the atomic net charges. In this work, the charge for Na⁺ was set to 1.0, and the charges for O and H

atoms of water were set with respect to the BJH–CF2 model, i.e., -0.6598 and $+0.3299$ for O and H atoms, respectively.

The ONIOM-XS MD simulation was performed in a canonical ensemble at 298 K with periodic boundary conditions. The system's temperature was kept constant using the Berendsen algorithm.⁴¹ A periodic box, with a box length of 18.19 Å, contains one Na⁺ and 199 water molecules, corresponding to the experimental density of pure water. The reaction-field method⁴² was employed for the treatment of long-range interactions. The Newtonian equations of motions were treated by a general predictor-corrector algorithm. The time step size was set to 0.2 fs, which allows for the explicit movement of the hydrogen atoms of water molecules. The ONIOM-XS MD simulation was started with the system's re-equilibration for 30 000 time steps, followed by another 205 000 time steps to collect configurations every 10th step.

3. RESULTS AND DISCUSSION

The hydration shell structure of Na⁺ can be described by means of Na–O and Na–H RDFs, together with their corresponding integration numbers, as depicted in Figure 1. With regard to the ONIOM-XS MD simulation, a well-defined first Na–O peak with a maximum centered at 2.35 Å is observed. Interestingly, the nonzero minimum following the first Na–O peak clearly suggests some exchange processes between first-shell waters and water molecules in the outer region. Integration up to the

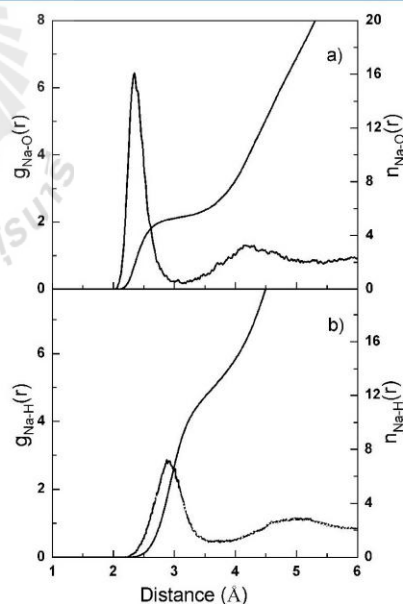


Figure 1. (a) Na–O and (b) Na–H radial distribution functions and their corresponding integration numbers.

first minimum of the Na–O RDF yields an average coordination number of 5.4 ± 0.1 . This observed value is in good agreement with the recent ND experiments¹² and AI-MD studies,^{13,18,19} which reported the coordination numbers of 5.3 and 5.2, respectively. The second peak of the Na–O RDF is less pronounced, indicating that the influence of Na⁺ beyond the first hydration layer is relatively weak; i.e., only a single layer of Na⁺ hydration is formed. The ONIOM-XS MD results are in good accord with the interpretation of X-ray absorption spectroscopy (XAS) experiments, which indicated that there is no long-range effect on the HB network of water due to the presence of monovalent cations.⁴³ With regard to the XAS results, it has been demonstrated that the changes in the XAS spectra observed upon addition of monovalent cation halide salts are due mainly to the interactions of water molecules with the halide anions. In addition, according to the recent femtosecond pump–probe spectroscopy study,⁴⁴ it has been suggested that the effect of alkali ions on the structure and dynamics of water is limited to the first hydration shell of ions; i.e., the HB network beyond the first shell is not different from that of bulk water.

As can be seen in Figure 1, the shape and height of the first Na–O and Na–H peaks clearly indicate the “structure-making” ability of Na⁺ in aqueous solution, i.e., the ability by which the ion can order the HB structure of its surrounding waters to form its specific Na⁺–water complexes. In this study, it should be clarified at the beginning that all discussion with respect to the “structure-making” ability of Na⁺ in water assumes a sufficiently dilute aqueous solution, i.e., the solution in which the influences of either counterion or ion-pairing are negligible. The “structure-making” effect of Na⁺ in aqueous solution has been discussed in detail in the recent QM/MM and quantum mechanical charge field (QMCF) MD studies²³ using the HF method and the same basis sets as employed in the present ONIOM-XS MD simulation. In fact, the QMCF framework⁴⁵ has been formulated to neglect the construction of non-Coulombic interaction potentials between solute and solvent particles. Nevertheless, it has been shown that the QMCF method with a sufficiently large QM size, i.e., where all exchange processes between the first and second hydration layer occur within the QM region, and a suitable embedding scheme has several advantages over the conventional QM/MM technique.²³ In particular, because the smoothing zone takes place at a relatively large distance to the ion, the error introduced by the nonconservation of momenta, as pointed out by Truhlar et al.,⁴⁶ becomes nearly negligible. In this work, as compared to the QMCF MD results,²³ the ONIOM-XS MD simulation reveals rather similar structural parameters for the Na⁺ hydrate, such as the average ion–water distance and the coordination number. However, the feature of the ONIOM-XS MD’s Na–O and Na–H RDFs are somewhat different, especially in terms of the half-width and intensity of the first-shell peaks. On the basis of ONIOM-XS MD simulation, the increased intensity of the first Na–O and Na–H peaks can be ascribed to the artificial “pressure” of the MM molecules on the QM region; i.e., the Coulombic interactions of the QM–MM coupling are computed according to fixed charges for both the QM and MM atoms. In this respect, a formal charge of +1.0 assigned to Na⁺ results in a slightly too strong ion–water interactions. Comparing to results from the QMCF MD technique, the partial charges of the QM particles are newly derived via population analysis in every step of the simulation.²³ In addition, the observed differences between the ONIOM-XS

and QMCF MD simulations could be due partly to the use of different QM size, i.e., of the QM radii of 4.2 and 5.7 Å, respectively. With regard to this point, it could be demonstrated that further improvement of the ONIOM-XS MD results is achievable by performing the simulation in conjunction with the use of larger QM size and a suitable embedding methodology, such as the partial charge schemes employed in the QMCF framework.

Figure 2 displays the probability distributions of the coordination numbers of Na⁺, calculated up to first minimum

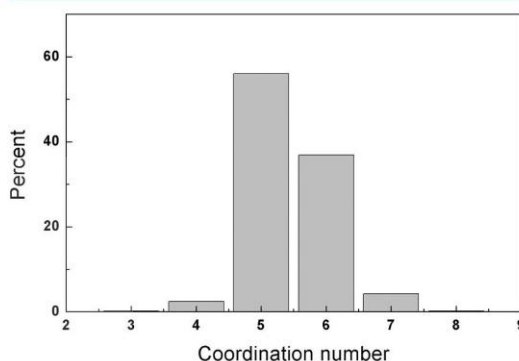


Figure 2. Distributions of the coordination numbers of Na⁺, calculated within the first minimum of the Na–O RDF.

of the Na–O RDF. It is obvious that this ion prefers the coordination numbers of 5 and 6, with the probability distributions of 56% and 37%, respectively, whereas the distributions of 4-fold and 7-fold coordinated complexes appear to be quite rare. This supplies information that only Na⁺(H₂O)₅ and Na⁺(H₂O)₆ complexes are the most prevalent species formed in aqueous solution. The flexibility of Na⁺ hydration can be described by the distributions of O---Na---O angle, as shown in Figure 3. In addition, the orientation of water molecules in the vicinity of Na⁺ is also given in Figure 4. In this context, the angle θ is defined by the Na---O axis and the dipole vector of first-shell water molecules. According to

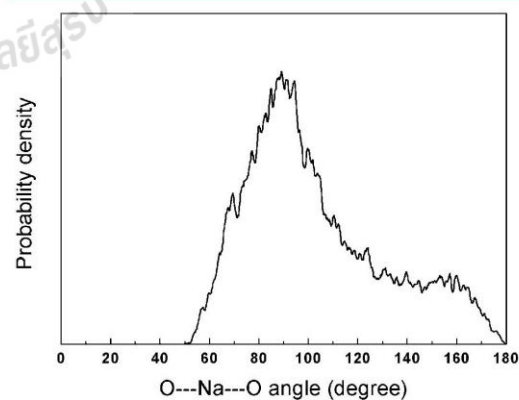


Figure 3. Distributions of the O---Na---O angle, calculated within the first minimum of the Na–O RDF.

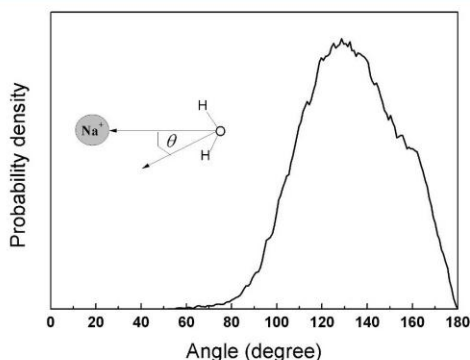


Figure 4. Probability distributions of θ angle in the first hydration shell of Na^+ , calculated within the first minimum of the Na–O RDF.

Figures 3 and 4, the observed broad distributions of both O---Na---O and θ angles clearly indicate a less ordered orientation of first-shell water molecules, i.e., showing that the hydration shell structure of Na^+ is somewhat flexible and that the “structure-making” effect of Na^+ in aqueous solution might not be strong.

The details with respect to the dynamical properties of the Na^+ hydrate can be visualized from plots of time dependence of the Na–O distance and number of first-shell waters, as depicted in Figure 5. During the ONIOM-XS MD simulation, it is

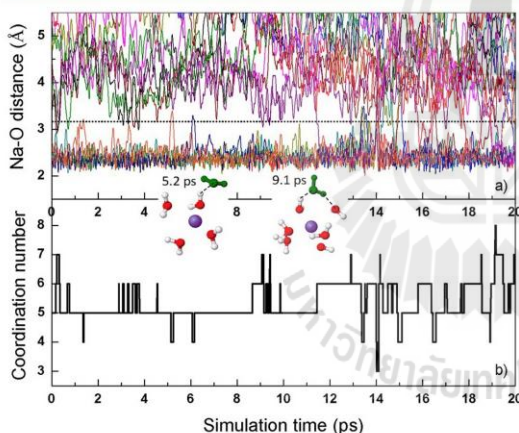


Figure 5. Time dependence of (a) Na^+ –O distance and (b) number of first-shell waters, as obtained from first 20 ps of the ONIOM-XS MD simulation. In (a), the dashed line parallel to the x -axis indicates the first minimum of the Na–O RDF.

observed that the structure of the hydrated Na^+ complexes is rather flexible in which the most favorable $\text{Na}^+(\text{H}_2\text{O})_5$ species can convert back and forth to the lower probability $\text{Na}^+(\text{H}_2\text{O})_6$ complexes. This leads to several rearrangements of the hydrated Na^+ complexes, as well as numerous attempts of first-shell waters to interchange with water molecules in the outer region. For example, at the simulation time of 5.2 ps, the arrangement of $\text{Na}^+(\text{H}_2\text{O})_4(\text{H}_2\text{O})$ complexes (CN = 4) can temporarily be formed; i.e., one first-shell water molecule (labeled in “green”) moved as far as 1 Å away from its optimal distance but it forms

a hydrogen bond to an inner-shell water molecule. In addition, other transition complexes, such as of the types $\text{Na}^+(\text{H}_2\text{O})_5(\text{H}_2\text{O})_2$ and $\text{Na}^+(\text{H}_2\text{O})_6(\text{H}_2\text{O})$ (CN = 7), can transiently be formed (e.g., at the simulation time of 9.1 ps, in which a “green” water molecule from the outer region approaches as close as 3 Å to the Na^+ ion and form hydrogen bonds to some inner-shell water molecules, forming $\text{Na}^+(\text{H}_2\text{O})_6(\text{H}_2\text{O})$ intermediate). The presence of such intermediates can be ascribed to the polarized first-shell waters, whose hydrogen atoms can form hydrogen bonds to the outer-shell water molecules, once they are arranged in a suitable geometrical position.

According to Figure 1a, the nonzero first minimum of the Na–O RDF implies that water molecules in the hydration shell of Na^+ are somewhat labile and they can possibly exchange with those in the outer region. The lability of water molecules in the hydration shell of Na^+ can be interpreted through the self-diffusion coefficient (D). In this study, the D value for first-shell waters was calculated from their center-of-mass velocity autocorrelation functions (VACFs) using the Green–Kubo relation,⁴⁷

$$D = \frac{1}{3} \lim_{t \rightarrow \infty} \int_0^t C_v(t) dt \quad (8)$$

On the basis of the ONIOM-XS MD simulation, the D value for water molecules in the vicinity of Na^+ is estimated to be $1.75 \times 10^{-5} \text{ cm}^2 \cdot \text{s}^{-1}$, which is not much different from the value of $2.23 \times 10^{-5} \text{ cm}^2 \cdot \text{s}^{-1}$ of pure water derived by the similar ONIOM-XS MD scheme.³² In this respect, it could be demonstrated that water molecules in the hydration shell of Na^+ are not strongly attached to the ion, i.e., they diffuse only slightly slower than those in the bulk. Such a phenomenon clearly corresponds to the weak “structure-making” ability of Na^+ in water. Regarding the ONIOM-XS MD results, it should be emphasized that the correct degree of lability of the first-shell waters is a crucial factor in determining the reactivity of Na^+ in aqueous solution.

The rates of water exchange processes at Na^+ were evaluated through mean residence times (MRTs) of the first-shell water molecules. In this work, the MRT data were calculated using the “direct” method,⁴⁸ as the product of the average number of water molecules in the first shell with the duration of the ONIOM-XS MD simulation, divided by the observed number of exchange events lasting a given time interval t^* . In general, a t^* value of 0.0 ps is recommended for the estimation of hydrogen bond lifetimes, whereas a t^* value of 0.5 ps is chosen as a good measure for water exchange processes.⁴⁸ The calculated MRT data with respect to t^* values of 0.0 and 0.5 ps are summarized in Table 2. To provide a useful discussion with respect to the “structure-making” ability of Na^+ , the MRT data

Table 2. Number of Water Exchange Events (N_{ex}) and Mean Residence Times (MRTs) of Water Molecules in the Bulk and in the Vicinity of Na^+ , K^+ , and Ca^{2+} , Obtained by ONIOM-XS MD Simulations

ion/solute	CN	t_{sim}	$t^* = 0.0 \text{ ps}$		$t^* = 0.5 \text{ ps}$	
			$N_{\text{ex}}^{0.0}$	$\tau_{\text{H}_2\text{O}}^{0.0}$	$N_{\text{ex}}^{0.5}$	$\tau_{\text{H}_2\text{O}}^{0.5}$
Na^+	5.4	41.0	164	1.35	36	6.18
K^{+31}	6.3	30.0	445	0.42	105	1.80
Ca^{2+31}	7.6	40.0	30	10.13	14	21.71
H_2O^{32}	4.7	30.0	607	0.23	65	2.17

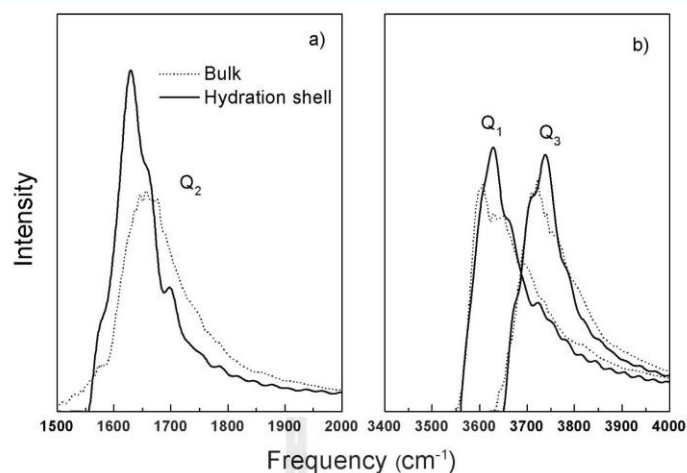


Figure 6. (a) Bending vibrations (Q_2) and (b) symmetric and asymmetric stretching vibrations (Q_1 and Q_3) of water molecules in the first hydration shell of Na^+ and in the bulk, obtained by ONIOM-XS MD simulations.

for water molecules in the vicinity of K^+ and Ca^{2+} , as derived by the similar ONIOM-XS MD framework,³¹ were also given for comparison. For both $t^* = 0.0$ and 0.5 ps, the MRT values of water molecules in the hydration shell of Na^+ are higher than those of bulk waters, showing a clear “structure-making” ability of Na^+ in aqueous solution. However, the ability of Na^+ in ordering the structure of its surrounding waters is much less than that of stronger “structure-makers”, like Ca^{2+} . In the case of K^+ , the MRT values of first-shell waters are close to the corresponding data for bulk waters, suggesting that K^+ may not be able to form any specific geometrical order of its hydration shell. In biological processes, the contrasting behaviors of Na^+ and K^+ are of special interest in determining the ability of ions to abandon their hydration shell to be pumped into the cell membrane.

More details regarding the dynamics of water molecules in the vicinity of Na^+ can be gained by computing the velocity autocorrelation functions (VACFs) of first-shell waters and their Fourier transformations. In this work, the normal-coordinate analysis developed by Bopp^{49,50} was used for obtaining three quantities Q_2 , Q_1 , and Q_3 , which are defined for describing bending vibration, and symmetric and asymmetric stretching vibrations of water molecules, respectively, as depicted in Figure 6. By the ONIOM-XS MD technique, because all atomic motions of first-shell water molecules are generated according to QM force calculations, the calculated vibrational spectra are usually scaled by an empirical factor, i.e., an approximate correction for errors in the force constants and for anharmonic effects.^{51–53} With regard to the systematic error of HF frequency calculations, all frequencies obtained by the ONIOM-XS MD simulation were multiplied by an appropriate scaling factor of 0.905.⁵¹ To reliably illustrate the “structure-making” ability of Na^+ in water, the corresponding Q_1 , Q_2 , and Q_3 frequencies obtained from the ONIOM-XS MD simulation of liquid water³² were utilized for comparison. All intramolecular vibrational frequencies (Q_1 , Q_2 , and Q_3) of water molecules in the hydration shell of Na^+ and in the liquid water are given in Table 3. For liquid water, all the bending and stretching vibrational frequencies showed peaks with recogniz-

Table 3. Vibrational Frequencies (Q_1 , Q_2 , and Q_3) of Water Molecules in the First Hydration Shell of Na^+ and in the Bulk, Obtained by ONIOM-XS MD Simulations (Numbers for the Shoulders in Parentheses)

phase	frequency (cm^{-1})		
	Q_2	Q_1	Q_3
hydration shell of Na^+	1629	3628	3738
pure water ³²	1660	3606 (3650)	3720 (3755)

able shoulders, especially for the symmetric and asymmetric vibrational modes. These observed spectra have been ascribed to the presence of several kinds, with varying strengths, of HBs formed in liquid water.³² In the hydration shell of Na^+ , water molecules are less mobilized and are arranged with respect to the influence of the ion, leading to more intense and better defined vibrational frequencies. As compared to bending frequencies of liquid water, the bending frequency of first-shell waters shows a clear “red-shift”, i.e., by about 31 cm^{-1} , whereas the symmetric (Q_1) and asymmetric (Q_3) stretching frequencies are found to be exhibited between the main peaks and the shoulders of the respective Q_1 and Q_3 frequencies of liquid water. These observed data, in particular the positions of Q_1 and Q_3 frequencies of first-shell waters, clearly demonstrate that Na^+ acts as weak “structure-maker” in aqueous solution. The results are consistent with the assignment of “structure-makers/breakers” according to Marcus,⁵⁴ indicating that Na^+ should be a weak “structure-maker”, i.e., it is considered as a borderline ion dividing “structure-makers” from “structure-breakers”. In terms of thermodynamics evidence, the details with respect to ion hydration entropies can provide a direct connection to ordering effects due to the insertion of ions into bulk water.^{55,56} For Na^+ , the hydration entropy of this ion analyzed via energetic partitioning of the potential distribution theorem free energy suggested that Na^+ is indeed a weak “structure-maker” and that the effect is relatively local around the ion.⁵⁶ Very recently, the hydration of Na^+ in aqueous solution has been studied by large angle X-ray scattering (LAXS) and double difference infrared spectroscopy (DDIR),

suggesting that this ion is weakly hydrated with only a single shell of water molecules and that it may be a “structure-breaker” even though its interactions with water are stronger than bulk water molecules interacting internally.⁵⁷ In this context, the results obtained by the ONIOM-XS MD simulation clearly provide more insights into the behaviors of Na⁺ hydrate, which are very crucial to correctly understand the reactivity of Na⁺ in aqueous solution.

4. CONCLUSIONS

In this study, an ONIOM-XS MD simulation has been performed to investigate the hydration shell structure and dynamics of Na⁺ in dilute aqueous solution. Regarding the detailed analyses of the ONIOM-XS MD trajectories, Na⁺ clearly acts as a “structure-maker” that can order the structure of waters in its surroundings to form two prevalent Na⁺(H₂O)₅ and Na⁺(H₂O)₆ species, with the probability distributions of 56% and 37%, respectively. Of particular interest, it is observed that these two probable hydrated Na⁺ complexes are rather flexible, in which the most stable Na⁺(H₂O)₅ species can convert back and forth to the lower probability Na⁺(H₂O)₆ complexes. This results in frequent structural rearrangements of the Na⁺(H₂O)₅ and Na⁺(H₂O)₆ complexes as well as numerous attempts of inner-shell water molecules to interchange with water molecules in the outer region. The overall observed data derived by means of the ONIOM-XS MD simulation clearly demonstrate the weak “structure-making” ability of Na⁺ in aqueous solution.

AUTHOR INFORMATION

Corresponding Author

*E-mail: anan_tongraar@yahoo.com, fax: 0066-44-224648.

Notes

The authors declare no competing financial interest.

ACKNOWLEDGMENTS

This work was supported by a grant funded under the SUT-PhD Program (Contract number: SUT-PhD/01/2554), Suranaree University of Technology (SUT), and the National Research University (NRU) Project of Thailand, Office of the Higher Education Commission. T.K. also acknowledges financial support from Mahidol University. High-performance computer facilities provided by the National Electronics and Computer Technology Center (NECTEC) are gratefully acknowledged.

REFERENCES

- Frank, H. *Chemical Physics of Ionic Solutions*; John Wiley & Sons: New York, 1956.
- Clementi, E. *Determination of Liquid Water Structure, Coordination Number of Ions and Solvation for Biological Molecules*; Springer-Verlag: New York, 1976, p 107.
- Hribar, B.; Southall, N. T.; Vlachy, V.; Dill, K. A. *J. Am. Chem. Soc.* **2002**, *124*, 12302.
- Morais-Cabral, J. H.; Zhou, Y. F.; MacKinnon, R. *Nature* **2001**, *414*, 37.
- Pálincás, G.; Radnai, T.; Hajdu, F. Z. *Naturforsch.* **1980**, *35a*, 107.
- Ohtomo, N.; Arakawa, K. *Bull. Chem. Soc. Jpn.* **1980**, *53*, 1789.
- Caminiti, R.; Licheri, G.; Paschina, G.; Pinna, G. *J. Chem. Phys.* **1980**, *72*, 4552.
- Skipper, N. T.; Neilson, G. W. *J. Phys.: Condens. Matter* **1989**, *1*, 4141.
- Ohtaki, H.; Radnai, T. *Chem. Rev.* **1993**, *93*, 1157.
- Kameda, Y.; Sugawara, K.; Usuki, T.; Uemura, O. *Bull. Chem. Soc. Jpn.* **1998**, *71*, 2769.
- Bondarenko, G. V.; Gorbaty, Y. E.; Okhulkov, A. V.; Kalinichev, A. G. *J. Phys. Chem. A* **2006**, *110*, 4042.
- Mancinelli, R.; Botti, A.; Bruni, F.; Ricci, M. A.; Soper, A. K. *Phys. Chem. Chem. Phys.* **2007**, *9*, 2959.
- Kulik, H. J.; Marzari, N.; Correa, A. A.; Prendergast, D.; Schwegler, E.; Galli, G. *J. Phys. Chem. B* **2010**, *114*, 9594.
- Impey, R. W.; Madden, P. A.; McDonald, I. R. *J. Phys. Chem.* **1983**, *87*, 5071.
- Obst, S.; Bradaczek, H. *J. Phys. Chem.* **1996**, *100*, 15677.
- Lee, S. H.; Rasaiah, J. C. *J. Phys. Chem.* **1996**, *100*, 1420.
- Toth, G. *J. Chem. Phys.* **1996**, *105*, 5518.
- White, J. A.; Schwegler, E.; Galli, G.; Gygi, F. *J. Chem. Phys.* **2000**, *113*, 4668.
- Ikeda, T.; Boero, M.; Terakura, K. *J. Chem. Phys.* **2007**, *127*, 34501.
- Galamba, N.; Cabral, B. J. C. *J. Phys. Chem. B* **2009**, *113*, 16151.
- Tongraar, A.; Liedl, K. R.; Rode, B. M. *J. Phys. Chem. A* **1998**, *102*, 10340.
- Azam, S. S.; Haq, Z.; Fatmi, M. Q. *J. Mol. Liq.* **2010**, *153*, 95.
- Azam, S. S.; Hofer, T. S.; Randolph, B. R.; Rode, B. M. *J. Phys. Chem. A* **2009**, *113*, 1827.
- Rode, B. M.; Schwenk, C. F.; Tongraar, A. *J. Mol. Liq.* **2004**, *110*, 105.
- Yoo, S.; Zeng, X. C.; Xantheas, S. S. *J. Chem. Phys.* **2009**, *130*, 221102.
- Warshel, A.; Levitt, M. *J. Mol. Biol.* **1976**, *103*, 227.
- Singh, U. C.; Kollman, P. A. *J. Comput. Chem.* **1986**, *7*, 718.
- Field, M. J.; Bash, P. A.; Karplus, M. *J. Comput. Chem.* **1990**, *11*, 700.
- Kerdcharoen, T.; Morokuma, K. *Chem. Phys. Lett.* **2002**, *355*, 257.
- Kerdcharoen, T.; Morokuma, K. *J. Chem. Phys.* **2003**, *118*, 8856.
- Wanprakhon, S.; Tongraar, A.; Kerdcharoen, T. *Chem. Phys. Lett.* **2011**, *517*, 171.
- Thaomola, S.; Tongraar, A.; Kerdcharoen, T. *J. Mol. Liq.* **2012**, *174*, 26.
- Svensson, M.; Humbel, S.; Froese, R. D. J.; Mutsuvara, T.; Sieber, S.; Morokuma, K. *J. Phys. Chem.* **1996**, *100*, 19357.
- Tasaki, K.; McDonald, S.; Brady, J. W. *J. Comput. Chem.* **1993**, *14*, 278.
- Dunning, T. H. Jr.; Hay, P. J. *Modern Theoretical Chemistry*; Plenum: New York, 1976.
- Hay, P. J.; Wadt, W. R. *J. Chem. Phys.* **1985**, *82*, 284.
- Check, C. E.; Faust, T. O.; Bailey, J. M.; Wright, B. J.; Gilbert, T. M.; Sunderlin, L. S. *J. Phys. Chem. A* **2001**, *105*, 8111.
- Stillinger, F. H.; Rahman, A. *J. Chem. Phys.* **1978**, *68*, 666.
- Bopp, P.; Jancsó, G.; Heinzinger, K. *Chem. Phys. Lett.* **1983**, *98*, 129.
- Frisch, M. J.; et al. *GAUSSIAN 03, Revision D.02*; Gaussian, Inc.: Wallingford, CT, 2005.
- Berendsen, H. J. C.; Grigera, J. R.; Straatsma, T. P. *J. Phys. Chem.* **1987**, *91*, 6269.
- Adams, D. J.; Adams, E. H.; Hills, G. *J. Mol. Phys.* **1979**, *38*, 387.
- Cappa, C. D.; Smith, J. D.; Messor, B. M.; Cohen, R. C.; Saykally, R. J. *J. Phys. Chem. B* **2006**, *110*, 5301.
- Bakker, H. J.; Kropman, M. F.; Omta, A. W. *J. Phys.: Condens. Matter* **2005**, *17*, S3215.
- Rode, B. M.; Hofer, T. S.; Randolph, B. R.; Schwenk, C. F.; Xenides, D.; Vchirawongkwin, V. *Theor. Chem. Acc.* **2006**, *115*, 77.
- Heyden, A.; Lin, H.; Truhlar, D. G. *J. Phys. Chem. B* **2007**, *111*, 2231.
- McQuarrie, D. A. *Statistical Mechanics*; Harper & Row: New York, 1976.
- Hofer, T. S.; Tran, H. T.; Schwenk, C. F.; Rode, B. M. *J. Comput. Chem.* **2004**, *25*, 211.
- Bopp, P. *Chem. Phys.* **1986**, *106*, 205.

- (50) Spohr, E.; Pálincás, G.; Heinzinger, K.; Bopp, P.; Probst, M. M. *J. Phys. Chem.* **1988**, *92*, 6754.
- (51) Scott, A. P.; Radom, L. *J. Phys. Chem.* **1996**, *100*, 16502.
- (52) Merrick, J. P.; Moran, D.; Radom, L. *J. Phys. Chem. A* **2007**, *111*, 11683.
- (53) Johnson, R. D., III; Irikura, K. K.; Kacker, R. N.; Kessel, R. J. *Chem. Theory Comput.* **2010**, *6*, 2822.
- (54) Marcus, Y. *Chem. Rev.* **2009**, *109*, 1346.
- (55) Collins, K. D. *Biophys. Chem.* **2012**, *167*, 43.
- (56) Beck, T. L. *J. Phys. Chem. B* **2011**, *115*, 9776.
- (57) Mähler, J.; Persson, I. *Inorg. Chem.* **2012**, *51*, 425.



APPENDIX D

MANUSCRIPT



Characteristics of Li^+ as a “structure-maker” in aqueous solution: A comparative study of conventional QM/MM and ONIOM-XS MD simulations

Pattrawan Sripa¹, Anan Tongraar^{1*} and Teerakiat Kerdecharen²

¹ School of Chemistry, Institute of Science, Suranaree University of Technology, and
NANOTEC-SUT Center of Excellence on Advanced Functional Nanomaterials,

Nakhon Ratchasima 30000, Thailand

² Department of Physics and NANOTEC Center of Excellence, Faculty of Science,
Mahidol University, Bangkok 10400, Thailand

Abstract

The hydration structure and dynamics of Li^+ in liquid water have been investigated by means of two combined quantum mechanics/molecular mechanics (QM/MM) molecular dynamics (MD) techniques, namely a conventional QM/MM MD and a more sophisticated QM/MM MD based on the ONIOM-XS method, called briefly ONIOM-XS MD. Based on the two QM/MM-based MD simulations, the feature of the first hydration shell of Li^+ is almost identical, showing a well-defined tetrahedral geometry with the average coordination numbers of 4.1 and 4.2, respectively. However, significant differences between the conventional QM/MM and ONIOM-XS MD simulations appear in the detailed analyses of the geometrical arrangement and the dynamics of the Li^+ hydrates. As compared to the conventional QM/MM MD study, the ONIOM-XS MD simulation clearly reveals that the structure of the hydrated Li^+ is more flexible and that water molecules in the first hydration shell are more labile, leading to a higher probability of finding other hydrated complexes, in particular the $\text{Li}^+(\text{H}_2\text{O})_5$ species. In this respect, the ONIOM-XS MD results clearly imply that the “structure-making” ability of this ion in aqueous solution is not too strong.

1. Introduction

Lithium ion (Li^+) is the smallest cation (*i.e.*, apart from the proton) that plays a vital role in technical and medical applications [1,2]. During the past decades, several attempts, from both the experimental and theoretical sides, have been made to elucidate the behavior of this ion, in particular the details with respect to its hydration structure and dynamics in the innermost hydration shell [3-23]. In experiments, the coordination numbers of Li^+ have been reported between 4 and 6, depending on the concentration [3-13]. For example, X-ray and neutron scattering measurements revealed that Li^+ has six nearest-neighbor water molecules [3-5], while some spectroscopy studies have suggested a hydration number of four [6,7]. Regarding the experimental observations, however, it is known that some uncertainties exist since most of the techniques employed have difficulties in reliably elucidating the structural data, especially at a low concentration [7,13]. In conjunction with experiments, computer simulations, in particular Monte Carlo (MC) and molecular dynamics (MD), have been carried out to predict the microscopic details of this hydrated ion [14-21]. Earlier MC and MD studies, most of which relied on molecular mechanical (MM) force fields, have also reported various coordination numbers of Li^+ , ranging from 4 to 6 [14-19]. In this respect, the observed discrepancies have been ascribed to the difficulty in constructing reliable potentials that included essential many-body interactions, *i.e.*, the properties of the Li^+ hydrate are rather sensitive to the quality of the potentials employed in the simulations. Recently, more sophisticated quantum-mechanics-based MD simulations, such as Car-Parrinello *ab initio* MD (CP-MD) [20-22] and combined quantum mechanics/molecular mechanics (QM/MM) MD [23-25], have predicted a sole coordination number of four. Regarding the CP-MD technique, the major advantage of this approach is that the overall system’s interactions can directly be obtained from QM calculations. However, some severe limitations stem from the use of simple generalized gradient approximation (GGA) functionals such as BLYP and PBE and of the relatively small system size. In particular, it has been reported that the use of simple density functionals in the CP-MD studies fails to correctly describe the structural and dynamical properties even for the underlying liquid water [26,27]. Alternatively, the QM/MM MD technique has been employed in elucidating the details of such condensed-phase systems [23-25,28-30].

According to the conventional QM/MM MD technique [23-25,28-30], the system is partitioned into a part described by quantum mechanics and another part treated by means of

* Corresponding author; E-mail: anan_tongraar@yahoo.com, fax: 0066-44-224648.

MM force fields. During the QM/MM MD simulation, when exchange of particles between the QM and MM regions takes place, a smoothing function [31] is employed to ensure a smooth change of forces at the transition between the QM and MM regions. By this scheme, however, the smoothing function is applied only for the exchanging particles that are crossing the QM/MM boundary. This leads to considerable problems since an interchange of particles between the QM and MM regions would more or less affect the forces acting on the remaining QM particles. In addition, it has been demonstrated that the conventional QM/MM MD framework cannot clearly define the system's energy expression during the exchange of solvent molecules between the QM and MM regions [32,33]. To solve these problems, a more reliable QM/MM MD technique based on the ONIOM-XS (Own N-layered Integrated molecular Orbital and molecular Mechanics – extension to Solvation) method, called briefly ONIOM-XS MD, has been proposed [32,33]. By the ONIOM-XS MD technique, the forces acting on all QM particles will be smoothed during the particle exchanges and, thus, it better defines the system's energy expression. Recently, the ONIOM-XS MD technique has been successfully applied for various condensed phase systems [32-36], providing more reliable results (*i.e.*, when compared to the conventional QM/MM MD studies) which are in better agreement with experiments. For example, in the case of pure water [36], the ONIOM-XS simulation, as compared to the HF/MM results, revealed that the structural arrangement of water with respect to 4 hydrogen bonds (HBs) decreases significantly, while the distributions of 2- and 3-fold HB species become more visible. The ONIOM-XS MD results were in good accord with the recent experimental observations, which reported considerable amounts of 2- and 3-fold HB clusters in liquid water [37,38]. In addition, for the studies of Na⁺ and K⁺ in aqueous solutions [34,35], the results obtained by the ONIOM-XS MD simulations have provided more insights into the contrasting behaviors of these two ions with respect to their "structure-making" and "structure-breaking" abilities.

In this study, the hydration structure and dynamics of Li⁺ in aqueous solution will be investigated by means of the conventional QM/MM and ONIOM-XS MD simulations. The results obtained by the two QM/MM-based MD simulation types will be compared and discussed with respect to the important treatment of the ONIOM-XS method for describing the "structure-making" ability of Li⁺ in aqueous solution.

2. Methods

2.1 Conventional QM/MM MD

According to the conventional QM/MM MD scheme [28-30], the QM region refers to a sphere which contains a central Li⁺ and its nearest-neighbor waters, which is treated by quantum mechanics, and the MM part corresponds to the bulk waters, which is described by MM force fields. The total interaction energy of the system is defined as

$$E_{total} = \langle \Psi_{QM} | \hat{H} | \Psi_{QM} \rangle + E_{MM} + E_{QM-MM}, \quad (1)$$

where $\langle \Psi_{QM} | \hat{H} | \Psi_{QM} \rangle$ denotes the interactions within the QM region, and E_{MM} and E_{QM-MM} represent the interactions within the MM and between the QM and MM regions, respectively. Note that the E_{MM} and E_{QM-MM} terms are described by classical MM force fields. The total force of the system is described by

$$F_{tot} = F_{MM}^{class} + (F_{QM}^{OM} - F_{MM}^{OM}), \quad (2)$$

where F_{MM}^{class} , F_{QM}^{OM} and F_{MM}^{OM} are the MM force of the total system, the QM force in the QM region and the MM force in the QM region, respectively. In this respect, the F_{MM}^{OM} term accounts for the coupling between the QM and MM regions. Regarding the interchange of water molecules between the QM and MM regions, the forces acting on each particle in the system are switched according to which region the water molecule is entering or leaving and can be defined as

$$F_i = S_m(r)F_{QM} + (1 - S_m(r))F_{MM}, \quad (3)$$

where F_{QM} and F_{MM} are the quantum mechanical and molecular mechanical forces, respectively. $S_m(r)$ is the smoothing function [31],

$$S_m(r) = 1, \quad \text{for } r \leq r_0, \\ S_m(r) = \frac{(r_1^2 - r^2)^2 (r_1^2 + 2r^2 - 3r_0^2)}{(r_1^2 - r_0^2)^3}, \quad \text{for } r_0 < r \leq r_1, \\ S_m(r) = 0, \quad \text{for } r > r_1, \quad (4)$$

where r_0 and r_1 are the distances characterizing the start and the end of the QM region, respectively, and applied within an interval of 0.2 Å to ensure a continuous change of forces at the transition between the QM and MM regions.

2.2 ONIOM-XS MD

By the ONIOM-XS MD technique [32-36], the system is composed of a "high-level" QM region and the remaining "low-level" MM bulk waters, in which a thin switching layer located between the QM and MM regions is employed for smoothing the energy and forces of the combined system according to the solvent exchange. In this respect, three parameters, namely n_1 , l and n_2 , are defined as the number of particles involved in the QM region, the switching layer and the MM region, respectively, and N is the total number of particles (*i.e.*, $N = n_1 + l + n_2$). According to the ONIOM extrapolation scheme [39], the potential energy of the system can be expressed in two ways. If the switching layer is included into the high-level QM region, the energy expression is written as

$$E^{ONIOM}(n_1 + l; N) = E^{QM}(n_1 + l) - E^{MM}(n_1 + l) + E^{MM}(N). \quad (5)$$

Otherwise, if the switching layer is considered as part of the "low-level" MM subsystem, the energy expression is

$$E^{ONIOM}(n_1; N) = E^{QM}(n_1) - E^{MM}(n_1) + E^{MM}(N). \quad (6)$$

In Eqs. (5) and (6), the E^{QM} and E^{MM} terms represent the interactions derived by the QM calculations and by the classical MM force fields, respectively. Since the interactions between the QM and MM regions are also described by means of MM potentials, these contributions are already included in the $E^{MM}(N)$. With regard to the ONIOM-XS MD scheme, when a particle moves into the switching layer (either from the QM or MM region), both Eqs. (5) and (6) will be evaluated. Then, the potential energy of the entire system can be expressed as a hybrid between both energy terms (5) and (6),

$$E^{ONIOM-XS}(r_1) = (1 - \bar{s}(r_1)) \cdot E^{ONIOM}(n_1 + l; N) + \bar{s}(r_1) \cdot E^{ONIOM}(n_1; N), \quad (7)$$

where $\bar{s}(r_1)$ is an average over a set of switching functions for individual exchanging particles in the switching layer $s_i(x_i)$,

$$\bar{s}(r_1) = \frac{1}{l} \sum_{i=1}^l s_i(x_i), \quad (8)$$

In general, the switching function applied in Eq. (8) can be of any form. In this study, a polynomial expression is employed,

$$s_i(x_i) = 6 \left(x_i - \frac{1}{2} \right)^5 - 5 \left(x_i - \frac{1}{2} \right)^3 + \frac{15}{18} \left(x_i - \frac{1}{2} \right) + \frac{1}{2}, \quad (9)$$

where $x_i = ((r - r_0)/(r_1 - r_0))$, and r_0 and r_1 are the radius of the inner and outer surfaces of the switching shell, respectively, and r_i is the distance between the center of mass of the exchanging particle and the center of the QM sphere (*i.e.*, the position of Li⁺). The above polynomial form and parameter sets were derived to have an S-shape that converges to 0 and 1 at r_0 and r_1 , respectively [32]. Finally, the gradient of the energy can be written as

$$\begin{aligned} \nabla_R E^{ONIOM-XS}(r_1) &= (1 - \bar{s}(r_1)) \cdot \nabla_R E^{ONIOM}(n_1 + l; N) + \bar{s}(r_1) \cdot \nabla_R E^{ONIOM}(n_1; N) + \\ &\quad \frac{1}{(r_1 - r_0)} \nabla \bar{s}(r_1) \cdot (E^{ONIOM}(n_1; N) - E^{ONIOM}(n_1 + l; N)) \end{aligned} \quad (10)$$

Here, it should be emphasized that the ONIOM-XS MD technique allows both energies and forces to be smoothed, whereas only forces were taken into account through the conventional QM/MM MD scheme.

2.3 Simulation details

According to both the conventional QM/MM and ONIOM-XS MD simulations, it is known that the selection of the QM method, QM size and basis set is crucial for obtaining reliable results. In practice, these parameters must be optimized, compromising between the quality of the simulation results and the available computational facilities. In this work, all QM interactions were evaluated by performing *ab initio* calculations at the Hartree-Fock

18.19 Å, contains one Li^+ and 199 water molecules, corresponding to the experimental density of pure water. The reaction-field method [45] was employed for the treatment of long-range interactions. The Newtonian equations of motions were treated by a general predictor-corrector algorithm. The time step size was set to 0.2 fs, which allows for the explicit movement of the hydrogen atoms of water molecules. The initial configuration of the system was taken from our previous QM/MM MD study [23]. The conventional QM/MM and ONIOM-XS MD simulations were separately performed with the system's re-equilibration for 30,000 time steps, followed by another 200,000 time steps to collect configurations every 10^{th} step.

3. Results and discussion

The structural properties of the hydrated Li^+ are explained in terms of Li-O and Li-H RDFs and their corresponding integration numbers, as depicted in Fig. 1, comparing the results as obtained by the conventional QM/MM and ONIOM-XS MD simulations. Based on the two QM/MM-based MD simulations, the features of the first Li-O peaks are almost identical, *i.e.*, showing a well-defined first hydration shell with the maxima centered at 1.96 and 1.93 Å, respectively. The shape and height of the first Li-O and Li-H RDFs reveal a clear "structure-making" ability of Li^+ in aqueous solution. Nevertheless, the first hydration shell of Li^+ is not completely separated from the outer region, indicating that some water exchange processes can take place between these two regions. Integrations up to the first minimum of the conventional QM/MM and ONIOM-XS MD's Li-O RDFs yield the average coordination numbers of 4.1 and 4.2, respectively. Note that the details with respect to the first hydration shell of Li^+ are close to those reported in the recent QM/MM MD [24,25] and CP-MD [21] studies. Regarding the conventional QM/MM and ONIOM-XS MD results, the observed similarity of the first Li-O and Li-H RDFs is understandable since most of the particles embedded within the first hydration shell of Li^+ are treated by the similar QM forces. In this respect, since the ONIOM-XS MD technique has been developed in order to improve the forces of QM particles according to immediate exchanges of particles between the QM and MM regions, a significant difference between the conventional QM/MM and ONIOM-XS MD results is expected to be found at the region nearby the QM-MM boundary. Interestingly, it has been demonstrated that the differences between the conventional QM/MM and ONIOM-XS MD simulations are more visible for

(HF) level of theory using the DZP basis set [40]. Under these constraints, it should be realized that the instantaneous electron correlation and the charge transfer effects may not be typically well-described by the HF theory, and that the use of the DZP basis set could result in a high basis set superposition error and an exaggeration of the ligand-to-metal charge transfer. For the QM size, a QM radius of 4.6 Å and a switching width of 0.2 Å were chosen, which correspond to the parameters r_0 and r_1 of 4.4 and 4.6 Å, respectively. This QM size is considered to be large enough to include most of the non-additive contributions and the polarization effects, *i.e.*, at least within the whole first hydration shell and major parts of the second hydration layer of Li^+ . In this sense, it is assumed that the remaining interactions beyond the QM region could be well accounted for by the MM potentials. As can be seen in the next section (cf. Fig. 1), the smooth shape of the Li-O radial distribution functions (RDFs) between 4.4 and 4.6 Å clearly supplies information that interchange of water molecules between the QM and MM regions occurs smoothly. For the interactions within the MM and between the QM and MM regions, a flexible BJH-CF2 model, which describes intermolecular [41] and intramolecular [42] interactions, was employed for water. Note that this flexible water model allows explicit hydrogen movements and, thus, ensures a smooth transition when water molecules move from the QM region with its full flexibility to the MM region and *vice versa*. The pair potential functions for describing Li^+ - H_2O interactions were newly constructed. The 2354 HF interaction energy points for various Li^+ - H_2O configurations, obtained from Gaussian03 [43] calculations using the DZP basis set were fitted to the analytical form of

$$\Delta E_{\text{Li}^+-\text{H}_2\text{O}} = \sum_{i=1}^3 \left(\frac{A_i}{r_{ie}^3} + \frac{B_i}{r_{ie}^6} + C_i \exp(-D_i r_{ie}) + \frac{q_i q_c}{r_{ie}} \right), \quad (11)$$

where A_i , B_i , C_i and D_i are the fitting parameters (see Table 1), r_{ij} denotes the distances between the ion and the i -th atoms of the water molecule and q_i are the atomic net charges. In this work, the charge for Li^+ was set to 1.0, and the charges for O and H atoms of water were set with respect to the BJH-CF2 model, *i.e.*, -0.6598 and 0.3299 for O and H atoms, respectively.

Both the conventional QM/MM and ONIOM-XS MD simulations were performed in a canonical ensemble at 298 K with periodic boundary conditions. The system's temperature was kept constant using the Berendsen algorithm [44]. A periodic box, with a box length of

the situation where the number of ligands that are crossing the QM-MM boundary is large, *i.e.*, a system where ion-water interactions are weak and water molecules surrounding the ion are labile [34,35]. In this work, the remarkable difference between the conventional QM/MM and ONIOM-XS MD results appears at the region beyond the first hydration shell of Li^+ . As can be seen in Fig. 1a, the recognizable second peak of the ONIOM-XS MD's Li-O RDF is located at a shorter distance of 3.71 Å, compared to the corresponding value of 3.95 Å obtained by the conventional QM/MM MD simulation. This observed difference clearly implies an important treatment of the ONIOM-XS MD technique in obtaining a more reliable description of the Li^+ hydrate.

Fig. 2 displays the probability distributions of the coordination numbers of Li^+ , calculated up to first minimum of the Li-O RDFs. In both the conventional QM/MM and ONIOM-XS MD simulations, the Li^+ ion clearly favors a coordination number of 4, followed by 5 in smaller amounts. However, the probability distributions of the 4-fold and 5-fold coordinated complexes obtained by the two QM/MM-based MD techniques are significantly different, being of 90.7 and 9.2 %, and of 75.2 and 23.9%, respectively. Interestingly, the ONIOM-XS MD results clearly supply information that the hydration structure of the Li^+ ion is somewhat flexible and that, besides the prevalent $\text{Li}^+(\text{H}_2\text{O})_4$ species, the $\text{Li}^+(\text{H}_2\text{O})_5$ complex could more frequently be formed in aqueous solution. The flexibility of the Li^+ hydration can be described by the distributions of the O---Li---O angle, as shown in Fig. 3. By means of the ONIOM-XS MD simulation, as compared to the conventional QM/MM MD results, the observed broader distributions of the O---Li---O angle clearly indicate a higher flexibility of the hydrated Li^+ . In particular, as can be seen in Fig. 3, a recognizable shoulder between 150° and 180° corresponds to a higher probability of finding the arrangement with respect to the 5-fold coordinated complexes. Consequently, these observed differences could further be expected to reflect in different dynamics details of the ligands surrounding the Li^+ ion.

The dynamical properties of the Li^+ hydrate can be visualized through the plots of time dependence of the Li-O distance and number of first-shell waters, as depicted in Figs. 4 and 5 for the conventional QM/MM and ONIOM-XS MD simulations, respectively. In the ONIOM-XS MD simulation, as compared to the conventional QM/MM MD results, water molecules surrounding the Li^+ ion are more labile, showing more frequent exchanges of water molecules between those in the hydration shell of Li^+ and the bulk. Consequently, this

leads to a higher probability of finding $\text{Li}^+(\text{H}_2\text{O})_5$ or even $\text{Li}^+(\text{H}_2\text{O})_3$ species. In this respect, it is observed that the most favorable $\text{Li}^+(\text{H}_2\text{O})_4$ species can temporarily convert back and forth to the lower probability $\text{Li}^+(\text{H}_2\text{O})_5$ complexes, or even to a less favorable $\text{Li}^+(\text{H}_2\text{O})_3$ formation. For example, at the simulation time of 4.2 ps, an arrangement of the 5-fold coordinated complex is temporarily formed, *i.e.*, one water molecule from the outer region (labeled in "green") transiently approaches as close as 2.2 Å to the Li^+ ion, forming an $\text{Li}^+(\text{H}_2\text{O})_4(\text{H}_2\text{O})$ intermediate. At the simulation times of 8.7 and 17.3 ps, the $\text{Li}^+(\text{H}_2\text{O})_5$ intermediates are formed according to associative (A) exchange processes, *i.e.*, a new (fifth) water molecule from the outer region (labeled in "blue" and "green", respectively) comes into the first hydration shell of Li^+ , and then, one of water molecules from the initial hydration shell is repelled. Interestingly, other intermediates, such as the $\text{Li}^+(\text{H}_2\text{O})_3$ species, also exist in aqueous solution (*e.g.*, at the simulation time of 2.1 ps, in which one first-shell water molecule is found to temporarily move as far as 1 Å away from its optimal distance).

The lability of water molecules in the first hydration shell of Li^+ can be interpreted through the self-diffusion coefficient (D). In this study, the D values for first-shell waters were calculated from their center-of-mass velocity autocorrelation functions (VACFs) according to the Green-Kubo relation [46],

$$D = \frac{1}{3} \lim_{t \rightarrow \infty} \int_0^t C_v(t) dt. \quad (12)$$

By the conventional QM/MM and ONIOM-XS MD simulations, the D values for water molecules in the vicinity of Li^+ are estimated to be 1.01×10^{-5} and $1.38 \times 10^{-5} \text{ cm}^2 \cdot \text{s}^{-1}$, respectively. Apparently, these D values are relatively lower than the corresponding values of 3.23×10^{-5} and $2.73 \times 10^{-5} \text{ cm}^2 \cdot \text{s}^{-1}$ of pure water derived by the conventional QM/MM and ONIOM-XS MD techniques [36], respectively. This indicates that water molecules in the first hydration shell of Li^+ are well attached to the ion, showing a clear "structure-making" ability of Li^+ in water. Comparing the conventional QM/MM and ONIOM-XS MD results, however, the D values are somewhat different, *i.e.*, the D values of water molecules in the hydration shell of Li^+ are of about 3 and 2 times slower than those of bulk waters, respectively. In this respect, it is apparent that the ONIOM-XS MD simulation reveals the "structure-making" ability of Li^+ which is significantly less than that predicted by the conventional QM/MM MD scheme. Note that the correct degree of lability of the first-shell

waters is a crucial factor in determining the reactivity of Li^+ in aqueous solution. On the basis of the ONIOM-XS MD technique, the D value of water molecules in the first hydration shell of Li^+ can be compared to that of Na^+ , which is reported to be $1.75 \times 10^{-5} \text{ cm}^2 \cdot \text{s}^{-1}$ [35]. In the case of Na^+ , it has been demonstrated that water molecules in the first hydration shell are quite labile and they diffuse slightly more slowly than those in the bulk, showing that Na^+ is indeed a weak “structure-maker” in aqueous solution [35]. For Li^+ , as compared to Na^+ , the ONIOM-XS MD results clearly suggest that the “structure-making” ability of this ion is not too strong. Regarding the Li-O RDF in Fig. 1a, the less pronounced second peak clearly supplies information that the effect of Li^+ on the water structure does not propagate beyond the first hydration shell.

The rates of water exchange processes at Li^+ were evaluated through mean residence times (MRTs) of the first-shell water molecules. In this work, the MRT data were calculated using the “direct” method [47], being the product of the average number of water molecules in the first shell with the duration of the simulations, divided by the observed number of exchange events lasting a given time interval t^* . With regard to the “direct” method, it has been suggested that a t^* value of 0.0 ps is suitable for the estimation of hydrogen bond lifetimes, while a t^* value of 0.5 ps is recommended as a good measure for water exchange processes [47]. The calculated MRT data for water molecules in the bulk and in the vicinity of Li^+ and of other ions with respect to t^* values of 0.0 and 0.5 ps are summarized in Table 2, comparing the results as obtained by the conventional QM/MM and ONIOM-XS MD simulations. For both $t^* = 0.0$ and 0.5 ps, the MRT values of water molecules in the hydration shell of Li^+ obtained from both the conventional QM/MM and ONIOM-XS MD simulations are higher than the corresponding values of bulk waters, confirming a clear “structure-making” ability of Li^+ in aqueous solution. By means of the ONIOM-XS MD simulation, however, the ability of Li^+ in ordering the structure of its surrounding waters is significantly weaker than that predicted by the conventional QM/MM MD scheme. According to the data in Table 2, the MRT values of water molecules in the vicinity of K^+ derived by the conventional QM/MM and ONIOM-XS MD simulations were found to be quite similar. However, it has been reported that the average coordination number of K^+ and the amount of exchange events are somewhat different [34]. In the case of Ca^{2+} , a significant difference between the two QM/MM-based MD simulations is found for $t^* = 0.5$ ps, in which the ONIOM-XS MD simulation revealed a relatively large number of exchange events (with the smaller MRT value) when compared to those obtained by the conventional

QM/MM MD simulation [34]. Recently, the ONIOM-XS MD technique has also been applied for studying the preferential solvation and dynamics of Li^+ in aqueous ammonia solution [48]. Of particular interest, as compared to the conventional QM/MM MD study, which predicts a clear water preference with the arrangement of the $\text{Li}^+[(\text{H}_2\text{O})_4][(\text{H}_2\text{O})_4]$ type, the ONIOM-XS MD simulation clearly reveals that this ion can order both water and ammonia molecules to form the preferred $\text{Li}^+[(\text{H}_2\text{O})_3\text{NH}_3][(\text{H}_2\text{O})_1(\text{NH}_3)_3]$ complex. In addition, it was observed that the “structure-making” ability of Li^+ in this media is not too strong and that the second solvent of this ion is less structured, implying a small influence of Li^+ in ordering the solvent molecules in this shell. Undoubtedly, the overall observed differences between the two QM/MM-based MD simulations clearly confirm that the use of the more accurate ONIOM-XS MD technique is highly recommended for obtaining more detailed descriptions of such condensed-phase systems.

4. Conclusions

The characteristics of Li^+ with respect to its “structure-making” ability in aqueous solution were investigated by means of the conventional QM/MM and ONIOM-XS MD simulations. Based on the two QM/MM-based MD techniques, it was observed that Li^+ acts as a clear “structure-maker” in water, *i.e.*, this ion is able to order the structure of its surrounding water molecules, forming a prevalent $\text{Li}^+(\text{H}_2\text{O})_4$ species. Comparing the conventional QM/MM and ONIOM-XS MD results, however, significant differences were found in the detailed analyses of the geometrical arrangement and the dynamics of the Li^+ hydrates. In the course of the ONIOM-XS MD simulation, it was observed that the structure of the hydrated Li^+ is more flexible and that, besides the prevalent $\text{Li}^+(\text{H}_2\text{O})_4$ species, other ion-water complexes, in particular the $\text{Li}^+(\text{H}_2\text{O})_3$, could more frequently be formed in aqueous solution. Together with the analyses on the dynamical data, the ONIOM-XS MD results clearly supply information that the “structure-making” ability of Li^+ is not too strong. These observed differences clearly confirm the important treatment of the ONIOM-XS MD technique in obtaining more detailed information on this hydrated ion.

5. Acknowledgment

This work was supported by a grant funded under the SUT-PhD Program (Contract number: SUT-PhD/01/2554), Suranaree University of Technology (SUT), and the National Research University (NRU) Project of Thailand, Office of the Higher Education Commission. A.T. also acknowledges support by the National Nanotechnology Center (NANOTEC), National Science and Technology Development Agency (NSTDA), Ministry of Science and Technology, Thailand, through its program of Center of Excellence Network. T.K. acknowledges financial support from Mahidol University. High-performance computer facilities provided by the National e-Science Infrastructure Consortium are gratefully acknowledged.

References

- [1] N.J. Birch, *Chem. Rev.* 99 (1999) 2659.
- [2] C.J. Phil, C.A. Wilson, V.M.-Y. Lee, P.S. Klein, *Nature* 423 (2003) 435.
- [3] T. Radnai, G. Pálmkás, G.I. Szász, K. Heinzinger, *Z. Naturforsch. A* 36 (1981) 1076.
- [4] J.E. Enderby, G.W. Neilson, *Rep. Prog. Phys.* 44 (1981) 593.
- [5] I. Howell, G.W. Neilson, *J. Phys.: Condens. Matter* 8 (1996) 4455.
- [6] K.H. Michaelian, M. Moskovits, *Nature* 273 (1978) 135.
- [7] H. Othaki, T. Radnai, *Chem. Rev.* 93 (1993) 1157.
- [8] Y. Marcus, *Chem. Rev.* 88 (1988) 1475.
- [9] G.W. Neilson, A.K. Adya, *Ann. Rep. Chem. Sect C* 93 (1996) 101.
- [10] K. Yamataka, M. Yamagami, T. Takamuku, T. Yamaguchi, H. Watika, *J. Phys. Chem.* 97 (1993) 10835.
- [11] W.W. Rudolph, M.H. Brooker, C.C. Pye, *J. Phys. Chem.* 99 (1995) 3793.
- [12] M.T. Rodgers, P.B. Armentrout, *J. Phys. Chem. A* 101 (1997) 1238.
- [13] D.T. Richens, *The Chemistry of Aqua Ions*, Wiley, New York, 1997.
- [14] G.I. Szász, K. Heinzinger, W.O. Riede, *Z. Naturforsch. A* 36 (1981) 1067.
- [15] S. Obst, H. Bradaczek, *J. Phys. Chem.* 100 (1996) 15677.
- [16] S.H. Lee, J.C. Rasaiah, *J. Phys. Chem.* 100 (1996) 1420.
- [17] R.W. Impey, P.A. Madden, I.R. McDonald, *J. Phys. Chem.* 87 (1983) 5071.
- [18] J. Chandrasekhar, D.C. Spellmeyer, W.L. Jorgensen, *J. Am. Chem. Soc.* 106 (1984) 903.
- [19] G.Tóth, *J. Chem. Phys.* 105 (1996) 5518.
- [20] S.B. Rempe, L.R. Pratt, G. Hummer, J.D. Kress, R.L. Martin, A. Redondo, *J. Am. Chem. Soc.* 122 (2000) 966.
- [21] A.P. Lyubartsev, K. Laasonen, A. Laaksonen, *J. Chem. Phys.* 114 (2001) 3120.
- [22] T. Ikeda, M. Boero, K. Terakura, *J. Chem. Phys.* 126 (2007) 34501.
- [23] A. Tongraar, K.R. Liedl, B.M. Rode, *Chem. Phys. Lett.* 286 (1998) 56.
- [24] H.H. Loeffler, B.M. Rode, *J. Chem. Phys.* 117 (2002) 110.
- [25] H.H. Loeffler, A.M. Mohammed, Y. Inada, S. Funahashi, *Chem. Phys. Lett.* 379 (2003) 452.
- [26] S. Yoo, X.C. Zeng, S.S. Xantheas, *J. Chem. Phys.* 130 (2009) 221102.
- [27] J.X. Grossman, E. Schwegler, E.W. Draeger, F. Gygi, G. Galli, *J. Chem. Phys.* 120 (2004) 300.

Piskorz, I. Komaromi, R. L. Martin, D. J. Fox, T. Keith, M. A. Al-Laham, C. Y. Peng, A. Nanayakkara, M. Challacombe, P. M. W. Gill, B. Johnson, W. Chen, M. W. Wong, C. Gonzalez, J. A. Pople, *GAUSSIAN 03*, Revision D.1; Gaussian, Inc.: Wallingford, CT, 2005.

[44] H.J.C. Berendsen, J.P.M. Postma, W.F. van Gunsteren, A. DiNola, J.R. Haak, *J. Phys. Chem.* 81 (1984) 3684.

[45] D.J. Adams, E.H. Adams, G.J. Hills, *Mol. Phys.* 38 (1979) 387.

[46] D.A. McQuarrie, in *Statistical Mechanics*; Harper & Row, New York, 1976.

[47] T.S. Hofer, H.T. Tran, C.F. Schwenk, B.M. Rode, *J. Comput. Chem.* 25 (2004) 211.

[48] P. Kabbalee, A. Tongraar, T. Kercharoen, *Chem. Phys.* 446 (2015) 70.

[28] D. Xenides, B.R. Randolph, B.M. Rode, *J. Chem. Phys.* 122 (2005) 174506.

[29] B.M. Rode, C.F. Schwenk, A. Tongraar, *J. Mol. Liq.* 110 (2004) 105.

[30] B.M. Rode, C.F. Schwenk, T.S. Hofer, B.R. Randolph, *Coord. Chem. Rev.* 249 (2005) 2993.

[31] B.R. Brooks, R.E. Bruccoleri, B.D. Olafson, D.J. States, S. Swaminathan, M. Karplus, *J. Comput. Chem.* 4 (1983) 187.

[32] T. Kercharoen, K. Morokuma, *Chem. Phys. Lett.* 355 (2002) 257.

[33] T. Kercharoen, K. Morokuma, *J. Chem. Phys.* 118 (2003) 8856.

[34] S. Wanprakhon, A. Tongraar, T. Kercharoen, *Chem. Phys. Lett.* 517 (2011) 171.

[35] P. Sripa, A. Tongraar, T. Kercharoen, *J. Phys. Chem. A* 117 (2013) 1826.

[36] S. Thamolai, A. Tongraar, T. Kercharoen, *J. Mol. Liq.* 174 (2012) 26.

[37] P. Wernet, D. Nordlund, U. Bergmann, M. Cavalleri, M. Odelius, H. Ogasawara, L. Å. Näslund, T.K. Hirsch, L. Ojamäe, P. Glatzel, L.G.M. Pettersson, A. Nilsson, *Science* 304 (2004) 995.

[38] S. Myneni, Y. Luo, L. Å. Näslund, M. Cavalleri, L. Ojamäe, H. Ogasawara, A. Pelmentschikov, P. Wernet, P. Vaterlein, C. Heske, Z. Hussain, L.G.M. Pettersson, A. Nilsson, *Journal of Physics: Condensed Matters* 14 (2002) L213.

[39] M. Svensson, S. Humbel, R.D.J. Froese, T. Mutsaers, S. Steber, K. Morokuma, *J. Phys. Chem.* 100 (1996) 19357.

[40] T.H.Jr. Dunning, P.J. Hay, in *Methods of Electronic Structure Theory*, III, Plenum, New York, 1977.

[41] F.H. Stillinger, A. Rahman, *J. Chem. Phys.* 68 (1976) 666.

[42] P. Bopp, G. Janesó, K. Heinzinger, *Chem. Phys. Lett.* 98 (1983) 129.

[43] M. J. Frisch, G. W. Trucks, H. B. Schlegel, G. E. Scuseria, M. A. Robb, J. R. Cheeseman, J. A. Montgomery, T. Vreven, K. N. Kudin, J. C. Burant, J. M. Millam, S. S. Iyengar, J. Tomasi, V. Barone, B. Mennucci, M. Cossi, G. Scalmani, N. Rega, G. A. Peterson, H. Nakatsuji, M. Hada, M. Ehara, K. Toyota, R. Fukuda, J. Hasegawa, M. Ishida, T. Nakajima, Y. Honda, O. Kitao, H. Nakai, M. Klene, X. Li, J. E. Knox, H. P. Hratchian, J. B. Cross, V. Bakken, C. Adamo, J. Jaramillo, R. Gomperts, R. E. Stratmann, O. Yazyev, A. J. Austin, R. Cammi, C. Pomelli, J. W. Ochterski, P. Y. Ayala, K. Morokuma, G. A. Voth, P. Salvador, J. J. Dannenberg, V. G. Zakrzewski, S. Dapprich, A. D. Daniels, M. C. Strain, O. Farkas, D. K. Malick, A. D. Rabuck, K. Raghavachari, J. B. Foresman, J. V. Ortiz, Q. Cui, A. G. Baboul, S. Clifford, J. Cioslowski, B. B. Stefanov, G. Liu, A. Liashenko, P.

TABLE CAPTIONS

Table 1 Optimized parameters of the analytical pair potentials for the interactions of water with Li^+ (interaction energies in $\text{kcal}\cdot\text{mol}^{-1}$ and distances in \AA).

Table 2 Number of water exchange events (N_{ex}) and mean residence times (MRTs) of water molecules in the bulk and in the vicinity of Li^+ and some other ions, as obtained by the conventional QM/MM and ONIOM-XS MD simulations.

Pair	A ($\text{kcal}\cdot\text{mol}^{-1}\cdot\text{\AA}^4$)	B ($\text{kcal}\cdot\text{mol}^{-1}\cdot\text{\AA}^5$)	C ($\text{kcal}\cdot\text{mol}^{-1}$)	D (\AA^{-1})
Li-O	-1050.70523	1157.41401	5931.628	2.9058482
Li-H	-69.95421	131.67480	15.710	0.7012464

FIGURE CAPTIONS

Figure 1 a) Li-O and b) Li-H RDFs and their corresponding integration numbers, as obtained by the conventional QM/MM and ONIOM-XS MD simulations.

Figure 2 Distributions of the coordination numbers of Li^+ , calculated within the first minimum of the Li-O RDFs, as obtained by the conventional QM/MM and ONIOM-XS MD simulations.

Figure 3 Distributions of the O---Li---O angle, calculated within the first minimum of the Li-O RDFs, as obtained by the conventional QM/MM and ONIOM-XS MD simulations.

Figure 4 Time dependence of a) Li⁺---O distance and b) number of first-shell waters, as obtained from first 20 ps of the conventional QM/MM MD simulation. In Figure 4a), the dash line parallel to the x-axis indicates the first minimum of the Li-O RDF.

Figure 5 Time dependence of a) Li⁺---O distance and b) number of first-shell waters, as obtained from first 20 ps of the ONIOM-XS MD simulation. In Figure 5a), the dash line parallel to the x-axis indicates the first minimum of the Li-O RDF.

Table 2

Ion/solute	CN	t_{sim}	$t^* = 0.0$ ps		$t^* = 0.5$ ps	
			$N_{\text{ex}}^{0.0}$	$\tau_{\text{H}_2\text{O}}^{0.0}$	$N_{\text{ex}}^{0.5}$	$\tau_{\text{H}_2\text{O}}^{0.5}$
Conventional QM/MM MD						
Li^+	4.1	40.0	37	4.43	9	18.22
K^+ [34]	7.0	30.0	514	0.41	112	1.87
Ca^{2+} [34]	7.8	40.0	26	12.00	8	39.00
H_2O [36]	4.9	40.0	944	0.21	84	2.33
ONIOM-XS MD						
Li^+	4.2	40.0	79	2.13	13	12.92
Na^+ [35]	5.4	41.0	164	1.35	36	6.18
K^+ [34]	6.3	30.0	445	0.42	105	1.80
Ca^{2+} [34]	7.6	40.0	30	10.13	14	21.71
H_2O [36]	4.7	30.0	607	0.23	65	2.17

Figure 1

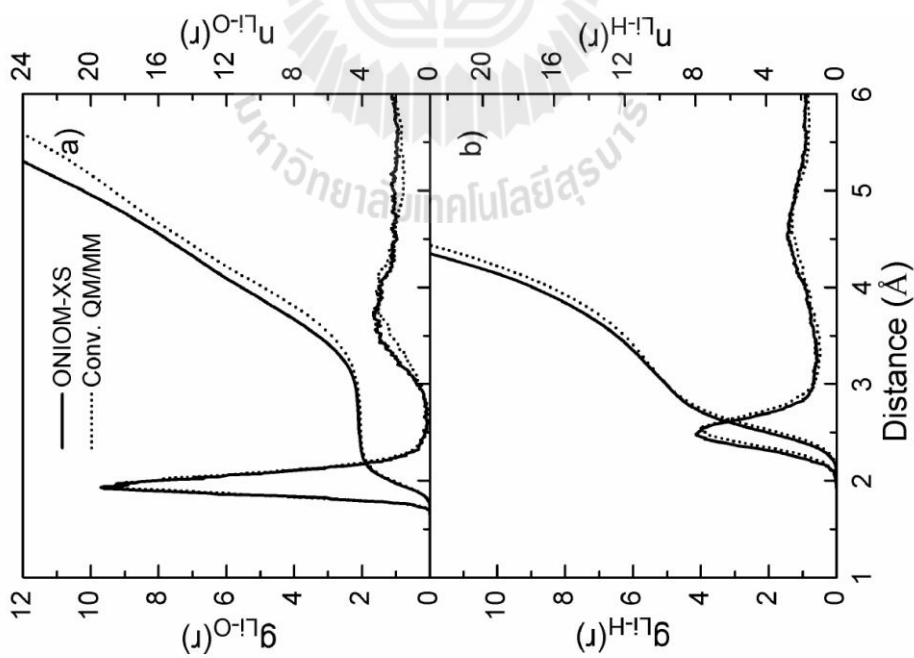


Figure 2

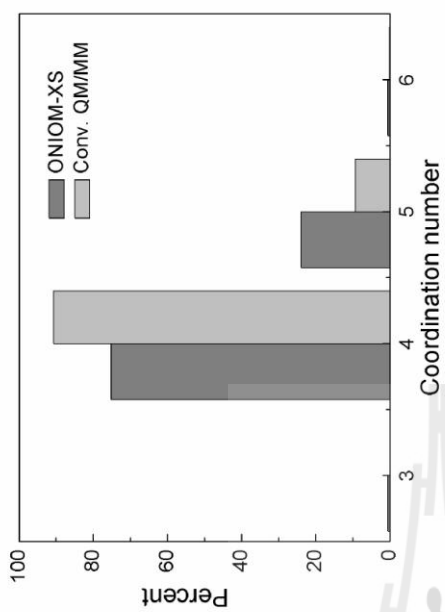


Figure 3

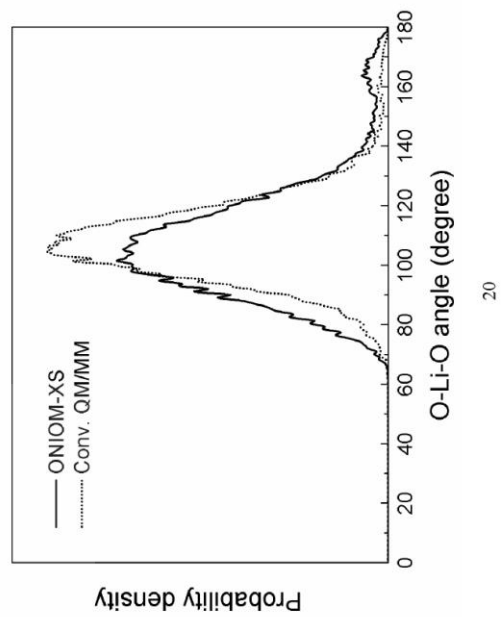


Table of Contents (TOC) Image

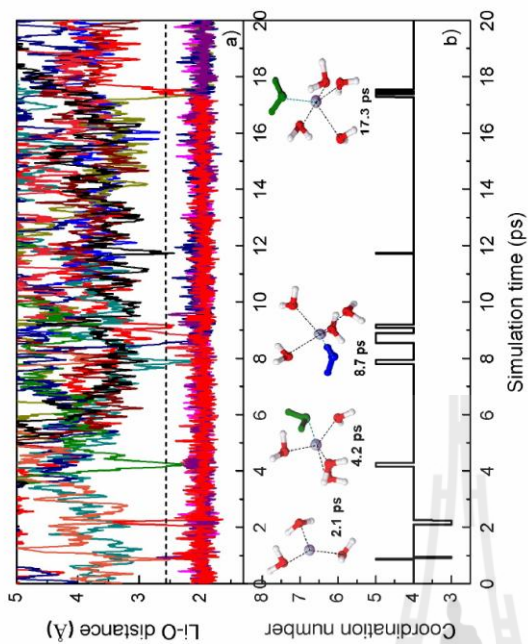


Figure 4

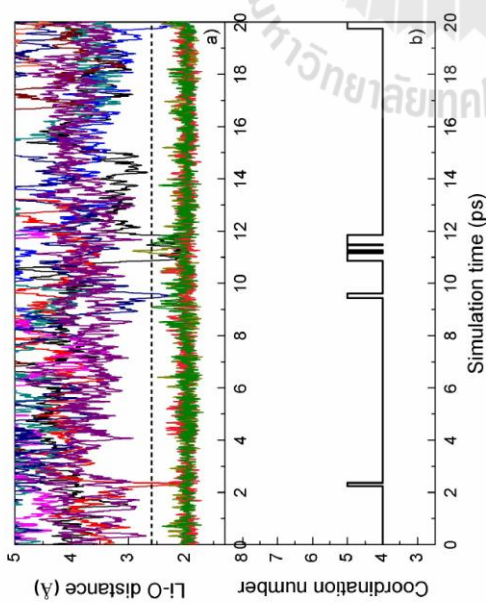
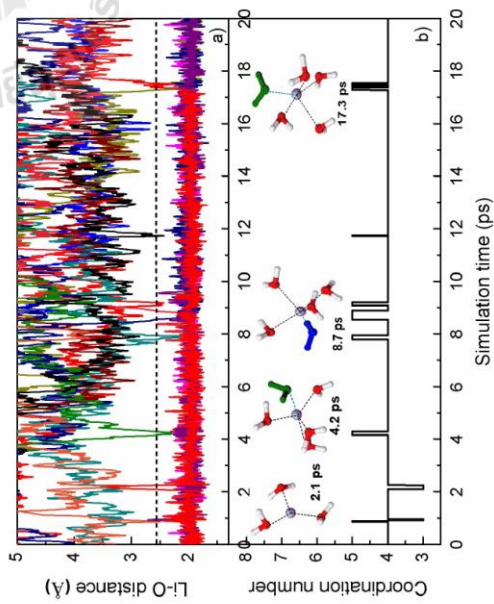


Figure 5



21

Time dependence of a) $\text{Li}^+\text{---O}$ distance and b) number of first-shell waters, as obtained from first 20 ps of the ONIOM-XS MD simulation.

CURRICULUM VITAE

MISS PATTRAWAN SRIPA

Education Background:

- Present Ph.D. Candidate (Chemistry), Suranaree University of Technology,
Nakhon Ratchasima, Thailand
- 2005-2008 B.Sc. (Chemistry), Ubon Ratchathani University, Ubon Ratchathani,
Thailand

Experiences:

- 2010 – 2014 Teaching assistant at Suranaree University of Technology
Courses : Fundamental Chemistry Laboratory I
Fundamental Chemistry Laboratory II
- 2014 Visiting study in Prof. Donald G Truhlar group research at the
University of Minnesota, United States of America for the period of
April 1 through September 30, 2014.

Grant and Fellowships:

- 2011-2014 The SUT-PhD Program (Contract number: SUT-PhD/01/2554),
Suranaree University of Technology (SUT)